The importance of miR-17~92 during CD28 co-stimulation of murine $CD4^+$ T cells

Inauguraldissertation

zur
Erlangung der Würde eines Doktors der Philosophie
vorgelegt der
Philosophisch-Naturwissenschaftlichen Fakultät
der Universität Basel

von
Marianne Dölz
aus Riehen BS, Schweiz

Basel, 2019

Originaldokument gespeichert auf dem Dokumentenserver der Universität Basel
edoc.unibas.ch

Dieses Werk ist lizenziert unter einer Creative Commons CC BY-NC-SA 4.0 International Lizenz

Genehmigt von der Philosophisch-Naturwissenschaftlichen Fakultät
auf Antrag von

Prof. Dr. Gennaro De Libero

Prof. Dr. Christoph Hess

Basel, den 25. Juni 2019

Prof. Dr. Martin Spiess
Dekan

1. Acknowledgement

I would like to thank Prof. Dr. Lukas Jeker for the supervision and advice during my PhD. I was lucky and grateful to have the freedom of exploring this project in almost any direction that I wanted to follow. I learned a lot about science and research, techniques and life in general.

Special thanks also to my committee Prof. Dr. Gennaro de Libero and Prof. Dr. Christoph Hess, for their support and advice. Thank you for taking time and effort of accompanying this project.

A great contribution came from all past and present members of the Jeker group and our “neighbors”. Werner, thank you for giving me advice, feedback and inputs during labmeetings. Madi, you not only made me laugh everyday but also were a great support. Thank you for being my soul mate, our “second brain” sessions, your hands in some dissections and your friendship. Mara, thank you for being my answer to everything in the first years of my PhD. Thanks to Hélène, Corinne, Giuseppina, Caroline who genotyped hundreds of mice for this project. Romina, thank you for ordering whatever I needed and making sure it would arrive instantaneously. Anne and Mathias, it was great to have our (almost) daily lunch meetings, with scientific and not so scientific discussions, lots of laughter, your friendship and support. Annaïse and Corina, thank you for asylum, entertaining coffee breaks and sharing your brains when Madi was not available. There were so many more people outside the lab who supported me especially during the last year of my PhD. Thank you for believing in me, distracting me when necessary, and encouragement.

A big thanks also goes to our collaborators. Glenn, thank you for your advice and support on the seahorse and metabolism part of this project. John and Mark, thank you for your effort, input, feedback and help with the HITS-CLIP data.

I would have been lost in my data sets without the help of Julien and the Bioinformatics core facility who implemented the user-friendly shiny app tool. Thank you very much for your work.

I would like to thank the entire mouse facility for their efforts and patience (especially when Pyrat got installed).

Most importantly, I would like to thank my family for their loving support and patience in the last years. First, my parents who taught me to be curious, critical, explorative, ambitious, patient and sometimes a bit perfectionist. You are a major part of my motivation. Fabian (and his family), for your love, a lot of patience, forcing me to take breaks and keeping me balanced throughout all ups and some downs of this project. Jürgen and Rahel, for teaching me to listen to criticism, giving me honest feedback and encouragement. I wish you all the best.

I was grateful to have many friends outside the institute with all different sorts of other background. Thank you for all our adventures, laughter, fun, but also for listening, discussions, understanding and giving me new perspectives. With your encouragement and advice, some hurdles changed their shape and suddenly did not appear so huge any more.

Finally, I would like to thank all doctors, physiotherapists and chiropractors for taking care of my mental and physical health during my PhD.

Table of contents

2. Abstract

The prototypic costimulatory molecule CD28 is essential for proper $CD4^+$ T cell activation and initiation of clonal expansion. CD28 ligation regulates metabolic adaptation, the production of cytokines, survival, differentiation but also T follicular helper cell generation and germinal center response. Moreover, CD28 signaling induces the expression of microRNA cluster miR-17~92 during $CD4^+$ T cell activation. However, despite the importance of this receptor, the molecular understanding of how CD28 exerts its function remains incomplete.

In this thesis, we extend previous reports by showing that miR-17~92 expression directly correlates with $CD4^+$ T cell activation, and miR-17~92-deficiency phenocopies CD28-deficiency in mice. We therefore hypothesized that transgenic miR-17~92 expression could substitute for the loss of CD28. Using a B6.CD4cre.R26^{flox}stop^{flox}miR1792tg.CD28ko mouse model, we demonstrate that transgenic miR-17~92 expression compensates for CD28 expression during $CD4^+$ T cell activation and differentiation *in vitro*, but also *in vivo* during acute LCMV infection.

Even though many targets of miR-17~92 have been identified so far, the mechanisms by which miR-17~92 contributes to $CD4^+$ T cell activation have not yet been fully explained. We generate transcriptomic datasets from activated $CD4^+$ T cells with distinct amounts of miR-17~92 expression, with which we identify a new list of *bona fide* canonical miR-17~92 target genes. Furthermore, we demonstrate with a second dataset that these genes are not only regulated by miR-17~92 but also by CD28 expression. This shows that in addition to the activation of transcription during CD28 dependent $CD4^+$ T cell activation, also the repression of genes which is mediated by miR-17~92 is essential. Moreover, the identified target genes mediate a rescue of the CD28ko transcriptome in rescue cells.

We furthermore identify a new miR-17 target regulator of calcineurin 3 (RCAN3) among the list of target genes. Our data strongly support a model in which miR-17~92, in addition to known pathways like PI3K, also regulates the NFAT pathway. This qualifies this miRNA cluster as an important regulator of CD28 co-stimulation, which could have broad implications for a better understanding of T cell activation and immunotherapy.

3. Introduction

3.1. T cell activation

3.1.1. Activation needs co-stimulation

The activation of $CD4^+$ T cells is a cornerstone for a proper adaptive immune response. Only with the help of $CD4^+$ T cells, B cells can undergo affinity maturation and class switch in order to reach an optimal antigen recognition and antibody response. Bretscher and Cohn proposed in 1970 that there are actually two signals needed in order to get full T cell activation [1], and this concept was further extended by Lafferty and Cunningham [2]. Schwartz and Jenkins later showed that T cell activation starts with binding of the T cell receptor (TCR) to an antigen presented on a major histocompatibility complex (MHC) molecule, but without other signals, the cell may turn unresponsive and anergic [3, 4], suggesting that activation of T cells needs co-stimulatory signals.

Co-stimulatory signals can either be generated from members of the CD28 family (which is the most important for T cells) or Tumor Necrosis Factor (TNF) receptor superfamily (for example CD40, which is more relevant for B cells). Early reports distinguished between TCR and CD28 signaling based on their differential reaction to Cyclosporin A (CsA), which on one hand led to the conclusion that TCR signaling is calcium (Ca^{2+}) dependent, but secondly that CD28 has another, Ca^{2+} independent signaling mechanism that was not inhibited by CsA [5]. Later, several groups reported that CD28 can be phosphorylated and then binds to Phosphatidyl Inositol 3-Kinase (PI3K) [6-8]. This binding of PI3K to CD28 is essential for downstream processes of T cell activation since it recruits the enzyme to the cell surface, providing proximity to target substrates which initiate pathways like glucose uptake, and cytoskeletal re-organization [9].

3.1.2. T cell receptor signaling cascade

The classical TCR is composed of an α and a β chain that span the cell membrane. Both of the chains have a variable and a constant region, and the combination of the extracellular variable regions is crucial for antigen specific binding. However, the

binding of antigen by α/β is not sufficient to initiate signaling. Instead, the TCR needs interaction partners for its function [10, 11], which then represent the starting point for further signaling: CD3 signaling chains as well as the ζ-chains are associated with the α - and β chain, forming the TCR complex. The intracellular parts of these additional signaling chains bear so-called immunoreceptor tyrosine-based activation motifs (ITAMs) which are important for downstream signaling [12]. The signaling processes are in fact a cascade of phosphorylation and dephosphorylation events, which are tightly regulated and initiate recruitment and interaction of key molecules. During antigen recognition, the TCR recognizes the antigen that is presented on MHC. In the case of $CD4^+$ T cells, the CD4 expressed on the T cell surface binds to the MHC class II molecule presenting the antigen to the TCR [13]. This binding moves the intracellular part of CD4 closer to the intracellular part of CD3, which is essential for the phosphorylation of ITAM: the Src-family kinase Lck is associated with CD4 and thought to be the main responsible kinase for the phosphorylation of ITAM (Figure 1) [14]. The activity of Lck is regulated by CD45, which can dephosphorylate both Lck tyrosine phosphorylation sites, opening its conformation [15]. Another regulating enzyme is C-terminal Src kinase (Csk), whose activity leads to a “closed” confirmation of Lck [16], which is a catalytically inactive state.

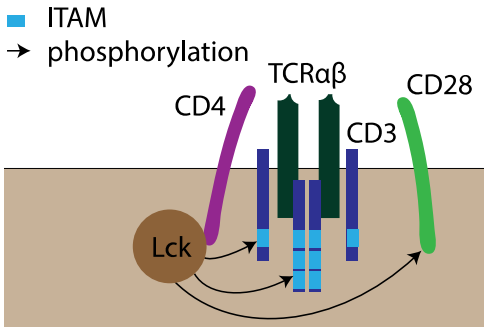

Figure 1. ITAMs of the T cell receptor complex are phosphorylated by Lck
The TCR α and β chains bind to MHCII:antigen. CD4 binds to MHCII, bringing the associated Lck in closer proximity to the TCR complex, so that ITAMs as well as CD28 can be phosphorylated

The phosphorylation of the ITAMs is the beginning of several downstream pathways: tandem Src Homology 2 (SH2) and SH3 domain-containing enzymes (e.g. ZAP70) recognize their binding motif, initiating further signaling. Once Lck has phosphorylated the ITAM on the intracellular part of CD3, ZAP70 binds to it and is as well phosphorylated by Lck [17]. This ZAP70 activation is the pre-requisite for subsequent T cell receptor signaling [18]: It phosphorylates the scaffold protein linker of activated

T cells (LAT) [19] and another adaptor protein called SLP-76. The two of them are linked by the adaptor protein Gads, which leads to a three-protein complex (LAT:Gads:SLP-76), which is key for T cell activation, acting as a scaffold. This scaffold can be generated by TCR signaling alone, while all subsequent events in T cell activation are dependent on co-stimulatory signals. ZAP70 activation additionally leads to the recruitment and activation of PI3K [20], but more importantly, PI3K is getting recruited and phosphorylated by the intracellular domain of CD28. CD28 is previously phosphorylated upon TCR signaling by p56Lck and p59Fyn [21] which enables binding of further molecules to this receptor. PI3K subsequently phosphorylates Phosphatidylinositol 4,5-bisphosphate (PIP_2) at the inner membrane [22], resulting in Phosphatidylinositol (3,4,5)-trisphosphate (PIP_3), which is essential for many signaling molecules that bind to PIP_3 via their PH domain (Figure 2).

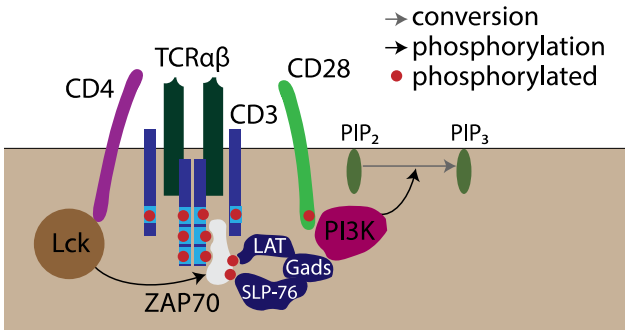

Figure 2. Phosphorylated ITAMs recruit SH2 domain containing molecules like ZAP70, so that a scaffold for further signaling can be created.

Phosphorylated ITAMs are bound by SH2 domain-containing molecules like ZAP70, which in turn get activated and phosphorylated. This creates new binding- and phosphorylation sites for e.g. LAT and SLP-76, which are linked to a complex via Gads. PI3K is recruited to this complex as well as to the phosphorylated part of CD28, so that PI3K can phosphorylate PIP_2, resulting in PIP_3.

3.1.3. Phosphatidylinositol-3 kinase activity and other downstream effects of T cell activation

Already in early reports from 1989, Thompson et al. described the augmentation of T cell responses, i.e. stronger cytokine production, if the stimulation of human T cells via CD3 complex was complemented with stimulation of CD28 [23]. The most important function of the co-stimulatory receptors is the enhancement of PI3K

expression [24]. The joint action of the LAT:Gads:SLP-76 scaffold and PI3K or both together initiate processes which are essential for proper T cell activation, starting from metabolic changes to cell adhesion, actin polymerization and alterations in transcription. Transcriptional changes initiated by TCR are mostly modulated by phospholipase C-γ (PLC-γ): PI3K phosphorylates PIP_2 on the cell membrane which leads to PIP_3, to which PLC-γ binds via its PH-domain. PLC-γ then binds to the LAT:GADS:SLP-76 complex, and is phosphorylated by Itk (IL-2 inducible T cell kinase, which is recruited to the membrane via its PH domain binding to PIP_3). Phosphorylated PLC-γ can then break down PIP_2 into diacylglycerol (DAG), which will stay bound to the membrane, and a diffusible second messenger called inositol 1,4,5-triphosphate (IP_3) [25]. These two cleavage products initiate distinct downstream pathways (Figure 3).

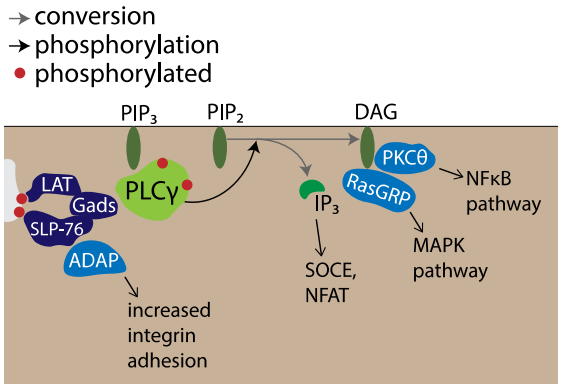

Figure 3. PLC-γ cleaves PIP_2 into IP_3 and DAG, initiating downstream pathways

PLC-γ interacts with LAT:Gads:SLP-76 scaffold before it cleaves PIP_2 to IP_3 and DAG, both leading to transcriptional changes. Other molecules like ADAP can also bind to the scaffold, initiating other downstream mechanisms, in this case increased integrin adhesion.

DAG recruits other molecules to the membrane, like PKCΘ and RasGRP. RasGRP activates Ras [26], which is an initiator of the MAPK pathway leading to Erk1 expression [27], which promotes generation of activator protein 1 (AP-1). AP-1 is a heterodimer consisting of Fos and Jun [28], which is transcriptionally inactive until Jun kinase (JNK) phosphorylates Jun, thereby activates AP-1 and initiates the transcription of many genes that are essential for T cell activation. AP-1 is an important interaction partner of nuclear factor of activated T cells (NFAT). PKCΘ is also recruited to the membrane by DAG, promoting a pathway which results in the activation of nuclear factor kappa-light-chain-enhancer of activated B cells (NFκB) [29].

TCR stimulation furthermore leads to increased integrin adhesion [30]. This process is mediated by the LAT:GADS:SLP-76 complex as well: the adaptor protein ADAP is recruited to the complex, which recruits two more proteins SKAP55 and RIAM. This complex in turn activates a small GTPase Rap1 [31], which promotes LFA-1 aggregation and its conformational change [32]. In this state, LFA-1 has a higher affinity for ICAM-1, which is important for the T cell if it should extravasate from e.g. a blood vessel to the surrounding tissue.

For a stable interaction between the antigen presenting cell (APC) and the T cell, which is essential for the proper activation of the T cell, the cytoskeleton has to reorganize [33]. This process depends on Vav, which is recruited to PIP_3 via its PH domain. At the same time, it also interacts with the LAT:GADS:SLP-76 complex via its SH2 domain. Also WASp is recruited to the LAT:GADS:SLP-76 complex, binding via the adaptor protein Nck. Vav activates Cdc42, which induces a conformational change in WASp [34]. This binds to WIP, and the complex recruits Arp2 and 3, which induces actin polymerization.

The PI3K is also especially important for the metabolic changes underlying T cell activation [35, 36]. Protein kinase B, also known as Akt [37], binds to PIP_3 in the membrane, where it is phosphorylated by PDK1. Phosphorylated Akt initiates a couple of important downstream pathways, for example it promotes the mammalian target of rapamycin (mTOR) pathway [38], leading to metabolic changes (Figure 4).

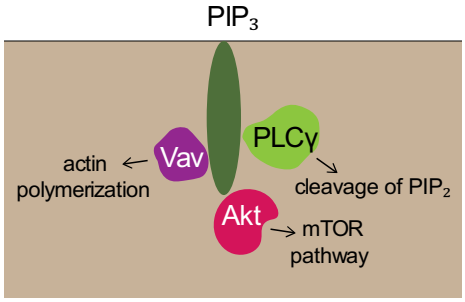

Figure 4. PIP_3 is an important interaction partner for different pathways of T cell activation
PIP_3 interacts with Vav, inducing Cdc42 activation and later actin polymerization. Furthermore, PIP_3 activates Akt, leading to mTOR pathway activation. PLC- γ importance is shown in Figure 3.

All of these processes that are partially or fully dependent on the activity of PI3K already argue for the importance of co-stimulation in the T cell activation process. We will now go into detail on the downstream mechanism of IP_3, which will be of particular interest in this thesis.

3.1.4. IP_3 initiates Store Operated Calcium Entry (SOCE)

IP_3 binds to Ca^{2+} channels in the endoplasmic reticulum (ER) membrane, so that Ca^{2+} is released from the ER store [39, 40], leading to an acute drop of Ca^{2+} abundance inside the ER lumen. This induces a conformational change [41] and clustering of stromal interaction molecules (STIM1/2) within the ER membrane [42, 43]. The STIM molecules then interact with the plasma membrane and ORAI [44, 45], which belong to the family of Ca^{2+}-release activated Ca^{2+} channels (CRAC). The concentration of intracellular Ca^{2+} is mainly controlled by CRAC channels, in T cells ORAI1/2 [42, 46-48], which are located in the plasma membrane. The CRAC channels open upon interaction with STIM1/2 [44], which allows extracellular Ca^{2+} influx and activation of further signaling to replenish Ca^{2+} stores in the ER. Since the Ca^{2+} concentration of the ER regulates the Ca^{2+} influx, this process is called store operated Ca^{2+} entry (SOCE) [40, 49, 50]. The Ca^{2+} in the cytosol bind to calmodulin, changing its conformation so that it interacts with and activates calcineurin. Upon conformational change of calmodulin and activation of calcineurin, NFAT is de-phosphorylated in multiple serine and threonine residues in its regulatory domains and translocates to the nucleus [51] where it initiates transcriptional activation (Figure 5).

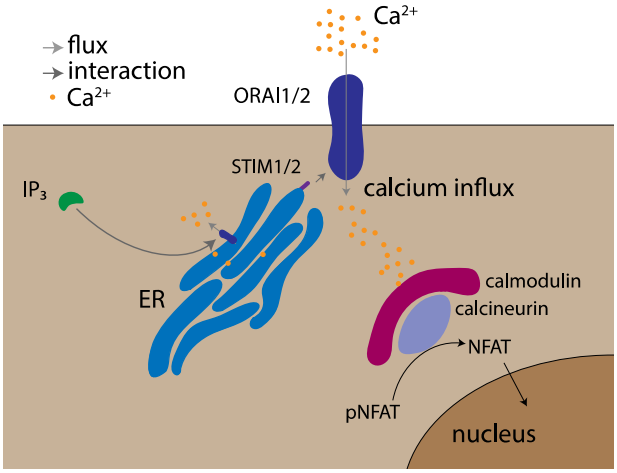

Figure 5. IP_3 induces Store Operated Calcium Entry (SOCE)

IP_3 interacts with ER calcium channels, so that Ca^{2+} is released from ER Ca^{2+} stores. STIM1/2 sense this drop in Ca^{2+} within the ER, and interact with ORAI1/2 to initiate extracellular Ca^{2+} influx. Ca^{2+} binds to calmodulin, leading to a conformational change and interaction with calcineurin. Calcineurin then de-phosphorylates NFAT, enabling nuclear translocation.

The phosphatase activity of calcineurin can be blocked by CsA and FK506 (also known as Tacrolimus) in a calmodulin independent manner [52, 53], which is one important aspect of immunosuppressive medication that is used in the clinics [54].

Mice that are deficient in ORAI1/2 or STIM1/2 expression in T cells display impaired T cell mediated immune responses, marked by impaired cytokine production and antigen-dependent proliferation [47, 55, 56]. Also for humans, mutations of ORAI and STIM result in severe combined immunodeficiency [46], underlining the importance of this pathway for proper T cell activation and function.

3.1.5. NFAT and its targets

NFAT was found in the end of the 1980s in the extract of activated T cells and several cell lines [57]. Shaw et al. described "*an inducible DNA-binding factor that is expressed minutes before the activation of the interleukin 2 (IL-2) gene*". NFAT was found not only in the cytoplasm but also in the nuclear fraction of stimulated Jurkat cells [58], with a different sensitivity to inhibition by FK506 and CsA, indicating that the translocation to the nucleus must be regulated by calcineurin. Meanwhile, the importance of the NFAT family was also demonstrated in other cell types of the hematopoietic system like megakaryocytes [59], dendritic cells [60] and B cells [61] as well as for developmental processes [62] and in other tissues, for example pancreatic β cells [63] and osteoclasts [64].

The NFAT family consists of five members [65-67]: NFAT1 (NFATc2, NFATp), NFAT2 (NFATc1, NFATc), NFAT3 (NFATc4, NFATx), NFAT4 (NFATc3) and NFAT5 (TonEBP, OREBP) [68]. Each of them is expressed in a different tissue-specific pattern and none is restricted to lymphocytes in its expression [66]. All of the family members are evolutionary related to the Rel-nuclear-factor-κB family of transcription factors (TF), but only NFAT1-4 are regulated by intracellular Ca^{2+} abundance via calcineurin [69].

In T cells, three of the Ca^{2+} regulated NFAT family members are expressed in two or more splice forms: NFATc1, NFATc2 and NFATc3 [68, 70]. All of them contain essential domains: First of all, the NFAT homology region that contains interaction domains for calcineurin (TAD-A, transactivation domain) and NFAT kinases (regulatory domain, serine-rich regions that are phosphorylated by kinases such as dual-specificity tyrosine-phosphorylation regulated kinase 1, DYRK1). This region is also strongly

targeted and thereby de-phosphorylated by calcineurin [53, 71, 72] in order to permit nuclear localization [57, 73]: for example NFATc2 is heavily phosphorylated on 14 sites, and 13 of them can be de-phosphorylated by calcineurin [74].

Secondly, the Rel homology region harbors the DNA-binding domain of the protein [75, 76] via a DNA-binding loop that also confers base-specific recognition at its N-terminal region, but also has a protein interaction domain at its C-terminus. This protein interaction domain is of special importance regarding the targets of the NFAT family: the diversity of interaction partners enable NFAT to act on a variety of different pathways, which are essential for T cell activation and differentiation.

NFAT can have an activating or deactivating transcriptional function depending on its binding partners [68]. For the initiation of transcription, NFAT needs to form a complex with AP-1, MEF2, or GATA proteins. The most commonly known interaction partner of NFAT is AP-1 [28, 77]. This interaction can promote expression of *IL-2* [78], *CD25* [79], interferon gamma (*IFNγ*) [80], *IL-4* [81], RAR related orphan receptor gamma t (*Rorγt*) [82] or Forkhead box p3 (*FoxP3*) [83]. The transcription of *IL-2* is initiated when NFAT interacts with AP-1 to form a heterodimer that binds DNA [28, 75, 77, 84]. However, addition of exogenous IL-2 only poorly rescues *in vitro* proliferation capacity of CD4cre.ORAI2$^{fl/fl}$ murine CD4^{+} T cells [47] which argues that cytokines are not the exclusive NFAT downstream targets that strongly influence proliferation. Moreover, the regulation of IL-2 is a good example of how complex the regulation actually might be: NFAT-AP1 promotes *IL-2* transcription, whereas NFAT-Foxp3 actually represses this process [85]. Furthermore, additional factors like runt-related TFs (Runx1 and 3) regulate NFAT-induced *IL-2* transcription as well.

Other binding partners of NFAT have also been described to initiate transcription: upon interaction with C/EBP, binding to the *PPAR-γ* promoter is promoted [86], subsequent binding of NFAT to PPAR-γ then leads to binding of the *IL-2* promoter while blocking the DNA binding of NFAT, thereby inhibiting *IL-2* transcription [87]. Interaction with MAF [88, 89], GATA3 [89] or IRF4 [90] leads to binding in *IL-4* promoter or enhancer regions. Upon interaction with T box expressed by T cells (Tbet), NFAT binds to the 5' enhancer of interferon γ (*IFNγ*) [89, 91]. *TNF* promoter is bound when EGR1 or EGR4 interact with NFAT [92], and synergy with MEF2 recruits the coactivator p300 for the transcription of *Nur77* [93]. During early T cell activation,

NFAT actually binds both promoters of *IFNγ* and *IL-4* [94], and as soon as T cell differentiation has been initiated the inappropriate locus is silenced.

Besides effects on cytokine production, NFAT activity also mediates metabolic reprogramming and clonal expansion [95]. Vaeth et al. demonstrated that SOCE, calcineurin and NFAT induce glycolysis and oxidative phosphorylation by regulating the expression of glucose transporters, glycolytic and mitochondrial enzymes. However, they also show that these pathways do not entirely depend on NFAT and that also the PI3K-Akt-mTOR pathway is to some extent regulated by SOCE and calcineurin.

Ca^{2+} signaling can have a stimulatory but also an inhibitory role in gene expression [96]. Feske et al. performed gene expression analysis on two T cell lines from patients with defects in Ca^{2+} signaling and found that about a third of the genes were down-regulated in the control, but not in patient samples upon activation, among these they identified *Lck*, *Fas*, *E2F-3*, *IRF-2* and Signal transducer and activator of transcription 1 (*STAT1*).

Sustained Ca^{2+} signaling induced by TCR in the absence of co-stimulation induces a state of anergy in B and T cells [97-99], in the latter this is marked by the expression of anergy-associated genes like *GRAIL* which negatively regulates T cell activation signals by targeting them for degradation. NFATc2 knockout cells were shown to be more resistant to anergy induction than wild-type cells and T cell anergy was induced in the absence of AP-1 [97], underlining NFATs critical role in anergy induction.

3.1.6. Regulation of NFAT

One downstream effect of CD28 co-stimulation is that Akt [100] is activated via PI3K pathway. Glycogen-synthase kinase 3 (GSK3) [101], similar to casein kinase 1 (CK1) [102] as well as p38 and JNK [103, 104], is a kinase that re-phosphorylates NFAT and thereby mediates nuclear export, but upon Akt activity GSK3 is phosphorylated which inhibits its kinase activity [105, 106]. Thereby, CD28 indirectly promotes NFAT signaling via PI3K signaling and the prevention of its export to cytoplasm [106, 107].

Calcineurin is regulated by so-called calcipressins, some of which are CABIN1 [108], AKAP79 [109, 110] and members of the Down's syndrome critical region (DSCR, also called regulator of calcineurin (RCAN) [111, 112]. In mice that are deficient for Cabin1,

Esau et al. reported increased cytokine expression in stimulated T cells [113], demonstrating the negative regulation of calcineurin by calcipressins.

There are three regulators of calcineurin (RCAN1-3) described in humans. They bind and inhibit the activity of calcineurin via the CIC motif [112], thereby preventing the dephosphorylation and nuclear translocation of NFAT [114]. The RCAN molecules differ in their N-terminal region, but are conserved among their central and C-terminal regions [112]. Expression of RCAN3 was reported in peripheral blood leukocytes, heart, skeletal muscle, liver and kidney [115]. However, in murine T cells mostly RCAN3 is expressed while RCAN2 is barely detectable and RCAN1 shows low expression (Figure 6) ([116], http://rstats.immgen.org/Skyline/skyline.html).

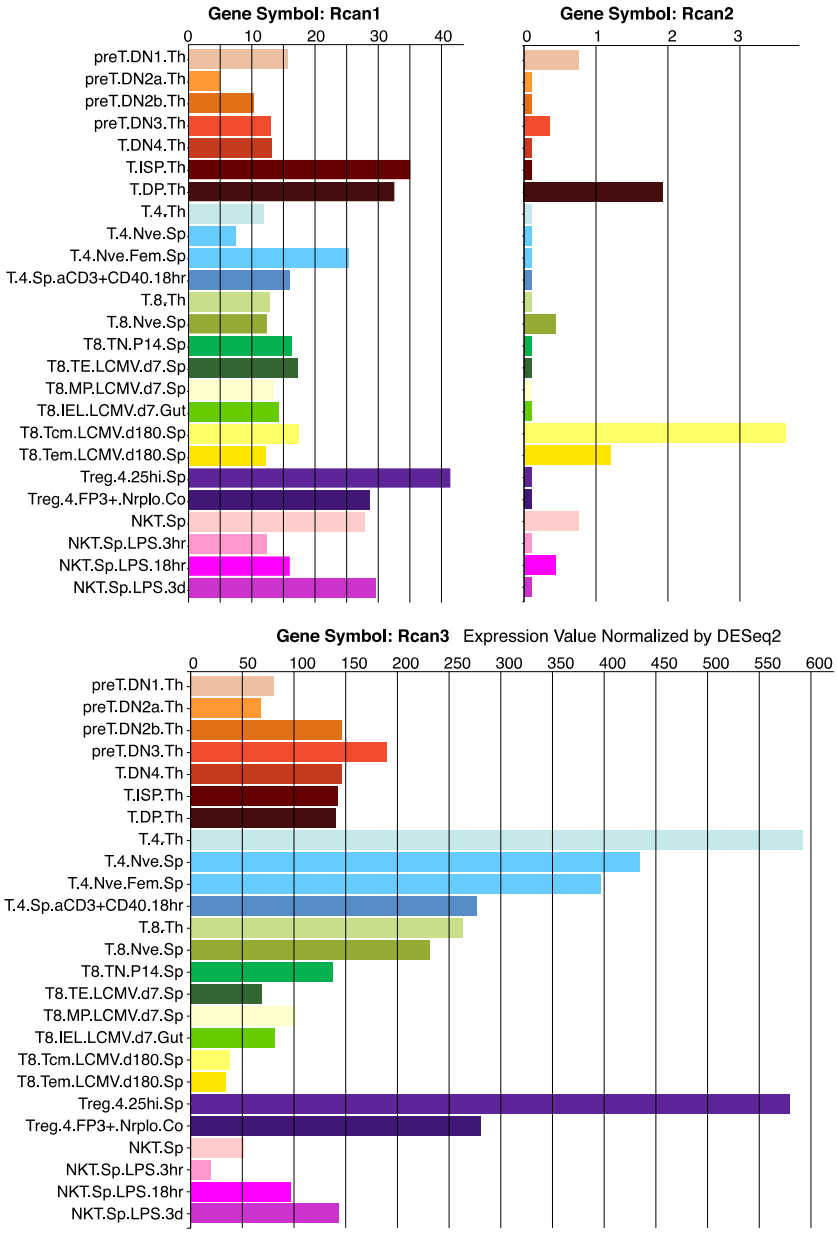

Figure 6. ImmGen Skylines of RCAN1, RCAN2, RCAN3 in murine T cells Normalized expression value of RCAN1-3 are shown in distinct T cell subsets.

3.1.7. Differentiation of CD4⁺ T cells

We can experimentally determine the activation state of a CD4⁺ T cell by staining for early (e.g. CD25, also known as IL-2Rα), and CD69 [117] and late (e.g. CD44/CD62L [118]) activation markers. Furthermore, activated CD4⁺ T cells are expected to blast, proliferate and produce cytokines, typically IL-2, in a CD28 dependent manner as described in previous sections.

When activated in the presence of different cytokines, as it is typically the case in different types of infection, CD4⁺ T cells differentiate into different T Helper (T_H) cell subsets. The decision to differentiate into a certain T_H subset is mainly initiated by the surrounding of the CD4⁺ T cell: the antigen, the type of cell that presents it and also the presence of cytokines (that can be released provided by cells of the innate immune system as well) act in concert to drive a specific type of differentiation. However, after the initiation of the process there are multiple feedback mechanisms inside the cell that emphasize the signal, leading to commitment. Among them are epigenetic changes and locus availability [119, 120], which is of major importance also for NFAT activity (see section 3.1.5). This can also be simulated to some extent *in vitro* by the addition of cytokines and blocking antibodies during the activation process. The individual T follicular Helper (T_{FH}), T_H1, T_H2, T_H17, and regulatory T (T_{reg}) cells are characterized by the expression of different subset specific hallmark TFs and cytokines (Figure 7).

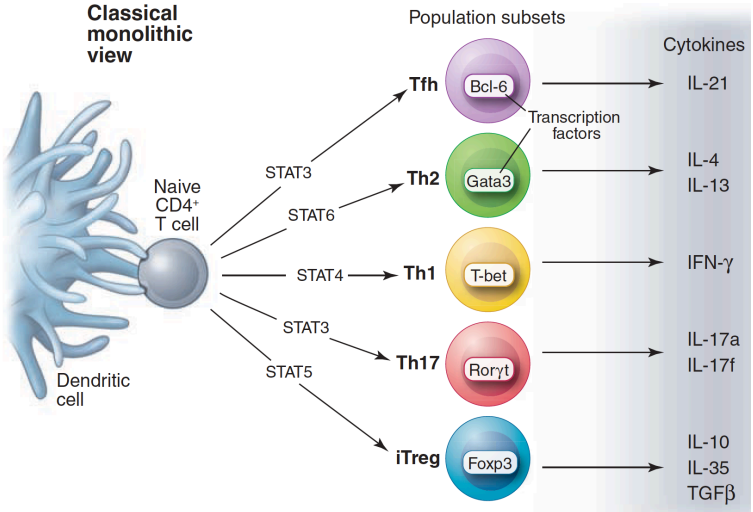

Figure 7. Classical view of T helper populations (Figure taken from [121])

In this thesis, T_{FH} and T_H1 cells are of particular interest. T_H1 cells are an important part of intracellular pathogen immunity, because they are able to activate macrophages [122] e.g. by the secretion of IFNγ. T_H1 are defined by the expression of the hallmark TF Tbet [123], which actively suppresses T_H2 fate and induces production of IFNγ. This phenomenon is restricted to $CD4^+$ T cells: $CD8^+$ T cells can produce IFNγ without Tbet expression [124]. Via signaling on STAT1, IFNγ activates the TF T-bet [125], which is also supported by STAT5 signaling coming from IL-2R. Tbet then promotes IFNγ production [123]. When TCR signaling stops, *IL12Rβ2* is induced [126], so that IL-12 can promote STAT4 signaling [127], which additionally promotes IFNγ and enhances STAT1 signaling. This illustrates how NFAT as a part of a positive feedback loop is essential for the differentiation of a T_H cell subset, in this case T_H1, but also in T_H2 and T_H17 similar synergistic action of sequential processes have been described [128].

The interaction between T_{FH} providing specialized help to B cells is essential for the formation of germinal centers (GC) [129]. These are histologically distinct structures within the B cell follicles of secondary lymphoid organs, and the main place where B cell affinity maturation and class switch recombination occur. T_{FH} are characterized by the expression of their master regulatory factor Bcl-6 [130], and further characterized by the expression of CXCR5, programmed death 1 (PD-1), inducible T cell co-stimulator (ICOS) and IL-21 [131]. Bcl-6 represses Blimp-1 [132] and opposes the differentiation into other helper lineages [130], but it also modulates microRNA (miRNA) expression [133]. T_{FH} are dependent on the global expression of miRNA (see section 3.2), which was shown in mice with CD4 intrinsic deficiency for DGCR8: the differentiation and function of T_{FH} was severely reduced [134]. Even though more and more evidence accumulates of which signals are needed for Bcl-6 induction and T_{FH} differentiation, i.e. IL-21 and IL-6 [131], T_{FH} so far cannot be generated *in vitro*. However, there are well established viral models (like acute lymphocytic choriomengitis model virus (LCMV), Armstrong [135]) to address the differentiation of this T cell subset *in vivo*, such models will also be applied in this thesis.

3.1.8. CD28

3.1.8.1. The family of CD28

The so-called receptor family of CD28 is grouped by their similar structure. All of the family members are expressed on lymphocytes and bind B-7 family ligands. Their role can be divided into activating and inhibitory molecules [136]. Expression of each of those molecules depends on context, activation state and cell type as well as on the presence of cytokines [137]. Moreover, the peptide affinity of the TCR complex to the antigen decides about the amount of co-stimulatory signals, which has led to some confounding results in different studies [137]. The net result of cell activation with co-stimulation is finally a complex combination of overlapping and opposing signals, which will only be briefly described here.

Cytotoxic T lymphocyte antigen 4 (CTLA-4) and PD-1 are typical examples for inhibitory receptors of the CD28 family. T cells from CTLA-4 deficient mice are hyper responsive to antigen [138, 139], and show increased T_{FH} and GC B cell differentiation in a CD28 dependent manner [140]. CTLA-4-Ig is a widely used tool to study co-stimulation: upon application of αCTLA-4 antibodies, TCR and TCR/CD28 triggered proliferation is inhibited [141] and T cell dependent antibody responses are strongly reduced [142].

PD-1 binds its ligand PD-L1 [143], and signals via this pathway regulate initial activation, which represents an important aspect of immune regulation [144]. Mice that are deficient for this receptor develop lupus-like symptoms and splenomegaly [145]. On the other hand, expression of PD-1 is elevated in some cancer and chronic viral infections, which led to the development of the PD-1 immune checkpoint blockade therapy [146]. In this approach, PD-1 signaling is blocked in order promote immunity to cancer. Lately, it was shown that this therapy might depend on the activating signaling via CD28 [147, 148].

ICOS and CD28 are activating receptors. The expression of ICOS is only induced via independent signaling pathways NFAT or MEK-ERK during $CD4^+$ T cell activation [149], while CD28 is expressed on naïve as well as activated cells. Weber et al. showed that while ICOS is dispensable for early events in T_{FH} differentiation like the upregulation of Bcl-6, it is essential for late GC reactions [150]. However, CD28 regulates key events in early T_{FH} generation but is dispensable for maintenance of T_{FH} cells. Interestingly,

the reduced GC response known from CD28 deficient mice is similarly seen in ICOS deficient patients [151].

Overall, the family of CD28 receptors is very diverse, some of the function is redundant yet the expression of each receptor is timing- and context dependent. Moreover, receptors of opposing role can be competing for the same ligand: CD28 and CTLA-4 both bind to the same receptors B7.1 and B7.2 (also called CD80 and CD86) [152], whereas CTLA-4 binds with a higher affinity. In this thesis, we will focus on CD28 in early $CD4^+$ T cell activation.

3.1.8.2. Structure and important motifs of CD28

CD28 is expressed on naïve $CD4^+$ T cells and binds to B7.1 (CD80) and B7.2 (CD86) which are expressed on APCs. When CD28 is bound to its ligand, the cytoplasmic part is phosphorylated by Lck. Different motifs of the intracellular part have been described to be essential for different functions. Of note, since the structure of the intracellular part of CD28 is very similar to CTLA-4 and ICOS, some of the motifs are shared between these domains as illustrated in Figure 8.

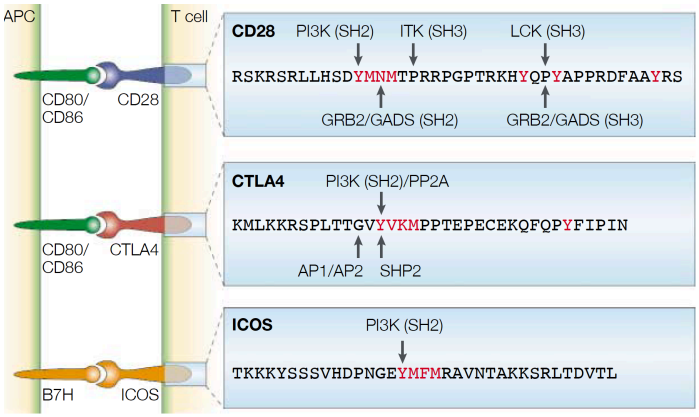

Figure 8. Motifs in the cytoplasmic tail of CD28 are partially shared with other family members (figure taken from [137])

The tyrosine residues in a YXN motif can recruit the adaptor protein Growth factor receptor-bound protein 2 (Grb2) via a non-ITAM motif YXXM. This is a shared motif between CD28, ICOS and CTLA-4, which acts as a consensus binding site for the p85 subunit of PI3K. More specifically, in CD28 this motif is YMNM. The asparagine residue confers specificity for Grb2 and Gads (see section 3.1), which might account for differences in the signaling between ICOS, CTLA-4 and CD28 [137, 153].

The distal, proline-rich motif PXXP was shown to bind the SH3 domains of Lck and Itk. It is essential for the signaling leading to normal IL-2 secretion as well as for the downstream phosphorylation of key kinases like PDK1, GSK3β and PKCΘ. Mutation of this distal motif led to decreased proliferation and IL-2 production, while mutation of the proximal YMNM motif was phenotypically indifferent [154]. Actually, the importance of the YMNM motif is a matter of debate, since others reported inhibition of proliferation and IL-2 secretion [155] in the same mouse model.

In humans, recurrent mutations in CD28 were reported for peripheral T cell lymphomas. Some of these mutations led to an increase of the affinity for CD86, GRB2 and GADS/GRAP2 with consequently increased NFκB signaling in response to CD28 stimulation [156].

3.1.8.3. The role of CD28 in $CD4^+$ T cell differentiation

Studies with CD28 deficient mice have been reported since 1993. In the first publication from Shahinian et al., CD28 deficient mice were shown to have normal numbers in B and T cells but reduced serum immunoglobulin (Ig) for the subclasses IgG1, IgG2b and a slight reduction in IgG3 [157]. In the meantime, many other and more specific cell subsets were investigated: CD28 was shown to be essential for the generation of T_{FH} cells and GC B cells [158]. The dominant ligand for this differentiation to T_{FH} is CD86 [140]. Apart from priming, maintained CD28 stimulation is also required for the differentiation and maintenance of T_H1 as well as T_{FH} cells during response to viral infection, and for the clearance of *Citrobacter rodentium* from the gastrointestinal tract [159].

As for T_H2 differentiation, King et al. reported in 1996 that CD28 deficient mice generate reduced IL-4 and IL-5 production in a *Schistosoma mansoni* infection [160]. In their study, they concluded that early CD28 signaling during $CD4^+$ T cell priming was required for the generation of a T_H2 response.

T_{reg} cell populations are reduced in CD28 deficient mice in blood, spleen and lymph nodes. Moreover, naïve CD28ko $CD4^+$ T cells show reduced de novo T_{reg} differentiation potential *in vivo* and *in vitro*, which can be rescued by addition of exogenous IL-2 [161]. This might actually explain part of the T_{reg} phenotype, because CD28 was shown to regulate IL-2 production in two different pathways: on one hand it stabilizes the mRNA

of IL-2, and on the other the activation of PI3K with subsequent nuclear localization of NFAT leads to more *IL-2* transcription [162]. FoxP3creCD28$^{fl/fl}$ mice have normal populations of T_{reg}s but show highly activated effector cells, leading to lethal autoimmunity as of 8-12 weeks of age. Addition of exogenous IL-2 could rescue for the proliferation defect of CD28 deficient T_{reg}s *in vitro*, nevertheless these T_{reg}s still showed competitive disadvantage *in vivo* and were less suppressive as compared to wild type (wt) cells [163]. Furthermore, it was shown that CD28 expression during T_{reg} maturation is essential for the generation of CD44^{hi}CD62L^{lo} effector T_{reg}s and the induction of CCR6 expression. The deficiency of CCR6 expression when CD28 was absent led to a defect in skin homing, which was partially responsible for skin inflammation in this mouse model [164].

The only subset in which CD28 co-stimulation was shown to have inhibitory effects was T_H17 differentiation. Bouguermouh et al. reported that CD28 co-stimulation reduced T_H17 polarization in comparison to αCD3 stimulus alone [165]. They then neutralized IL-2 and IFNγ with blocking antibodies and found that this restores IL-17A production even in the presence of CD28 co-stimulation, which might suggest that T_H1 response is favored by CD28 co-stimulation.

In summary, CD28 co-stimulation contributes to the polarization of different T_H subsets, however different mechanisms might come into play here and suggest a complex network of differentiation.

3.1.8.4. CD28 and metabolism

Naïve CD4$^+$ T cells only show low activity of genes that are involved in glycolysis, glutaminolysis and lipid biosynthesis. They efficiently generate ATP via glycolysis, during which glucose is metabolized to pyruvate. However, since the metabolic need in naïve cells is quite low, they also only take up low amounts of glucose [166]. Upon activation, rapid transcriptional activation of genes is initiated and essential to meet the needs for cell growth and differentiation [167, 168]. For example, as soon as the T cell gets activated, glucose intake is greatly increased in CD28 dependent manner [37]. This is mainly regulated by glucose transporter 1 (GLUT1), whose expression is low in naïve but upregulated in activated T cells [169]. Increasing glucose uptake by transgenic expression of GLUT1 also leads to more activation, which suggests glucose

as a limiting factor in activation [170]. The pyruvate that is generated via glycolysis is further metabolized in aerobic glycolysis, which leads to lactate production, or in oxidative phosphorylation.

Activated and differentiated T cells can use various pathways for their energetic supply [171, 172] and metabolize glucose, fatty acids, glutamine or arginine [173]. The rewiring of metabolic pathways upon T cell activation is regulated by distinct pathways depending on the T cell subset. For example, activation of Akt (see section 3.1.3) leads to GLUT1 upregulation [169] and consequently more glucose uptake, while ERK activation increases glutamine uptake [174].

Especially important for the initial reprogramming of metabolism in T cells are the TF c-Myc and mTORC1. mTORC1 maintains the high expression of c-Myc, which binds to promotors of glycolytic genes to induce gene expression [171, 175]. Another important TF is hypoxia induced factor 1 α (HIF1α). HIF1α drives T_H17 differentiation and sustains elevated glycolysis [176] but prevents T_{reg} generation [177]. Together with its β subunit, HIF1α binds hypoxia responsive element sequences and activates transcriptional programs that help the cell to adapt to lower oxygen availability. Upon CD28 co-stimulation, HIF1α protein is upregulated, presumably through PI3K and mTOR activity [178-180].

3.2. Gene regulation through microRNAs

3.2.1. Posttranscriptional regulation and microRNAs

A wide range of mechanisms have been established that may regulate the expression of a gene or protein. Regarding mechanisms involving RNA, we distinguish between transcriptional regulation (e.g. initiation of transcription), which refers to the regulation of the DNA to RNA transcription, and post-transcriptional regulation, which focuses on the regulation that acts directly on RNA. Posttranscriptional regulation includes all sorts of different mRNA modifications which lead to e.g. stabilization, storage or decay. In this thesis, we are especially interested in the effects of miRNAs.
MiRNAs are usually 22nt in length and were shown to have essential roles in animals [181] as well as plants [182]. They can be encoded in a host gene but also in an intron [183], often in polycistronic miRNA "clusters", so that multiple miRNAs are generated from one transcript [184]. However, this does not necessarily mean that all members of the same cluster are expressed to the same extent, since post-transcriptional mechanisms can introduce an additional regulation also for miRNAs [184, 185].
A potentially important role for miRNAs was suggested by Blevins et al. in 2015: they reported that the absence of miRNA in lymphocytes led to more variation in protein expression within a population of cells [186]. In feed forward loops, the target gene (e.g. CD69) and the targeting miRNA (miR-17 and miR-20a) are expressed simultaneously, which reduces cell to cell variation. Additionally, single cell studies show that the effect of repression can actually be very striking [187]. Mukherji et al. suggested that miRNAs introduce a threshold of target mRNA expression [187], and at this threshold great sensitivity of regulation is reached. This means that miRNAs not only can fine-tune gene expression, but also act as switches if the target mRNA is expressed at threshold levels.

3.2.2. MicroRNA biogenesis

Transcription of the miRNA results in a long primary transcript (pri-miRNA) [188] which is capped and polyadenylated [189]. This primary transcript is processed in the nucleus by key enzymes Drosha and DGCR8 into 60-70nt pieces (pre-miRNA) [190], including a stem loop. The pre-miRNA is exported to the cytosol where it is further

processed by an RNAseIII endonuclease called Dicer into double stranded RNA duplices: the miRNA and its antisense strand [191] (Figure 9).

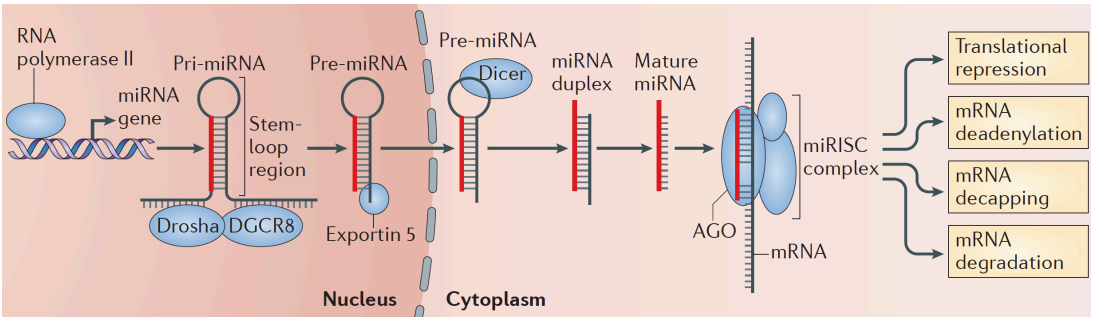

Figure 9. Canonical pathway of miRNA biogenesis (figure taken from [192])

The mature miRNA then forms an RNA induced silencing complex (RISC) with several proteins, for example Argonaute 2 (Ago2). RISC is guided by the miRNA to its targeting sequence. The major determining factor of this is the seed region of the miRNA: a 6-8nt sequence at the 5' end of the miRNA [182, 193]. Upon targeting of the mRNA, the protein expression is usually down regulated by mRNA decay or mRNA deadenylation [194-196]. Of note, one 3' untranslated region (UTR) can be targeted by more than one miRNA, which is also supported by bioinformatics predictions [197], and vice versa one miRNA family can have hundreds of targets [198].

Notably, mRNA targeting at the 3'UTR via Watson-Crick base pairing is some sort of a classical, straight-forward understanding of targets (canonical targets). Further targeting sites like the 5' end [199] of an mRNA or even non-protein coding transcripts [200] were reported. Additionally, seed-matched base pairing as a pre-requisite for miRNA function was challenged by reports about G:U wobbles and bulges in the seed region, leading to inexact pairing but preserved function [201, 202]. This introduced "non-canonical" targets to the field, which do not harbor the seed sequence of the targeting miRNA.

As for nomenclature, the field distinguishes between the same miRNA generated from different loci with numbering (e.g. miR-125b-1 and miR-125b-2). Moreover, we distinguish the sense and the antisense strand of the generated miRNA duplex, resulting in two miRNAs, a 5' and a 3' strand version (miR-17-5p and miR-17-3p). Importantly, which one finally is the more abundant ("guide" strand) and which one is less biologically active ("passenger" strand, also known as miRNA*) [203] is thought

to be determined by thermodynamic stability and Ago preference. Usually, the guide with the less stable 5' terminus is selected as the guide strand, but also Ago proteins prefer guides with a U as a starting nucleotide [204].

The miRNA biogenesis pathway described above explains the canonical pathway of miRNA biogenesis. Notably, also alternative mechanisms have been described, which are Dicer- or Drosha-independent [205, 206]. However, these non-canonical miRNAs only represent approximately 1% of the miRNAs and their functional relevance is unclear [203].

Posttranscriptional regulation by miRNAs was reported for approximately half of all protein-encoding genes [198]. It is of note that additional layers of regulation add even more complexity to the system: miRNA clusters are processed, resulting in differential expression for each cluster members [207, 208]. This suggests that actually miRNAs of the same cluster can play a role in different functions, at different time points, in different cell types, depending on their context.

Interfering with the miRNA biogenesis pathway has severe impacts on the immune system, which is was shown in several mouse models: deletion of Dicer [209] or Drosha [210] in a CD4cre-system led to multiorgan inflammatory syndrome which was most likely due to dysfunctional T_{reg} cells. Deletion of Dicer in immature thymocytes caused a severe reduction in double positive $CD4^+CD8^+$ and $CD4^+$ or $CD8^+$ single positive cells in the thymus as well as to a reduction in T cells in the periphery [209, 211]. Muljo et al. showed that T cells deficient for Dicer are biased towards T_H1 differentiation [212] due to their failure to suppress IFNγ production. The deletion of Dicer additionally also led to a reduced T_{reg} cell population, which then led to severe immunopathology [209] with splenomegaly, colitis and enlarged intestinal lymph nodes. When Dicer expression is ablated in T_{reg} cells only, the mice develop a fatal systemic autoimmune disease due to loss of their suppressive capacity [213]. DGCR8 deficiency in T_{reg} cells also led to a scurfy-like phenotype and unstable Foxp3 expression [214], supporting the concept that canonical miRNA expression is essential for functional T_{reg} control.

3.2.3. miR-17~92

While there is an overall massive increase in RNA transcription upon T cell activation, miRNA expression is globally down regulated within 12h of activation [84]. Moreover, within two days post activation the majority of all miRNA is downregulated in murine as well as human primary $CD4^+$ T cells. Further examination of key enzymes of the miRNA generation pathway showed that the expression of Ago2 was reduced, leading to a stop in miRNA processing [84]. One miRNA cluster breaking with this pattern is the expression of miR-17~92, which is induced during $CD4^+$ T cell priming with CD28 co-stimulation [140, 215, 216].

3.2.3.1. miR-17~92 and its paralogues

In mice, the miR-17~92 cluster, also known as oncomir-1 or chromosome 13 open reading frame 25 (C13orf25) [217], is encoded in the non-protein coding miR-17~92 host gene (MIR17HG) on chromosome 14. Expression of miR-17~92 was shown from early developmental stages to adult cells in different kinds of tissue, in variable amounts [218, 219]. The cluster codes for six miRNAs (miR-17, miR-18a, miR-19a, miR-20a, miR-19b, and miR-92) that can be grouped regarding their four seed families (miR-17 family, miR-18 family, miR-19 family and miR-92 family) as illustrated in Figure 10.

The cluster is highly conserved among vertebrates [184], and duplication events during evolution led to the development of two paralogue clusters miR-106a~363 cluster on the X and miR-106b~25 cluster on the fifth chromosome, which also give rise to individual miRNAs that can be grouped to the same seed families, so that from miR-17~92 and its paralogs, 15 adult miRNAs are generated [220].

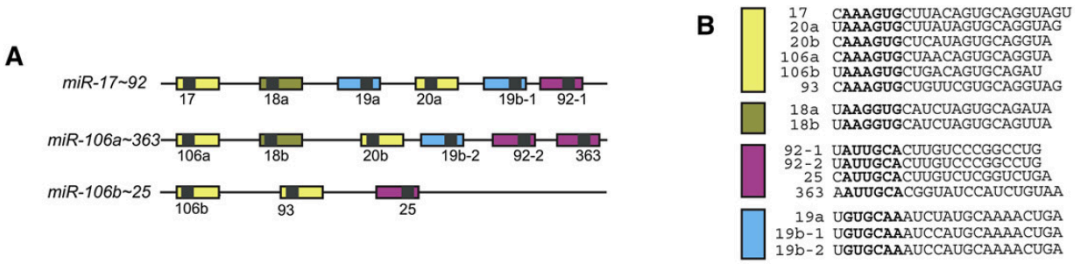

Figure 10. miR-17~92, its paralogue clusters and grouping of seed families (figure taken from [218]) A) illustrates the three paralogue clusters while B) shows the grouping of the different miRNAs of each cluster according to their common seed sequence

Germline knockout of miR-106a∼363 or miR-106b∼25 in mice was phenotypically indifferent while miR-17~92 knockout led to smaller size and perinatal lethality [218]. The combination of a knockout of miR-106b∼25 with a knockout of miR-17~92 led to an even more severe phenotype, which suggests that miR-17~92 can compensate for the loss of miR-106b∼25 and that homologous miRNA clusters that display similar expression patterns can be functionally redundant [221]. Furthermore, it was reported that there is functional cooperation between members of the miR-17~92 cluster [222].

3.2.3.2. miR-17~92 as an oncogene

The expression of miR-17~92 is known to be elevated in solid tumors and hematopoietic malignancies, e.g. in B cell lymphomas [217, 223]. Retroviral expression of miR-17~92 in a mouse B cell lymphoma model led to increased c-Myc expression and tumor formation [223]. Genetic ablation of the cluster in Myc-driven lymphomas reduces tumor cell growth [224]. This demonstrates the potential oncogenic role of miRNAs, especially miR-17~92, *in vivo*, which is also the reason why miR-17~92 is sometimes named oncomiR-1. Also vice versa, Myc induces miR-17~92 [225], and with this influences metabolism in Myc lymphoma cells [226]. In this publication, Izreig et al. show that miR-17 and miR-20 are especially important for this miR-17~92 dependent reprogramming. miR-17 targets the tumor suppressor LKB1, which regulates metabolism and cell growth through mTOR signaling [226]. However, the authors also suggest that since the effects on metabolic reprogramming by miR-17~92 are rather large, it might be that not individual metabolic genes but TFs are targeted by the miRNA cluster.

3.2.3.3. Known miR-17~92 targets in $CD4^+$ T cells

With the increasing amount of literature on miR-17~92, many roles for the expression of miR-17~92 and its targets have been reported [227, 228]. The ENCODE (Encyclopedia of DNA Elements) project provided some information on transcriptional regulation: this study with 118 TFs revealed 34 that were connected to the miR-17~92 cluster [229]. All E2Fs were shown to bind to the promoter region of miR-17~92, but in turn they are as well known to be regulated by the cluster [230], which is a good example for the action of miRNAs in autoregulatory loops.

Xiao et al. generated a mouse model in which miR-17~92 is artificially expressed in lymphocytes with hCD2-iCre [231]. This led to increased proliferation up to lymphoproliferative and autoimmune disease and premature death. In the same paper, the proapoptotic protein *BIM* (also known as Bcl-2-like protein 11, *BCL2L11*) and phosphatase and tensin homolog (*PTEN*) were suggested as targets of miR-17 and miR-19: limitation of the protein expression to one allele only led to a similar phenotype as in miR-17~92 overexpressing cells.

Among the first targets to be validated was *PTEN*, a repressor of PI3K, which is a target of miR-19a and miR-19b-1 [218]. Buckler et al. even reported that the requirement for CD28 during T cell activation is caused by the negative regulation of TCR signals by PTEN [232], which might even suggest that the induction of miR-17~92 is required for proper T cell activation, e.g. in the suppression of *PTEN*.

Jiang et al. examined the effect of miR-17~92 expression on T_H1 differentiation [208]. They showed that decreased miR-17~92 expression reduced proliferation and survival *in vitro*, and vice versa for miR-17~92 overexpression. In T_H1 differentiation, Tbet and IFNγ production were reduced in miR-17~92 knockout cells. As a mechanism, they showed that miR-19b targets *PTEN* while miR-17 targeted cAMP response element binding (*CREB1*) and transforming growth factor beta receptor II (*TGFβRII*), which facilitated effector T cell responses. Later, Wu et al. confirmed that the differentiation and expansion of T_H1 cells is diminished in $CD4^+$ T cells that are deficient for miR-17~92 expression [208, 233], and further reported that the formation of memory $CD4^+$ T cells after LCMV infection is reduced.

T_H2 differentiation is impaired in CD4cre.miR-17~92$^{fl/fl}$, while it is increased in CD4cre.miR-17~92^{tg} mice [234]. Simpson et al. showed that this was linked to miR-19a and miR-19b expression, and their targeting effect on the mRNA of *SOCS1*, *TNFAIP*, and *PTEN*.

The same pattern was reported for T_H17 differentiation [235]. However, Zhu et al. could not confirm this finding: in their hands, miR-20b expression reduced T_H17 differentiation *in vitro* and also suppressed extracerbated experimental autoimmune encephalitis (EAE) progression *in vivo* [236]. Additionally, Montoya et al. showed that miR-18a acts as an inhibitor of T_H17 differentiation by targeting *SMAD4*, *HIF1α* and *RORα* [237]. This especially interesting because these targets had been shown to be

targeted by other members of the cluster before – but in that case promoting differentiation and cytokine production. This suggests that the role of individual members of the same miRNA cluster is probably time and context dependent.

Similar to T_H17 differentiation, the reports regarding T_{reg} cells and miR-17~92 expression are controversial: Jiang et al. reported that artificial miR-17~92 expression prevents inducible T_{reg} differentiation [208]. In contrast to this, de Kouchkovsky et al. found that Foxp3cre.miR1792$^{fl/fl}$ mice were not able to control EAE [215], antigen specific T_{reg}s could not accumulate and also IL-10 production was reduced, which suggested that there is an important role for miR-17~92 in T_{reg}s as well. Interestingly, two years after this publication Yang et al. reported that CD4cre.miR1792$^{fl/fl}$ as well as Foxp3cre.miR1792$^{fl/fl}$ mice were less susceptible to EAE [238]. Moreover, they found that Foxp3cre.miR1792$^{fl/fl}$ CD4 cells were more suppressive *in vitro*. In their experiments they validated *EOS*, a Foxp3 co-regulator, as a target gene of miR-17. *EOS* was reduced upon miR-17 induction, whereas the expression of Foxp3 was unchanged. They suggested that the differences of their data in comparison to the previous study might be explained by the fact that their T_{reg}s were not deficient in IL-10 production. Another explanation could be that two distinct Foxp3cre mouse models were used, which might explain differences in the knockout specificity.

The differentiation of T_{FH} and consequently GC B cells was shown to be dependent on miR-17~92 [134]. Baumjohann et al. confirmed in this publication the contribution of *PTEN* as a miR-17~92 target to T_{FH} differentiation. However, they also showed that this gene could not be the only contributor to T_{FH} differentiation in this context and additionally proposed *RORα* as a target gene. Limiting *RORα* to one allele only also led to a partial rescue in CD4cre.miR1792$^{fl/fl}$ cells, confirming that this gene was a target of miR-17~92 in T_{FH} differentiation. *PTEN* is an inhibitor of PI3K, and PH Domain and Leucine Rich Repeat Protein Phosphatase 2 (*PHLPP2*, whose 3'UTR has one binding site for miR-17 and two for miR-92) acts on the same pathway by inactivating Akt. Using a mouse model in which miR-17~92 as well as paralogue clusters were knocked out, Kang et al. showed that knockdown of *PHLPP2* partially rescued the effect of miR-17~92 (and paralogues) knockout in T_{FH} differentiation [216]. After differentiation into T_{FH}, the expression of miR-17~92 was reported to decline [216], probably due to Bcl-6 repression [133].

Lastly, it was shown in a murine chronic graft-versus-host-disease (cGVHD) model that miR-17~92 expression in donor T and B cells is essential for the induction of scleroderma and bronchiolitis obliterans [239]. miR-17~92 enhanced the differentiation of pathogenic T_H1 and T_H17 cells as well as T_{FH} and GC B cells, which are required for the generation of autoantibody production. The systemic application of anti-miR-17 in a lupus-like cGVHD model led to a milder phenotype of disease, with reduced skin damage and T_H17 differentiation.

These partially contrasting studies from the literature exemplify the complexity of regulation with miRNAs. It is therefore difficult to pinpoint "the one and only" role of miR-17~92 in $CD4^+$ T cells. So far, we can conclude from existing studies that miR-17~92 promotes proliferation and survival, and to some extent differentiation as well as cytokine production of distinct T_H subsets. However, it also becomes increasingly clear that single targets alone cannot explain for the large number of effects that were reported [240] and that instead, the understanding of the cooperation of different miRNAs targeting different genes at the same time might lead to a global understanding. One example for this is the cooperation of different miR-17~92 members in the regulation of TGFβ signaling, with miR-17 targeting *TGFβRII* and others targeting downstream signaling molecules *SMAD2* and *SMAD4* [184, 227]. In this case, cluster members can be functionally redundant, but also act synergistically [184].

3.2.3.4. miR-17~92 in human

In humans, the miR-17~92 host gene is located at chromosome 13q31, with the transcript spanning 800bp. This genomic region is also often amplified in solid cancer and lymphomas, and the mature miRNAs are expressed in high amounts. Especially, significant overexpression of pri-mir1792 was reported in a study where 46 lymphoma samples were examined [223]. Germline deletion of miR-17~92 in humans is only reported in heterozygous manner, resulting in developmental defects reported in patients with Feingold syndrome [241]. Next to skeletal abnormalities, these patients also can show microcephaly as well as learning and developmental disabilities [227]. Moreover, also for human $CD4^+$ T cells the miR-17~92 was shown to be important: miR-19a is elevated in human $CD4^+$ T cells from asthmatic lungs. It promotes T_H2

phenotype by suppression of negative regulators of T_H2 cytokines like *PTEN*, *SOCS1*, and *A20* [234]. Moreover, miR-92a was shown to control the frequency of T_{FH} precursors in type 1 diabetes islet autoimmunity by targeting *FOXO1*, *PTEN* and *KLF2*. In a humanized mouse model, miRNA-92a antagomir application ameliorated the phenotype by lowering immune activation in the pancreas [242].

4. Aim of the project and Hypotheses

Before this thesis project was started, it was known that CD4cre.miR-17~92$^{fl/fl}$ knockout mice show a phenotype which resembles CD28ko mice, and transgenic expression of miR-17~92 in CD4$^+$ T cells led to a more activated phenotype. This led to the hypothesis that miR-17~92 might promote CD4$^+$ T cell activation. Moreover, since miR-17~92 expression was known to be induced with CD28 co-stimulation, we suggested that exogenous expression of miR-17~92 might compensate for CD28 signaling during CD4$^+$ T cell activation. If this was the case, processes which are dependent on CD4$^+$ T cell activation, e.g. proliferation and differentiation, might be rescued as well. Mechanistically, miR-17~92 target genes should be repressed in overexpressing cells and increased if miR-17~92 expression was absent. Based on these hypotheses, we defined three main aims in this project:

Aim 1: Correlate miR-17~92 expression with CD4$^+$ T cell activation

In this first part of the project, we asked:

1) Is miR-17~92 expression correlating with CD4$^+$ T cell activation?
2) Does miR-17~92 promote a metabolic checkpoint which influences activation?

Aim 2: Investigate if transgenic miR-17~92 expression rescues CD28 deficiency in CD4$^+$ T cells

The following questions were asked to specifically address this aim:

3) Can we rescue CD4$^+$ T cell activation of CD28ko cells *in vitro*, e.g. IL-2 production, proliferation, and surface activation markers?
4) Can we rescue more complex processes like CD4$^+$ T cell differentiation *in vitro*?
5) Does transgenic miR-17~92 expression rescue CD28ko CD4$^+$ T cells *in vivo*, e.g. during LCMV response in the differentiation into T_H1 and T_{FH}?

Aim 3: Identify miR-17~92 targets that explain for influences on CD4$^+$ T cell activation

In this part of the thesis, we wanted to address the molecular mechanism behind the rescue with the following questions:

6) Which are *bona fide* canonical miR-17~92 target genes in our specific system?
7) Is the CD28ko transcriptome rescued by transgenic miR-17~92 expression?
8) How does miR-17~92 promote CD4$^+$ T cell activation?
9) Can we exploit the activating effect of miR-17~92 therapeutically?

5. Mouse models and Methods

5.1. Mice

5.1.1. B6.CD4cre.miR-17~92^{lox}

In this mouse model, the miR-17~92 cluster (Mir17, Mir18, Mir19a, Mir20a, Mir19b-1, Mir92-1) is flanked by loxP sites [218]. When crossing the mouse to CD4cre mice [243], the locus is excised in all cells that do or did express CD4 (B6.CD4cre.miR-17~92^{lox}, in the following abbreviated: miR1792lox). These mice were shown to have a defect in T_{FH} differentiation during LCMV infection. In addition, CD4^{+} T cells are known to be less proliferative.

5.1.2. B6.CD4cre.Rosa26^{lox}STOP^{lox}CAG-miR-17~92Tg

For these mice, the human miR-17~92 locus was cloned into the Rosa26 locus as a transgene, preceded by a floxed stop cassette [231]. Upon crossing to CD4cre mice [243] the stop cassette is excised and all cells do or did express CD4 start to artificially overexpress the human miR-17~92 cluster (B6.CD4cre.Rosa26^{lox}STOP^{lox}CAG-miR-17~92, in the following abbreviated: miR1792tg). Transgenic overexpression of miR-17~92 was reported to induce lymphoproliferative disease and splenomegaly in ageing mice.

5.1.3. B6.CD4cre.Rosa26^{lox}STOP^{lox}CAG-miR-17-92Tg.Cd28ko(SMARTA)

We crossed CD28ko mice [157] to the B6.CD4cre.Rosa26^{lox}STOP^{lox}CAG-miR-17~92 mice. In the CD28ko mice, part of Exon 2 of the receptor was replaced by a neomycin resistance cassette so that there is very little remaining CD28 expression in all cells. The resulting strain was for some experiments additionally crossed to the SMARTA line, which expresses an MHC II restricted transgenic TCR that is specific for LCMV-glycoprotein (GP) [244].

5.2. Methods

5.2.1. Genotyping

Toes were clipped at day 10 and digested in tail lysis buffer with proteinase K for at least 3h at 55°C shaking at 600rpm. Remaining debris were pelleted and discarded, DNA was then precipitated with isopropanol (1:1 ratio) and spun down. The pellet was washed with 70% Ethanol and resuspend in dH_2O. Most genotypings were performed according to the protocols indicated at the vendors webpage. As for SMARTA genotyping, in addition to the PCR blood was taken at the time of organ harvest for the experiments and mixed with Heparin. Erythrocytes were then lysed with ACK lysis buffer for 2min. Remaining lymphocytes were washed with FACS buffer and stained for CD3, CD4, Vα2 and Vβ8.3.

5.2.2. Organ and blood isolation

Organs were obtained after CO_2 euthanization and kept on ice during processing. Mesenteric lymph nodes (LN), inguinal LN, axillary LN, brachial LN, six cervical LN and spleen were taken for most of the experiments. Spleens were injected with 0.5ml ACK lysis buffer for erythrolysis before processing. The organs were meshed with 0.4µm filters to obtain single cell suspensions which were then washed with FACS buffer.

5.2.3. Naïve $CD4^+$ T cell isolation

Naïve $CD4^+$ T cells were isolated from cell suspensions with pooled lymph nodes and spleen. Isolation was performed with StemCell mouse naïve $CD4^+$ T cell isolation kit according to manufacturer's instructions. In brief, the cell suspensions were incubated with rat serum and CD4 isolation antibody for 7.5 minutes, then with memory depletion antibody for 2.5 minutes, and in the end with magnetic beads for another 2.5min before incubating with the isolation magnet for 2.5min. The resulting untouched naïve $CD4^+$ T cells were then washed with FACS buffer, and purity was routinely checked with a staining for CD4, CD44 and viability.

5.2.4. Plate-bound $CD4^+$ T cell activation

Plates were coated over night with 0.2µg αCD28 and 0.5µg αCD3 per ml PBS for most of the experiments (low stimulation as according to [134]). Plates were washed with

PBS before plating $2*10^5$ naïve $CD4^+$ T cells per well in 96 well flat-bottom in 200µl medium. For 24 well plates, $2*10^6$ naïve $CD4^+$ T cells per ml medium were plated.

5.2.5. In vitro differentiation

T_H1 differentiation conditions were generated with 50U IL-2, 5ng/ml IL-12 and 10µg/ml αIL-4 per ml T cell medium [245]. $iT_{reg}s$ were either differentiated with or without retinoic acid (0.9mM), but always with 250U IL-2, 0.75ng/ml TGFβ, 10µg/ml αIFNγ and 10µg/ml αIL-4 [246]. T_H17 were generated with 50ng/ml IL-6, 3ng/ml TGFβ, 5µg/ml αIFNγ and 10µg/ml αIL-4 per ml T cell medium [247]. For the differentiation, $2*10^5$ naïve $CD4^+$ T cells were plated on a pre-coated 96-well flat bottom plate (coated over night with 0.2µg αCD28, 0.5µg αCD3 per ml PBS) and harvested at 24h, 48h or 72h after plating.

5.2.6. Seahorse

This protocol was adapted from our collaborators from the Hess laboratory at the Department of Biomedicine, Basel. Calibration plates were coated over night with 200µl calibrant. Cell plates were coated with 18µl 0.1M $NaHCO_3$ pH8.0 6.67% CellTak (Seahorse XF96 flux pack, Bucher Biotech, CH). The following day, cell plates were washed with H_2O and left for drying during cell preparation. Compounds were prepared for a final in-well concentration of 1µM for Oligomycin, 2µM for FCCP and 11µM for Rotenone. $CD4^+$ T cells (naïve or activated) were harvested with glucose-free, unbuffered RPMI, washed and counted multiple times before plating $3*10^5$ cells per well. Mitochondrial perturbation was performed by sequential injection of glucose (80mM stock), oligomycin, FCCP and rotenone. Measurements of oxygen consumption rate (OCR, pMoles/min) and extracellular acidification rate (ECAR; mpH/min) were performed with a Seahorse XF96 flux analyzer (Seahorse Bioscience, USA). Data analysis was performed using Prism (Version7.0d), mitochondrial parameters were calculated as described by Gubser et al.[248].

5.2.7. FACS Staining

For cytokine stainings after *in vitro* differentiation or ex vivo e.g. for IL-2 staining, cells were stimulated with 50ng/ml PMA, 500ng/ml Ionomycin and 10 µg/ml Brefeldin A (BFA) for 3h at 37°C before staining. Cells were then first stained for viability with

viability dye 780 in PBS for 20min at 4°C and then washed with PBS. Non-specific binding was blocked with αCD16/αCD32 0.5mg/ml on ice for 10min. Surface stainings were performed in FACS buffer for 20-30min at 4°C. Cell fixation was performed with Fix-Perm for 20min on 4°C (1h for LCMV experiments). Intracellular staining was done in permeabilization buffer for 1h at 4°C.

Data was acquired with an LSR Fortessa (BD) and analyzed with FlowJo (version 10.4.1)

5.2.8. Proliferation assay with cell trace violet (CTV)

Freshly isolated naïve $CD4^+$ T cells were washed with PBS. 1µl of Cell Trace stock solution (dissolved in DMSO according to the manufacturer's instructions) was then used per ml PBS for $10*10^6$ cells. Cells were incubated at 37°C for 20min, then 5x the original staining volume of normal T cell culture medium was added for 5min to remove residual dye. Cells were washed and plated in complete culture medium supplied with 50U IL-2 per ml.

5.2.9. RNA extraction for qPCR

For any experiment involving RNA, cells were washed with PBS before counting and the RNA was kept on ice during the experiments, storage at -80°C. All pipetting was performed with filter-tips and RNAse-free tubes.

$5*10^5$ cells were washed resuspend in 400µl TRIreagent. RNA isolation was then performed according to the isolation protocol from TRIreagent supplier (SIGMA). In brief, 0.1ml of 1-bromo-3-chloropropane per ml of TRI Reagent was added, samples were mixed by vigorous shaking, incubated for 15min at room temperature and then centrifuged at 12'000g for 15min at 4°C for phase separation. The aqueous phase was then mixed with 0.5 ml of isopropanol per ml of TRI Reagent used, again centrifuged for 10min for RNA precipitation. RNA was then washed with 70% Ethanol and finally resuspend in RNAse-free water. RNA concentration and purity was determined with a Nanodrop2000 Spectrophotometer (ThermoScientific).

5.2.10. RNA extraction for RNA sequencing, protein extraction and digestion for proteomics

All procedures for the extractions were performed at the facilities with materials, protocols and supervision of the facility experts.

For RNA sequencing, $2.5*10^5$ cells were washed with PBS and resuspend in 200µl TRI Reagent. RNA was extracted from Trizol-samples in the RNA sequencing facility at the Biozentrum Basel with a Zymo Direct-zol kit which includes DNAse treatment. Quality control was run with a Bioanalyzer.

For targeted proteomics, $2.5*10^5$ cells were washed with PBS and pellets were frozen on dry ice. Proteins were extracted at the proteomics facility at the Biozentrum Basel and digested for mass spectrometry with Lys-C and Trypsin. Samples were spiked with heavy labeled synthetic peptides of our RCAN3 target protein for measurement.

5.2.11. RNA sequencing data analysis

Data analysis for the RNA sequencing data was performed by Julien Roux from the Swiss Institute of bioinformatics, Department of Biomedicine, Basel. He describes his procedure as the following:

"RNA quality was assessed with a Fragment Analyzer (Advanced Analytical) and RNA-seq library preparation (Illumina Truseq stranded kit) was performed at the Genomics Facility Basel of the ETH Zurich. Sequencing was performed on an Illumina NexSeq 500 machine to produce single-end 76-mers reads. Read quality was assessed with the FastQC tool (version 0.11.5).

Reads were mapped to the mouse genome (UCSC version mm10) with STAR (version 2.5.2a) [249] with default parameters, except filtering out reads mapping to more than 10 genomic locations (outFilterMultimapNmax=10), reporting only one hit in the final alignment for multimappers (outSAMmultNmax=1) and filtering reads without evidence in the spliced junction table (outFilterType="BySJout").

All subsequent gene expression data analysis was performed using the R software (version 3.5). Read alignment quality was evaluated using the qQCReport function of the R Bioconductor package QuasR (version 1.18). Gene expression was quantified using the qCount function of QuasR [250] as the number of reads (5'ends) overlapping with the exons of each gene assuming an exon union model (using the UCSC knownGenes annotation downloaded on 2015-12-18). To quantify intronic expression levels, exonic coordinates were extended by 10 bp on each side of the exons, and for each gene the resulting read count was subtracted to the read count obtained on the whole gene (extended by 10 bp on each side).

The R Bioconductor package edgeR (version 3.24.3)[251] was used for differential gene expression analysis. Between samples normalization was done using the TMM method [252]. Only genes with CPM (counts per million reads mapped) values more than 1 in at least 4 samples (the number of biological replicates) were retained. An generalized linear model including a genotype effect, an activation effect, and a replicate effect (nested within genotype) was fitted to the raw counts (function glmFit), and differential expression was tested using likelihood ratio tests (function glmLRT). P-values were adjusted by controlling the false-discovery rate (Benjamini-Hochberg method) and genes with a FDR lower than 1% were considered differentially expressed. Gene set enrichment analysis was performed with the function camera [253] from the edgeR package (using the default parameter value of 0.01 for the correlations of genes within gene sets) using gene sets from the curated gene set collection of the Molecular Signature Database (MSigDB v6.0)[254] with special focus on KEGG [255], Biocarta and Reactome [256] gene sets. We considered only sets containing more than 10 genes and gene sets with a false discovery rate lower than 5% were considered significant."

5.2.12. Reverse transcription (RT) and quantitative PCR (qPCR)

Reverse transcription was performed with RNA extracted with TRIzol and the SIGMA MMLV kit on 1µg RNA according to the manufacturer's instructions. qPCR was run with TaqMan FAST Universal PCR master mix on an Applied Biosystems® Real-Time PCR System. 18S was used as a reference gene.

5.2.13. Glucose uptake staining with 2-NBDG

$2*10^5$ naïve $CD4^+$ T cells were washed with complete T cell medium and then incubated with complete T cell culture medium plus 50µM 2-NBDG for 30min at 37°c. 5X the original staining volume of complete T cell culture medium was then added for 5min to remove residual dye. Cells were washed again with PBS and stained for viability and surface markers before FACS analysis.

5.2.14. Cell preparation for metabolomics

$5*10^6$ $CD4^+$ T cells were washed with PBS and centrifuged several times with decreasing the volume, so that the cell pellet could be frozen. The pellets were then

shipped on dry ice to the NIH West Coast Metabolomics center for further processing and metabolomic analysis.

5.2.15. GC-MS data

Detailed information on the procedure with frozen cell pellets performed by the Metabolomics Central Service Core facility at the University of California Davis Genome Center can be found in their protocol provided in the Appendix (see section 13.2). Data analysis for the metabolomic data was performed by Julien Roux from the Swiss Institute of bioinformatics, Department of Biomedicine, Basel. He describes his procedure as the following:

"Raw data (unnormalized peak heights) were obtained from the West Coast Metabolomics Center (University of California, Davis). Normalization and differential metabolite abundance was performed similarly to the RNA-seq differential expression analysis, but instead of edgeR, the Bioconductor package limma (function eBayes with options trend=TRUE and robust=TRUE)[257] was used on the log-transformed peak heights divided by the sum of peak heights for each sample (analogous to counts-per-million values for RNA-seq analyses)."

5.2.16. Enzyme-linked immunosorbent assay (ELISA)

IL-2 ELISA was performed with the BioLegend ELISA MAX mouse IL-2 set according to the manufacturer's instructions. After the last washing step, TMB substrate was added for the readout. Absorbance was measured with an ELISA plate reader (Synergy H1 Hybrid Reader, BioTek) at 450nm as well as 570nm wavelength, and normalized to wild type controls.

5.2.17. LCMV Armstrong infection model

Mice were infected with $2*10^5$ PFU LCMV-Armstrong strain intra peritoneally with U-100 insulin syringes (0.30mm (30G) x 8mm). LCMV-Armstrong was a gift from Annaïse Jauch, Recher laboratory. Eight days post infection, the animals were euthanized with CO_2 and the spleens were harvested for staining (for gating strategy, see Appendix, Figure 40). Restimulation of splenocytes was performed in flat bottom 96 well plates with 1µg/ml LCMV-specific peptide GP-64 in comparison to polyclonal 50ng/ml PMA,

500ng/ml Ionomycin stimulation for one hour, then 10µg/ml Brefeldin A was added for another three hours before staining.

5.2.18. Histology

Spleens were embedded in cryo embedding medium and frozen on dry ice before storage at -80°C. Sections were cut at a thickness of 6µm and dried on air. Single sections were then fixed with acetone for 5min and circled with PAP pen. Staining for CD19, CD4 and GL-7 was performed in FACS buffer with αCD16/CD32 in a wet chamber overnight. Slides were then washed with PBS on a shaker for 15min before drying and mounting. Imaging was performed with a 20x objective on a Nikon Ti2 microscope.

5.2.19. Adoptive transfer with subsequent LCMV infection

Naïve SMARTA$^+$ CD4$^+$ T cells from wt, CD28ko and rescue mice were isolated transferred into CD28ko recipients. Each recipient received 1*10^5 cells in 100µl PBS i.v.. The recipients were infected with 2*10^5 PFU LCMV Armstrong i.p. two days after cell transfer. Eight days after infection, the mesenteric and peripheral LN as well as the spleen were analyzed separately for the presence of Vα2$^+$Vβ8.3$^+$ T cells as well as CD44 expression (for gating strategy, see Appendix, Figure 41). One CD28ko mouse that did not receive donor cells was used as a negative control to display the recipient-intrinsic Vα2$^+$Vβ8.3$^+$ population.

5.2.20. CsA titration

The sensitivity of CD28ko and rescue cells to compounds interfering with Ca^{2+} signaling was tested. Increasing amounts of CsA were added to the cultures during activation: 2*10^5 naïve CD4$^+$ T cells were plated in 100µl complete T cell medium in pre-coated 96 well plates. 100µl of a serial dilution of CsA were then added to result in in-well concentrations of 100ng/ml, 50ng/ml, 25ng/ml, 12.5ng/ml, 6.5ng/ml, 3.125ng/ml, 1.5625ng/ml or 0ng/ml. Cells were then activated in the presence of these CsA concentrations for 48h before harvesting and staining for viability and activation markers.

5.2.21. ImageStream

Naïve $CD4^+$ T cells were isolated and activated for 48h in the presence of 6.25ng/ml CsA as described before. They were then harvested and washed with PBS before fixation for 20min at 4°C. Intracellular staining for NFATc2 was performed in a two-step staining with first 1h at room temperature (RT) with αNFATc2 in permeabilization buffer, and subsequently 1h at room temperature (RT) with goat anti-mouse IgG1 in permeabilization buffer. Nuclei were stained with DAPI in the last 5min of incubation. Acquisition was run on an ImageStreamX Mark2 Imaging flow cytometer (Amnis), and data analysis was performed with the IDEAS software (v6.2).

5.2.22. Statistical analysis

Statistical analysis was performed with GraphPad Prism (v7.0d, Graphpad Software). No Gaussian Distribution was assumed for any of the experiments, and tests were chosen individually depending on the type of experiment. The overall statistical significance was set to 5% (α=0.05), and error bars represent standard deviation (SD). We used Kruskal-Wallis tests for most of the experiments where more than two unpaired groups were compared in one parameter (e.g. $\%Fas^+GL7^+$ population in three genotypes), followed by Dunn's multiple comparison. We used two-way Anova for experiments in which samples were in different in two parameters (e.g. $\%CD44^{hi}CD62^{lo}$ population in three genotypes activated with or without αCD28), followed by Tukey's multiple comparison.

T-test was used for the analysis of targeted proteomics (each sample compared to wt) as instructed by the facility experts.

6. Results

So far, most studies in murine lymphocytes that investigated the role of miR-17~92 in $CD4^+$ T cells focused on either the comparison between miR-17~92 knockout to wt or miR-17~92 overexpression to wt. For example, Xiao et al. showed that elevated miR-17~92 expression in lymphocytes results in lymphoproliferative and autoimmune phenotypes with increased proliferation and cytokine expression in $CD4^+$ T cells [231]. This observation led us to our first hypothesis that miR-17~92 promotes T cell activation. However, like in most of the other studies on miR-17 B6.CD4cre.miR-17~92^{lox} 92 in lymphocytes, they did not do a side-by-side comparison of these two genotypes (see section 3.2.3.3). To directly compare the effect of lack or overexpression of miR-17~92 on the activation of $CD4^+$ T cells we took advantage of previously published mouse models B6.CD4cre.miR-17~92^{lox} (miR1792lox) and B6.CD4cre.Rosa26^{lox}STOP^{lox}CAG-miR-17~92 (miR1792tg) [218, 231, 243] and used CD4cre negative littermates as wt controls.

6.1. miR-17~92 expression promotes $CD4^+$ T cell activation

6.1.1. IL-2 production and proliferation is promoted by miR-17~92 expression

To test our hypothesis if miR-17~92 expression promotes T cell activation *ex vivo*, we followed previous literature [231] and investigated IL-2 production and proliferation in a side by side comparison in $CD4^+$ T cells from miR1792lox, wt and miR1792tg mice. In order to determine intracellular IL-2 production, freshly isolated murine naïve $CD4^+$ T cells were activated with PMA and ionomycin (iono) for three hours. Already at this very early time point we found an ~0.6-fold reduced production of IL-2 in miR1792lox cells in comparison to wt, whereas miR1792tg cells showed an ~1.7-fold increase in comparison to wt cells (Figure 11A). This pattern was also true for IL-2 secretion measured by ELISA from 48h culture supernatants (Figure 11B): miR1792lox cells secreted only half of the IL-2 that was secreted by wt cells while miR1792tg secreted ~1.2-fold more. The proliferation capacity was slightly, but not significantly (probably due to small number of samples) reduced in miR1792lox as compared to wt, and slightly increased in miR1792tg in comparison to wt (Figure 11C) even in the presence

of exogenous recombinant IL-2, which is consistent with previous reports [134, 231]. The direct comparison between miR1792lox and miR1792tg shows significantly more proliferation with increased miR-17~92 expression, which suggests that miR-17~92 positively correlates with proliferation. From these results, we concluded that miR-17~92 indeed promotes IL-2 production and proliferation in murine CD4⁺ T cells.

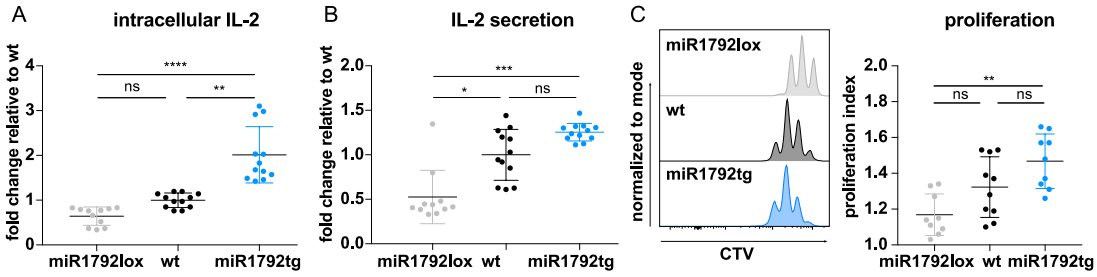

*Figure 11. miR-17~92 expression promotes IL-2 production and proliferation in CD4⁺ T cells. miR1792lox (grey), wt (black), miR1792tg (blue). Error bars show mean ±SD, Dunn's multiple comparison test, p values: ns=not significant, *<0.05 **<0.002 ***<0.0002 ****<0.0001. A) IL-2 intracellular staining in CD4⁺ T cells stimulated with PMA/Iono/BFA for 3h after isolation. Data represent four independent experiments with 3-4 biological replicates per group. B) IL-2 secretion measured by ELISA in supernatants of 48h cultured cells activated with plate-bound 0.2µg αCD28/ 0.5µg αCD3 per ml PBS for coating. Data represent four independent experiments with 3-4 biological replicates per group. C) Proliferation of CD4⁺ T cells activated for 48h with αCD3/αCD28 stimulation and 50U IL-2 per ml T cell medium. Data represent two independent experiments.*

6.1.2. miR-17~92 and metabolism in CD4⁺ T cell activation

Upon activation, CD4⁺ T cells are expected to undergo glycolytic switch [37] in a CD28-dependent manner (see section 3.1.8.4). The TF Myc which controls metabolic reprogramming in T cells [171] was also shown to induce miR-17~92 expression [225]. Izreig et al. reported that miR-17~92 expression is essential for the metabolic reprogramming of Myc⁺ tumor cells [226], and others had previously shown that metabolic checkpoints can restrict differentiation of distinct T cell subsets [258]. We therefore hypothesized that miR-17~92 expression promotes CD4⁺ T cell activation by promoting one specific metabolic pathway, leading to the passage through such a checkpoint. We examined the metabolic profile of naïve CD4⁺ T cells by metabolic flux analysis and by performing a glucose uptake assay using 2-NBDG. Glycolytic (extracellular acidification rate, ECAR) and respiratory (oxygen consumption rate,

OCR) activity of naïve CD4⁺ T cells, as determined by using a mitochondria stress test, appeared similar between genotypes (Figure 12A). There was, however, a marked difference in 2-NBDG uptake between all groups with miR1792tg T cells taking up 20% more 2-NBDG than wt cells (Figure 12B), whereas 2-NBDG uptake was proportionally lower in miR1792lox cells.

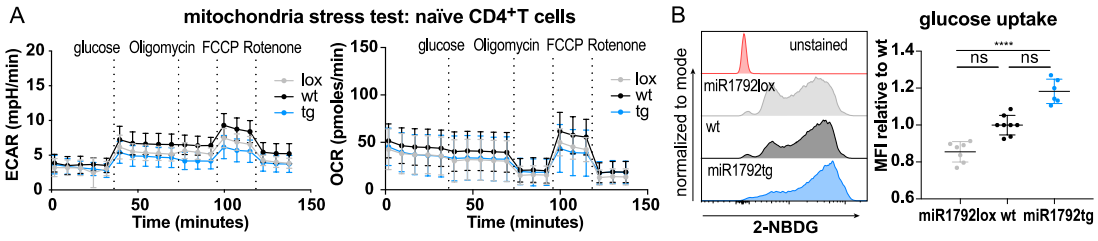

Figure 12. miR-17~92 expression modifies glucose uptake but not mitochondrial activity in naïve CD4⁺ T cells.

*miR1792lox (grey), wt (black), miR1792tg (blue) A) Mitochondria stress test measured with a 96-well seahorse in naïve CD4⁺ T cells. Eight biological replicates from two experiments are shown. left: Extracellular acidification rate (ECAR), right: Oxygen consumption rate (OCR) B) Glucose-uptake measured with 2-NBDG. red: unstained control, median fluorescence intensity of the high uptake population is compared to wt. Data represent three independent experiments. Dunn's multiple comparison test, p values: ns=not significant, ****<0.0001*

Since our previous results indicated that miR-17~92 cluster influences the outcome of CD4⁺ T cell activation, we also performed metabolic flux analysis on activated CD4⁺ T cells from all three genotypes. Activated CD4⁺ T cells that were deficient in miR-17~92 expression displayed slightly lower glycolytic rates than wt and miR1792tg T cells (Figure 13A) as well as lower basal and ATP coupled respiration (Figure 13B). These findings indicate that the miR-17~92 cluster might be involved in the regulation of metabolic reprogramming in activated CD4⁺ T cells.

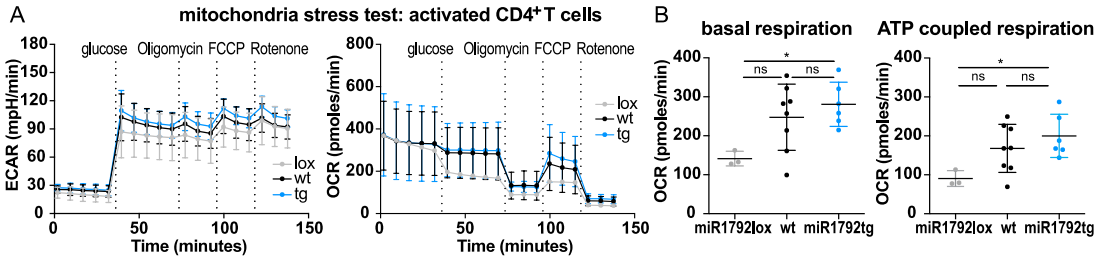

Figure 13. miR-17~92 expression modifies mitochondrial activity in activated CD4$^+$ T cells.

*A) Mitochondria stress test measured with a 96-well seahorse in 48h activated CD4$^+$ T cells. 3-8 biological replicates from four experiments are shown. Tukey's multiple comparison test, p values: *<0.0332 C) left: Extracellular acidification rate (ECAR), right: Oxygen consumption rate (OCR) B) Basal respiration (after glucose- but before oligomycin addition [248]) and ATP coupled respiration (before-after oligomycin addition [248])*

To further evaluate the metabolic profile of these cells and elucidate which pathways are influenced by miR-17~92 expression, we performed mass spectrometry-based global metabolomic analysis on activated T cell lysates. Principal component analysis (PCA) showed small differences in the metabolome between all three genotypes (Figure 14).

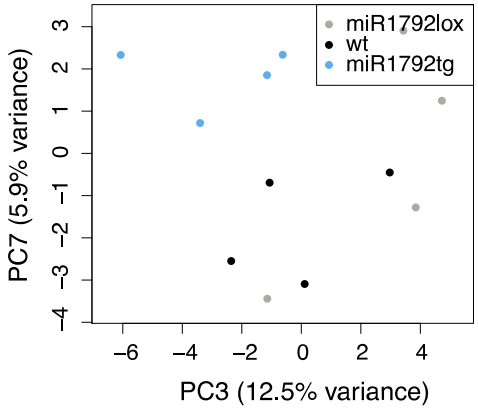

Figure 14. miR-17~92 expression introduces small differences in the metabolome of activated CD4$^+$ T cells.

CD4$^+$ T cells were activated for 48h with plate-bound αCD3 and αCD28 before harvest as described in the Methods section. miR1792lox (grey), wt (black), miR1792tg (blue)

However, direct comparison of miR1792lox and miR1792tg cells revealed only eight metabolites that were differentially abundant (minimum 2-fold change (FC), p value<0.01, logFC>1 indicates higher abundance in miR1792tg) (Table 1). Intriguingly, of the eight metabolites, seven associated with either cysteine, fatty acid or purine

metabolism. Lactic acid, which is the end-product of glycolysis, was also found to be less abundant in miR1792lox cells as compared to miR1792tg cells. This confirmed our seahorse data where miR1792lox cells showed slightly lower glycolytic rate.

Table 1. List of differentially abundant metabolites in the comparison between miR1792tg and miR1792lox.

metabolite	logFC	p-value	associated pathway
glutathione	1.8636	0.0004	cysteine
taurine	1.1961	0.0065	cysteine
lactic acid	1.1317	0.0047	glycolysis
oleic acid	-1.2940	0.0055	fatty acid
lauric acid	-1.3339	0.0012	fatty acid
arachidonic acid	-1.4744	0.0019	fatty acid
inosine	-1.6948	0.0009	purine
guanosine	-1.9344	6.70E-08	purine

For further analysis of the metabolomic data set, we took advantage of an RNA sequencing data set that we generated for the same project but will be analyzed in more detail later (see section 6.3.1). Here, we focused on samples of 48h activated $CD4^+$ T cells from miR1792lox, wt and miR1792tg mice of which we isolated total RNA for sequencing. We investigated the RNA sequencing data set for enzymes that are promoting the build-up or processing of the differentially abundant metabolites (Table 1) or metabolic pathways that are promoted. Direct target genes would be e.g. inhibitors of glycolysis, thereby possibly promoting activation of $CD4^+$ T cells following modulation of miR-17~92 expression. However, even if single metabolism-associated genes were differentially expressed, the RNA sequencing data did not show any metabolic pathway that was globally impacted by modulation of miR-17~92 expression. Moreover, changes in metabolite abundance were rather small. With this, we conclude that our data does not support the hypothesis that miR-17~92 expression promotes or represses one specific metabolic pathway during $CD4^+$ T cell activation. Instead, since we do see a slightly increased glycolytic activity, our data suggests that miR-17~92 expression might affect metabolism indirectly, i.e. by promoting a “more activated” cell phenotype which consequently is metabolically more active.

6.2. Transgenic miR-17~92 expression rescues CD28 deficiency

From the data illustrated above, and from previous publications we concluded that miR-17~92 indeed promotes T cell activation. Moreover, it promotes the processes that are known to be strongly dependent on CD28 co-stimulation, and in turn loss of miR-17~92 expression phenocopies loss of CD28 signaling. This was true for IL-2 production [162] and proliferation [259] but also more complex processes like T_{FH} differentiation [134]. Additionally, Xiao et al. had shown that miR1792tg cells proliferated more than wt cells when they received αCD3 stimulus without αCD28 co-stimulation [231]. This suggested that ectopic miR-17~92 expression does confer a co-stimulatory signal. Based on these observations, we hypothesized that miR-17~92 is part of the CD28 signaling cascade, and contributes to the essential "signal 2". To test this hypothesis, we created a new mouse model by crossing B6.CD4cre.Rosa26^{lox}STOP^{lox}CAG-miR-17~92 to CD28ko [157], resulting in B6.CD4cre.Rosa26^{lox}STOP^{lox}CAG-miR-17~92.CD28ko mice, called "rescue" in the following results. If our hypothesis holds true, we expect in this mouse model that the transgenic expression of miR-17~92 should (partially) compensate for loss of CD28 signaling. We first analyzed mesenteric lymph nodes (LN), peripheral LN, thymus, spleen and Peyer's patches of this new mouse model to determine the baseline phenotype of CD28ko and rescue in comparison to wt. We did not find any significant difference in organ size or $CD4^+$ T cell numbers, neither between CD28ko and wt nor between CD28ko and rescue (data not shown), as it had been shown for CD28 deficient mice by Shahinian et al. [157]. We furthermore stained for baseline populations of T_{FH} and T_{reg}s and also there did not find differences in CD28ko (and subsequent rescue). We therefore decided to isolate $CD4^+$ T cells to specifically test $CD4^+$ T cell activation *in vitro*.

6.2.1. Transgenic miR-17~92 expression rescues CD28 deficiency in vitro

We isolated naïve $CD4^+$ T cells from wt, CD28ko and rescue mice to investigate IL-2 and proliferation and see if the transgenic expression of miR-17~92 could compensate for the loss of this co-stimulatory signal. Following up our data on

miR1792lox/wt/miR1792tg comparisons (see Figure 11A), we stimulated CD28ko, wt and rescue cells for three hours with PMA and iono. CD28ko CD4$^+$ T cells produced half of the IL-2 amount that was measured in wt cells, while rescue cells produced ~2.5-fold more than wt (Figure 15A). This suggested that transgenic miR-17~92 could not only compensate for CD28 signaling, the transgene even led to increased production of IL-2 in the absence of CD28. Moreover, the proliferation capacity of wt clearly depended on αCD28 co-stimulation (proliferation index of wt with αCD28 1.51±0.13, without 1.28±0.07), which was expected from the literature [259], and CD28ko cells only proliferated at very basal levels (proliferation index of CD28ko with αCD28 1.17±0.07, without 1.16±0.08). However, the rescue cells proliferated like αCD3/αCD28 stimulated wt cells (Figure 15B) (proliferation index of rescue cells with αCD28 1.45±0.16, without 1.40±0.10), suggesting that transgenic miR-17~92 expression can compensate for the signal given by CD28 also for proliferation. Of note, since the proliferation experiment was performed in the presence of exogenous IL-2, this effect was unlikely to be due to differential IL-2 production.

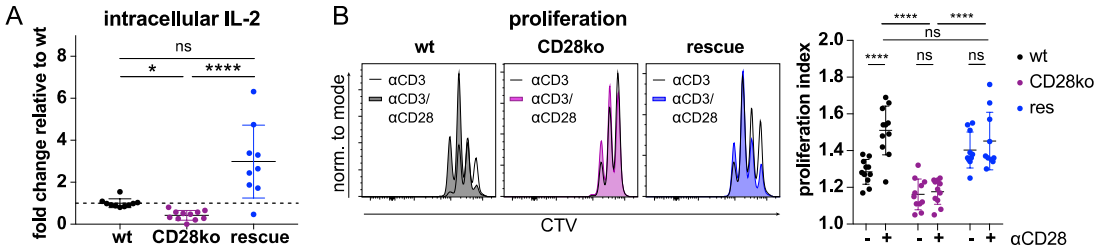

Figure 15. Transgenic miR-17~92 expression rescues IL-2 production and proliferation of CD28 deficient CD4$^+$ T cells in vitro.

*wt (black), CD28ko (purple), CD28ko with miR1792tg = rescue (dark blue). Data from three independent experiments with three to four biological replicates per group are shown. Error bars represent mean ±SD, statistical tests as indicated. A) Intracellular staining for IL-2 in viable CD4$^+$ T cells after three hours PMA/Iono/BFA stimulation. Dunn's multiple comparison test, p values: ns=not significant, *<0.05 ****<0.0001 B) Proliferation shown with CTV staining, gated on viable CD4$^+$ T cells. Left side: representative histograms of each genotype activated with (white) or without (colored) αCD28. Right: proliferation indices. Naïve CD4$^+$ T cells were stimulated for 48h with 0.5µg/ml plate-bound αCD3 with (+) or without (-) 0.2µg /ml αCD28 Tukey's multiple comparisons test, p values: ns=not significant, *<0.05 **<0.002 ***<0.0002 ****<0.0001*

We furthermore noticed that T cell blasting, another important hallmark of $CD4^+$ T cell activation, was reduced in CD28ko cell culture (microscope observation), which led us to quantify cell size by FACS. After 48h activation with αCD28 co-stimulation, the size of cells, shown as FSC-A (Figure 16), was increased in αCD28/αCD3 stimulated wt cells in comparison to samples that were stimulated with αCD3 alone (median fluorescence intensity (MFI) FSC-A of wt with αCD28 161k±12k, without 144k±9k). CD28ko cells were significantly smaller (MFI FSC-A of CD28ko with αCD28 130k±15k, without 126k±18k), and transgenic miR-17~92 expression rescued blasting of rescue cells to an extent that was comparable to αCD28/αCD3 stimulated wt cells (MFI FSC-A of rescue with αCD28 162k±11k, without 156k±16k). This indicated that also for the induction of blasting, transgenic miR-17~92 expression could compensate for the CD28 co-stimulatory signal.

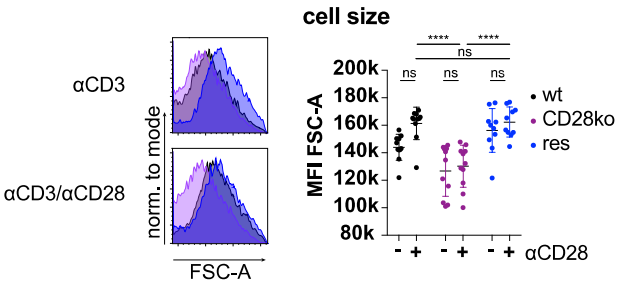

*Figure 16. miR-17~92 or CD28 signaling is essential for blasting of $CD4^+$ T cells during activation. Blasting of $CD4^+$ T cells shown as MFI of FSC-A of the lymphocyte gate. Naïve $CD4^+$ T cells were stimulated for 48h with 0.5µg/ml plate-bound αCD3 with (+) or without (-) 0.2µg/ml αCD28 Error bars represent mean ±SD, Tukey's multiple comparisons test, p values: ns=not significant, *<0.05, ****<0.0001*

Since we saw a rescue effect in IL-2 production, proliferation and blasting, we hypothesized that miR-17~92 mediated increase of cell activation could be marked by increased expression of typical early- and late surface activation markers. We therefore activated wt, CD28ko and rescue cells for 48h and stained for early activation markers CD25 and CD69. CD25, the high affinity IL-2 receptor α subunit, is essential for proper T cell activation and IL-2 uptake [79, 260] and known to be CD28 dependent. All genotypes and conditions developed similar percentages of $CD69^+CD25^+$ populations (Figure 17A). CD69 expression was not significantly changed among all conditions and genotypes, which was expected from the literature since it

is dependent on TCR signaling [117]. In contrast, the MFI of CD25 was strongly dependent on CD28 signaling (MFI CD25 of wt with αCD28 15.6k±2.7, without 10.9k±2.7k; CD28ko with αCD28 7.5k±2.6k, without 6.9k±3k) and rescued to wt MFI by transgenic miR-17~92 expression (MFI CD25 of rescue with αCD28 16.3±2.3k, without 15.9k±2.6k).

We additionally stained for "late" activation markers CD44/CD62L: while naïve cells show a CD44^{lo}CD62L^{hi} phenotype, activated cells are expected to express high CD44 but low CD62L. αCD28/αCD3 stimulated wt cells showed a significant increase in their CD44^{hi}CD62L^{lo} population (%CD44^{hi}CD62L^{lo} of wt with αCD28 25.4±9.9%, without 13.5±5.6%) as compared to αCD3 stimulation alone (Figure 17B), and CD28ko cells resembled αCD3 stimulated wt cells (%CD44^{hi}CD62L^{lo} of CD28ko with αCD28 8.5±5.2%, without 9.2±5.5%). However, exogenous miR-17~92 expression led to even higher percentages of CD44^{hi}CD62L^{lo} populations (%CD44^{hi}CD62L^{lo} of rescue with αCD28 38.5±10.4%, without 36.3±8.9%) in rescue cells as compared to wt.

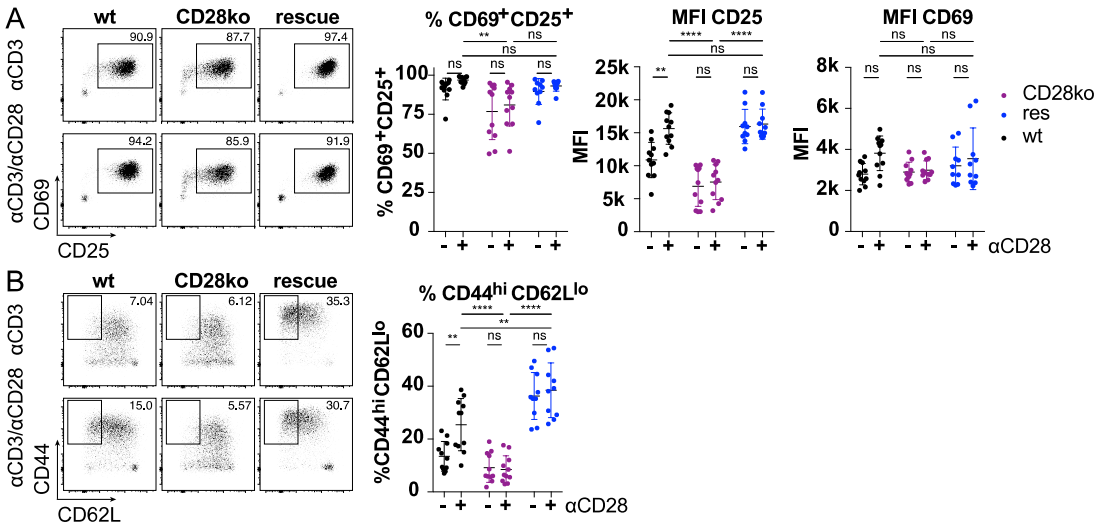

*Figure 17. miR-17~92 or CD28 signaling is essential for CD44 and CD25, but not for CD69 upregulation. Naïve CD4$^+$ T cells were stimulated for 48h with 0.5µg/ml plate-bound αCD3 with (+) or without (-) 0.2µg/ml αCD28. Tukey's multiple comparisons test, p values: ns=not significant, **<0.002 ***<0.0002 ****<0.0001 A) representative dot plots of early activation markers CD25/CD69 expression gated on viable CD4$^+$ T cells, gate marks CD25$^+$/CD69$^+$ population. left diagram: percentage of CD25$^+$/CD69$^+$ population, middle: MFI of CD25 in the CD25$^+$/CD69$^+$ population, right: MFI of CD69 in the CD25$^+$/CD69$^+$ population B) representative dot plots of CD44/CD62L expression gated on viable CD4$^+$ T cells, gate marks CD44^{hi}/CD6L^{lo} population. right: percentage of CD44^{hi}/CD62L^{lo} population*

Collectively, these *in vitro* activation experiments demonstrate that exogenous miR-17~92 expression can compensate for CD28 signaling in IL-2 production, proliferation, blasting and activation markers.

6.2.2. Exogenous miR-17~92 expression compensates for CD28 deficiency during in vitro differentiation

The miR-17~92 cluster was reported to promote the differentiation of T_H1 [208, 233], T_H2 [234] and T_H17 [235] cells, but inhibit iT_{reg} generation [208]. Moreover, CD28 was shown to be important for the same differentiation processes. This led us to hypothesize that transgenic miR-17~92 expression might also compensate for CD28 signaling during early differentiation. We therefore performed differentiation assays with wt, CD28ko, rescue and miR1792tg cells and analyzed the development of T_H1, T_H17 and iT_{reg} subsets during very early time points of differentiation.

When we investigated T_H1 differentiation (Figure 18), we found that already at 24h after plating in T_H1 skewing conditions, Tbet upregulation was induced in wt, but almost absent in CD28ko cells. Transgenic expression of miR-17~92 over compensated for Tbet induction in rescue cells, and miR1792tg cells showed similar percentages (wt 13.0±8.4%, CD28ko 3.3±3.1%, rescue 21.2±8.8%, miR1792tg 25.9±5.0% at 24h). At 48h, however, also CD28ko cells induced Tbet, even though not as efficiently as wt, while rescue and miR1792tg were still higher in Tbet expression as compared to wt (wt 60.0±26.3%, CD28ko 48.8±13.6%, rescue 71.3±14.2%, miR1792tg 77.5±18.1% at 48h). Until 72h post differentiation induction, all genotypes expressed similar percentages of Tbet (wt 80.5±7.8%, CD28ko 74.5±4.4%, rescue 74.9±6.2%, miR1792tg 78.3±3.4% at 72h) which suggested that Tbet induction is delayed in CD28ko cells, and rescued by transgenic miR-17~92 expression. IFNγ production was very low at 24h in all genotypes, however already at 48h post induction IFNγ production was induced in wt cells. This was almost absent in CD28ko, and over compensated in rescue cells while miR1792tg cells expressed the most IFNγ (wt 5.1±5.7%, CD28ko 1.2±1.5%, rescue 23.4±10.9%, miR1792tg 35.5±12.9% at 48h). In contrast to Tbet induction, CD28ko cells were not able to reach wt IFNγ induction at 72h, while rescue and miR1792tg continued to express more IFNγ as compared to wt cells (wt 12.7±4.3%, CD28ko 9.1±5.6%, rescue 27.3±6.2%, miR1792tg 38.4±9.6% at 72h). From this data we

concluded that miR-17~92 promotes different aspects of T_H1 differentiation, which confirms published data [208]. Importantly, the same processes are regulated by CD28 expression as well. Consequently, exogenous miR-17~92 expression rescued of delayed Tbet expression as well as IFNγ production in CD28ko cells.

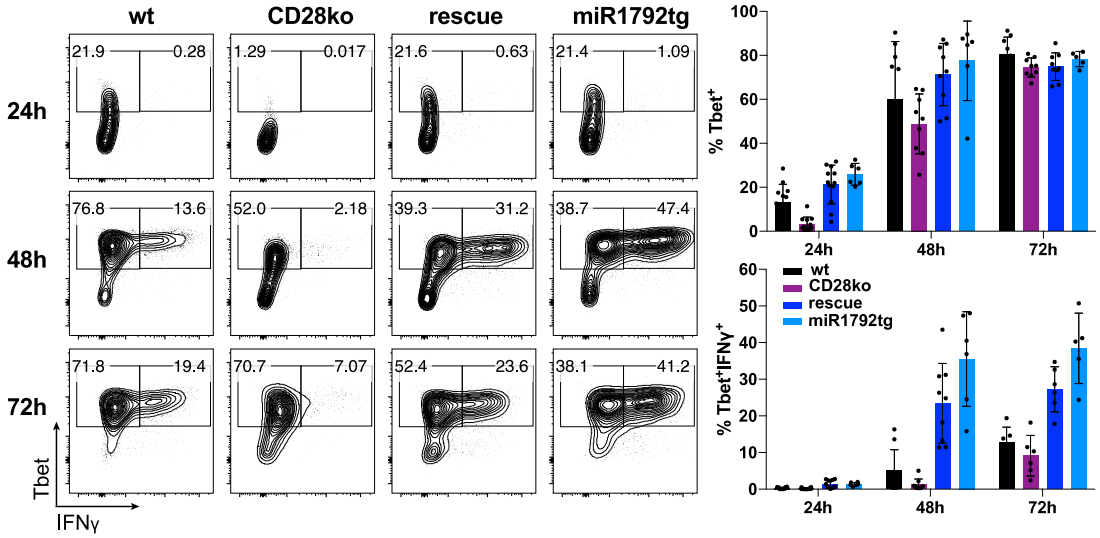

Figure 18. Transgenic miR-17~92 expression over compensates for CD28 signaling during in vitro T_H1 differentiation.

Naïve $CD4^+$ T cells were activated for 24h, 48h, and 72h with plate-bound antibodies (0.2µg/ml αCD28 0.5µg/ml αCD3) in the presence of skewing conditions for the generation of T_H1 (50U IL-2, 5ng/ml IL12 and 10µg/ml αIL4 per ml T cell medium). wt *(black, left), CD28ko (purple, second from left), rescue (dark blue, second from right) and miR1792tg (light blue, right). Data from two independent experiments are shown, with representative FACS plots of each timepoint and genotype. Error bars show mean ±SD, no statistical analysis was performed due to large variation. T_H1 differentiation was stained with IFNγ and Tbet in viable $CD4^+$ T cells, $Tbet^+$ cells include both gates while $Tbet^+IFNγ^+$ are shown in the right gate only*

Next, we investigated T_H17 differentiation (Figure 19). In contrast to T_H1 differentiation, induction of lineage-defining TF Rorγt induction was reduced in CD28ko but only partially rescued by exogenous miR-17~92 expression at 24h. Moreover, miR1792tg cells phenocopied CD28ko cells (wt 45.6±9.7%, CD28ko 32.7±4.4%, rescue 38.9±6.6%, miR1792tg 31.9±8.1% at 24h). Interestingly, Rorγt induction of CD28ko cells was reduced also in following time points, and partially rescued at 48h. In addition, the miR1792tg cells resembled wt cells in their Rorγt induction (wt 80.7±7.8%, CD28ko 31.1±8.9%, rescue 51.8±10.0%, miR1792tg 85.3±12.2% at 48h). At 72h post induction, Rorγt expression was still reduced in

CD28ko cells in comparison to wt and miR1792tg, but fully rescued by transgenic miR-17~92 expression (wt 69.3±14.0%, CD28ko 41.4±8.7%, rescue 67.8±14.6%, miR1792tg 76.7±12.5% at 72h). Similar to T_H1 differentiation, cytokine production only started at 48h. Wt produced IL-17A, while CD28ko cells were deficient and only partially rescued by transgenic miR-17~92 expression while miR1792tg cells phenocopied rescue cells (wt 9.9±3.8%, CD28ko 2.0±0.6%, rescue 5.4±1.0%, miR1792tg 5.4±0.8% at 48h). All genotypes produced IL-17A at 72h, however CD28ko cells still produced less IL-17A in comparison to wt, which was only partially rescued by transgenic miR-17~92 expression. Interestingly, miR1792tg cells resembled wt cells (wt 14.3±3.7%, CD28ko 5.9±2.8%, rescue 8.7±2.3%, miR1792tg 12.9±1.0% at 72h). We therefore concluded that for *in vitro* T_H17 differentiation, exogenous miR-17~92 expression can only partially compensate for CD28 signaling. Intriguingly, in this T cell subset the timing

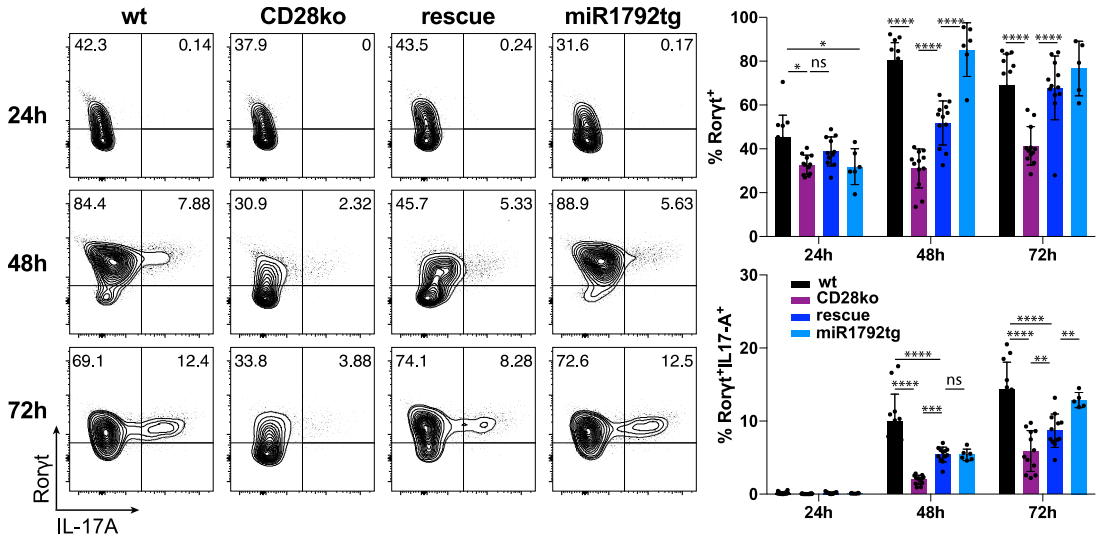

Figure 19. Transgenic miR-17~92 expression can partially compensate for CD28 signal during in vitro T_H17 differentiation.

*Naïve $CD4^+$ T cells were activated for 24h, 48h, and 72h with plate-bound antibodies (0.2µg/ml αCD28 0.5µg/ml αCD3) in the presence of skewing conditions for the generation T_H17 (50ng/ml IL6, 3ng/ml TGFβ, 5µg/ml αIFNγ and 10µg/ml αIL4 per ml T cell medium). wt (black, left), CD28ko (purple, second from left), rescue (dark blue, second from right) and miR1792tg (light blue, right). Data from two independent experiments are shown, with representative FACS plots of each timepoint and genotype. Error bars show mean ±SD, Tukey's multiple comparison, p values: ns, not significant, *<0.005, **<0.002, ***<0.001, ****<0.0001. T_H17 were stained for IL-17A and Rorγt in viable $CD4^+$ T cells, $Rorγt^+$ include the two top quadrants while $Rorγt^+IL17A^+$ cells are represented in the top right quadrant only.*

seems to be very relevant for the role of the cluster. Our experiments confirm published data that miR-17~92 overexpression prevents T_H17 differentiation [237] in early stage of *in vitro* differentiation, however in our setting at later time points the inhibitory effect is lost.

Finally, we performed iT_{reg} differentiation (Figure 20). At 24h post induction, the population of $Foxp3^+CD25^+$ cells was massively reduced in the CD28ko samples in comparison to wt, which was fully rescued by exogenous miR-17~92 expression. miR1792tg cells were similar to wt and rescue cells (wt 34.7±5.3%, CD28ko 16.2±3.2%, rescue 34.8±4.5%, miR1792tg 34.0±6.8% at 24h). Differentiation was increased in all genotypes at 48h, however CD28ko samples still showed reduced $Foxp3^+CD25^+$ populations in comparison to all other samples (wt 77.2±9.2%, CD28ko 42.4±11.0%, rescue 76.8±4.9%, miR1792tg 81.6±14.0% at 48h).

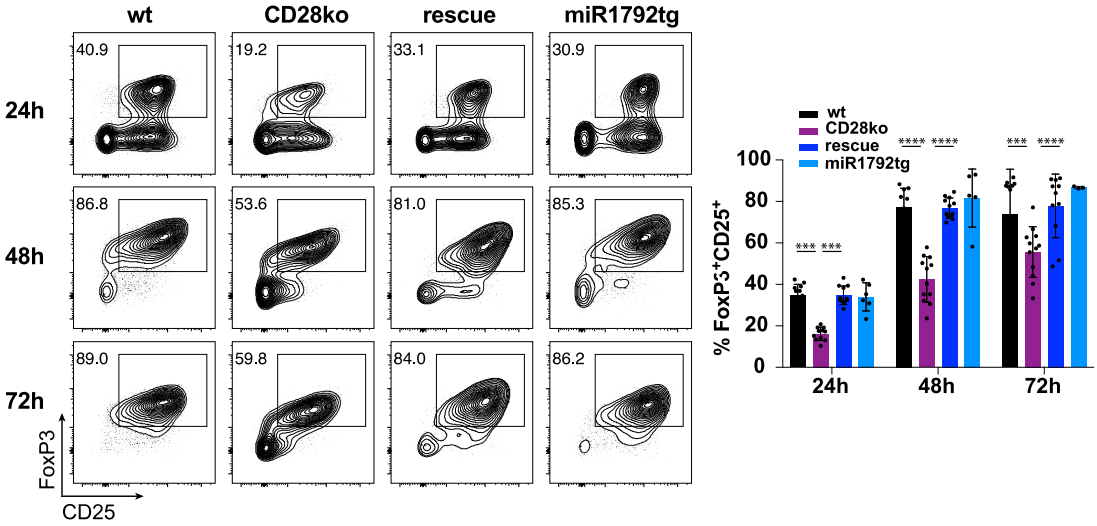

Figure 20. Transgenic miR-17~92 expression can compensate for CD28 signal during in vitro iT_{reg} differentiation.

*Naïve $CD4^+$ T cells were activated for 24h, 48h, and 72h with plate-bound antibodies (0.2µg/ml αCD28 0.5µg/ml αCD3) in the presence of skewing conditions for the generation of iT_{reg} (250U IL-2, 0.75ng/ml TGFβ, 10µg/ml αIFNγ and 10µg/ml αIL4 plus 0.9mM retinoic acid). wt (black, left), CD28ko (purple, second from left), rescue (dark blue, second from right) and miR1792tg (light blue, right). Data from two independent experiments are shown, with representative FACS plots of each timepoint and genotype. Error bars show mean ±SD, Tukey's multiple comparison, p values: ns, not significant, ***<0.001, ****<0.0001. Gate represents $FoxP3^+CD25^+$ iT_{reg}s*

While wt, rescue and miR1792tg stayed at high percentages at 72h post induction, CD28ko cells further increased their population (wt 73.8±21.7%, CD28ko 55.6±12.2%,

rescue 77.9±15.3%, miR1792tg 86.7±0.6% at 72h). We concluded that the induction of Foxp3$^+$CD25$^+$ differentiation is delayed in CD28ko cells, but can be fully rescued by transgenic miR-17~92 expression.

For the analysis of differentiation of T_H subsets and iT_{reg}s, we had pre-gated on viable CD4$^+$ cells. Interestingly, when we investigated the viability of cells in all of these subsets, we additionally found time-, genotype- and subset specific differences: in T_H1 differentiation, viability was comparable among genotypes at each time point. In contrast, during T_H17 differentiation at 72h CD28ko cells were markedly reduced in their viability as compared to wt cells. This was partially rescued by transgenic miR-17~92 expression, and miR1792tg cells were similar to wt cells (viability in T_H17 differentiation wt 63.1±9.1%, CD28ko 29.4±6.2%, rescue 50.3±8.3%, miR1792tg 62.8±17% at 72h) (Figure 21, middle). The same pattern could be observed in iT_{reg} differentiation: CD28ko cells showed reduced viability in comparison to wt, while transgenic miR-17~92 partially rescued viability (though not significantly, which again

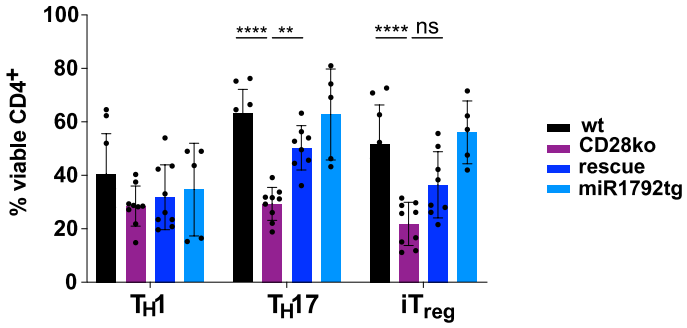

Figure 21. CD4$^+$ viability is decreased in CD28ko cells at 72h post differentiation induction in T_H17 and iT_{reg} differentiation

*Naïve CD4$^+$ T cells were activated for 72h with plate-bound antibodies (0.2µg/ml αCD28 0.5µg/ml αCD3) in the presence of skewing conditions for the generation of T_H1 (50U IL-2, 5ng/ml IL12 and 10µg/ml αIL4 per ml T cell medium), T_H17 (50ng/ml IL6, 3ng/ml TGFß, 5µg/ml αIFNγ and 10µg/ml αIL4 per ml T cell medium) and iT_{reg} (250U IL-2, 0.75ng/ml TGFß, 10µg/ml αIFNγ and 10µg/ml αIL4 plus 0.9mM retinoic acid). wt (black, left), CD28ko (purple, second from left), rescue (dark blue, second from right) and miR1792tg (light blue, right). Data from two independent experiments are shown, with representative FACS plots of each timepoint and genotype. Error bars show mean ±SD, Tukey's multiple comparison, p values: ns, not significant, *<0.005, **<0.002, ****<0.0001.*

might be due to sample size) and miR1792tg cells were comparable to wt cells (viability in iT_{reg} differentiation wt 57.5±14.6%, CD28ko 21.9±8.1%, rescue

36.5±12.4%, miR1792tg 56.1±11.7% at 72h) (Figure 21, right). This data suggests that in addition to subset-specific induction of TFs and cytokines, miR-17~92 is important for survival at later time points as well as it was demonstrated before [261]. However, since at early time points no difference was seen among genotypes in any of the subsets, this also suggests that survival cannot account for differences in the outcome of early differentiation assays.

Overall we found a defect for differentiation of CD28ko cells in all tested T cell subsets and could observe a partial or complete rescue effect by transgenic miR-17~92 expression. However, timing and extent of rescue varied between subsets: while T_H1 was even promoted in comparison to wt in rescue cells, T_H17 differentiation was only partially rescued and iT_{reg} differentiation was fully rescued to wt percentage. We concluded from these experiments that exogenous miR-17~92 expression rescues T_H1, T_H17 and iT_{reg} differentiation partially in the absence of CD28 stimulation, but the relative contribution is variable and context dependent. Moreover, since all of the tested subsets were affected, these results suggested that there might be targets of miR-17~92 that are common among different T_H subsets.

6.2.3. Transgenic miR-17~92 expression rescues CD28 deficiency in $CD4^+$ T cells in vivo

For an adaptive immune response, not only the secretion of cytokines by T_H subsets is important, but also the specialized help of T_{FH} to B cells, which is strongly dependent on CD28 co-stimulation [140] as well as miR-17~92 expression [134]. We therefore hypothesized that deficient T_{FH} differentiation in CD28ko mice could be rescued by transgenic miR-17~92 expression. To investigate the generation of T_{FH} and T_H1 responses *in vivo* we infected our mice with LCMV Armstrong. This virus strain is known to elicit an acute viral infection, causing T_{FH} and T_H1 differentiation, and is usually cleared by day eight post infection [262]. We infected wt, CD28ko and rescue mice and analyzed the spleens eight days post infection. In line with our *in vitro* data (Figure 17B), we observed a decreased CD44 expression in CD28ko $CD4^+$ T cells in comparison to wt cells, which was rescued by transgenic miR-17~92 expression (wt 67.5±14.8%, CD28ko 19.1±8.8%, rescue 40.2±13.6%) (Figure 22).

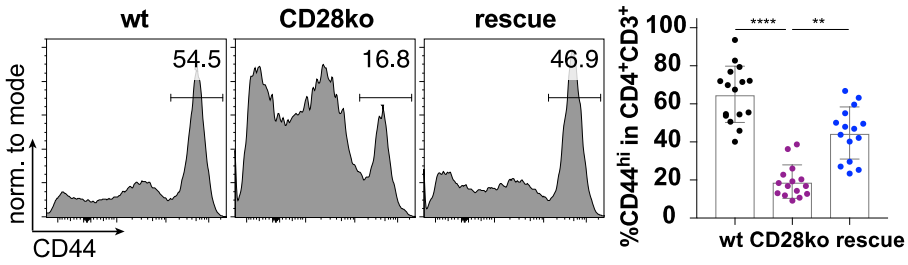

*Figure 22. CD44 upregulation in CD4$^+$ T cells is rescued by transgenic miR-17~92 expression in vivo six to eight weeks old mice were infected with 2*10^5 PFU LCMV Armstrong i.p. and spleens were analyzed at day eight post infection. wt (black, left), CD28ko (purple, middle), CD28ko with transgenic miR-17~92 expression= rescue (dark blue, right). left: representative histograms of CD44 expression gated on viable CD3$^+$CD4$^+$ cells, gate shows CD44^{hi} population. right: data summary of %CD44^{hi} population. Error bars represent mean ±SD, Dunn's multiple comparison test, p values: ns=not significant, *<0.05, **<0.002, ***<0.0002, ****<0.0001. Data represent four independent experiments with four mice per group.*

To identify T_{FH} we used key markers Bcl-6, ICOS, CXCR5 and PD-1 (Figure 23A). CD28ko mice showed a 5-fold reduced population in comparison to wt mice, which was rescued by transgenic miR-17~92 expression in Bcl-6/ICOS (wt 7.5±2.7%, CD28ko 1.1±0.7%, rescue 5.7±5.1%) as well as CXCR5/PD1 expression (wt 6.2±3.8%, CD28ko 1.3±0.8%, rescue 5.8±5.4%), independent from marker combination.

T_{FH} are essential for the formation of GC and the differentiation of GC B cells which are characterized by GL-7 and Fas expression. Consequently, also GC formation is strongly dependent on the CD28 co-stimulatory signal [140], therefore we investigated if GC B cells are rescued as a secondary effect of rescued T_{FH} cells. We observed a significantly reduced population of GC B cells in CD28ko as compared to wt mice, which was rescued with transgenic miR-17~92 expression (Figure 23B) (wt 8.0±2.3%, CD28ko 3.4±1.0%, rescue 6.9±3.7%). This was also visually apparent in histological staining (Figure 23C), where we stained cryo-sections of spleens for CD4 and CD19 to distinguish B and T cell zones and then identified GC B cells as GL-7$^+$. From this, we concluded that the T_{FH} population is rescued in their function, i.e. GC B cell formation and structural organization of the GC.

To test for T_H1 differentiation we used GP-64, a peptide with the immunodominant epitope of LCMV-Armstrong [263, 264], for restimulation. Tbet expression was 2-fold reduced in CD28ko as compared to wt cells but not significantly increased in rescue

cells (wt 23.2±14.4%, CD28ko 6.6±4.5%, rescue 17.8±14.3%) (Figure 24A, B). However, IFNγ production was 5-fold reduced in CD28ko in comparison to wt and fully restored by transgenic miR-17~92 expression (wt 9.4±4.2%, CD28ko 2.1±0.7%, rescue 7.9±3.4%)(Figure 24A, C). The ratio of IFNγ producing cells to total Tbet expressing cells was similar among all genotypes (Figure 24D), suggesting that if a CD28ko cell expresses Tbet, it also produces IFNγ. This demonstrates that in CD28ko cells, differentiation is blocked at the TF, rather than at the cytokine production level. As a control, we also used non-specific restimulation with PMA and iono, which resulted in the same pattern (data not shown).

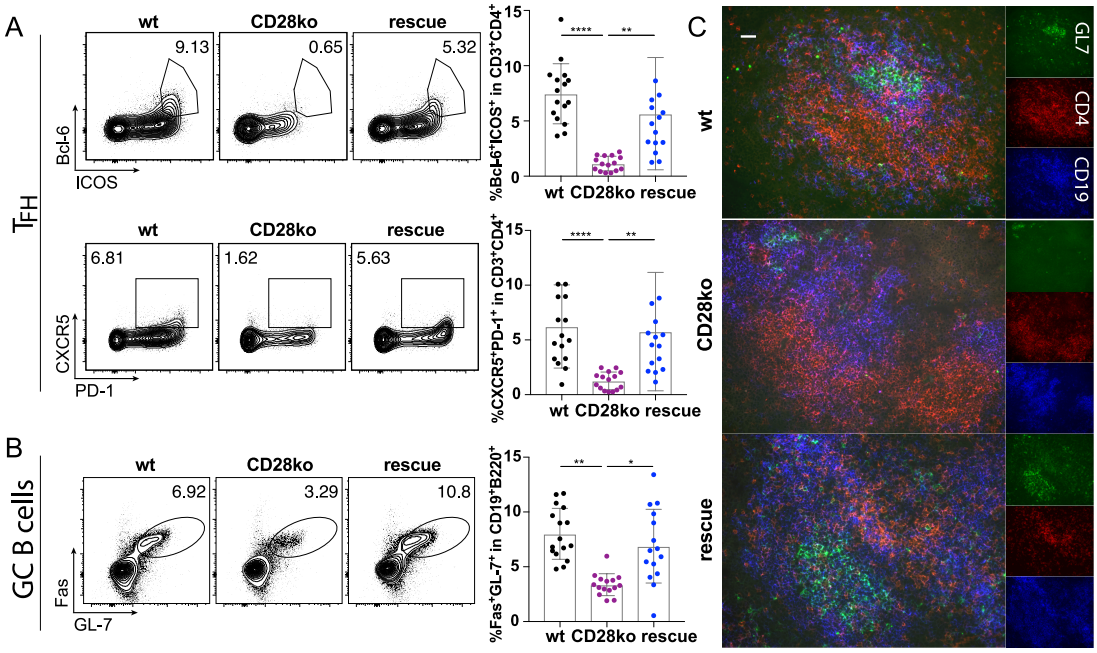

Figure 23. T_{FH} differentiation and function in CD28ko mice is rescued by transgenic expression of miR-17~92

*six to eight weeks old mice were infected with 2*10^5 PFU LCMV Armstrong i.p. and spleens were analyzed at day eight post infection. wt (black, left), CD28ko (purple, middle), CD28ko with transgenic miR-17~92 expression= rescue (dark blue, right). Error bars represent mean ±SD, Dunn's multiple comparison test, p values: ns=not significant, *<0.05, **<0.002, ***<0.0002, ****<0.0001. Data represent four independent experiments with four mice per group. A) T_{FH} population was stained with Bcl-6, ICOS, CXCR5 and PD-1, pre-gating on viable CD4$^+$CD3$^+$ cells. top row: representative contour plots of T_{FH} markers Bcl-6 and ICOS, gate shows Bcl-6$^+$ICOS$^+$ population. Bottom row: representative contour plots of T_{FH} markers CXCR5 and PD-1, gate shows CXCR5$^+$PD-1$^+$ population B) Germinal center B cells were stained with Fas and GL7, pre-gating on viable CD19$^+$B220$^+$ cells. Left: representative contour plots of Fas and GL7 expression, gate shows Fas$^+$GL7$^+$ population. C) Cryosections of spleens stained for GL-7 (green), CD4 (red) and CD19 (blue). White scale bar indicates 40µm*

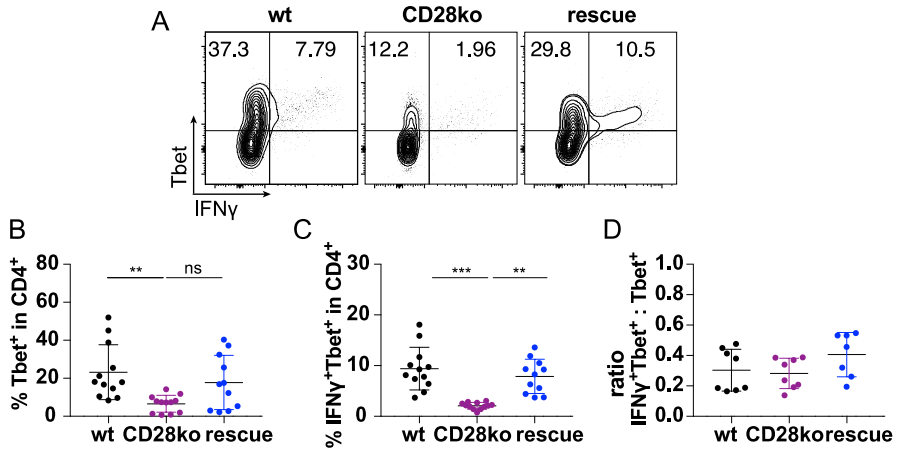

Figure 24. T_H1 differentiation during acute LCMV infection is rescued by transgenic miR-17~92 expression.

*six to eight weeks old mice were infected with $2*10^5$ PFU LCMV Armstrong i.p. and spleens were analyzed at day eight post infection. wt (black, left), CD28ko (purple, middle), CD28ko with transgenic miR-17~92 expression= rescue (dark blue, right) T_H1 response was addressed with restimulation of total splenocytes with GP-64 and BFA for 4h. Pre-gating on viable $CD3^+CD4^+$ cells. Top: representative contour plots of Tbet and IFNγ expression, bottom left: percentage of $Tbet^+$ cells (top quadrants in the plots), bottom middle: percentage of $Tbet^+IFNγ^+$ (top right quadrants of the plots) bottom right: ratio of $Tbet^+IFNγ^+$ to total $Tbet^+$ cells. Shown are three independent experiments with four samples per group. Error bars represent mean ±SD, Dunn's multiple comparison test, p values: ns=not significant, *<0.05, **<0.002, ***<0.0002, ****<0.0001.*

Collectively, our data suggested dose-dependent effects for many of the examined parameters. Therefore, we additionally performed experiments to compare these genotypes to miR1792lox, miR1792tg and heterozygous rescue mice (Figure 25). Heterozygous rescue mice are full knockout for CD28, but only express one allele of the miR-17~92 transgene (hetrescue). In these experiments, we found that again miR1792lox phenocopied CD28ko mice, which was expected from the literature [134]. Furthermore, we confirmed published data that miR1792tg mice display increased T_{FH} differentiation. In addition to increased T_{FH} population in relative numbers, we noted a miR-17~92 and CD28 expression dependent increase in PD-1 and ICOS upregulation in the total $CD4^+CD3^+$ population. This is presumably an effect of increased T cell activation, leading to induction of ICOS [265] as well as PD-1 expression [266]. Interestingly, heterozygous expression of the miR-17~92 transgene was sufficient to rescue T_{FH} and GC differentiation. As for T_H1 differentiation, we noted a non-significant trend that also this compartment is rescued.

Importantly, we addressed the viral clearance at day eight post infection in lung, liver, kidney and spleen [267]. Viral clearance was not affected by CD28 deficiency or miR-17~92 transgenic expression and the virus was fully cleared in all organs of all genotypes. This is consistent with literature that showed that viral clearance at this time point is CD8 mediated and CD28 independent [268]. Thus, we excluded viral clearance as a possible confounding factor.

Taken together, we concluded that also *in vivo* transgenic miR-17~92 expression rescues known defects of CD28ko cells, namely T_{FH} and GC B cell differentiation. While homozygous expression of the transgene rescued T_{FH} and GC as well as T_H1 formation, heterozygous expression was also sufficient for the rescue of T_{FH} and GC B cells but not for T_H1 formation.

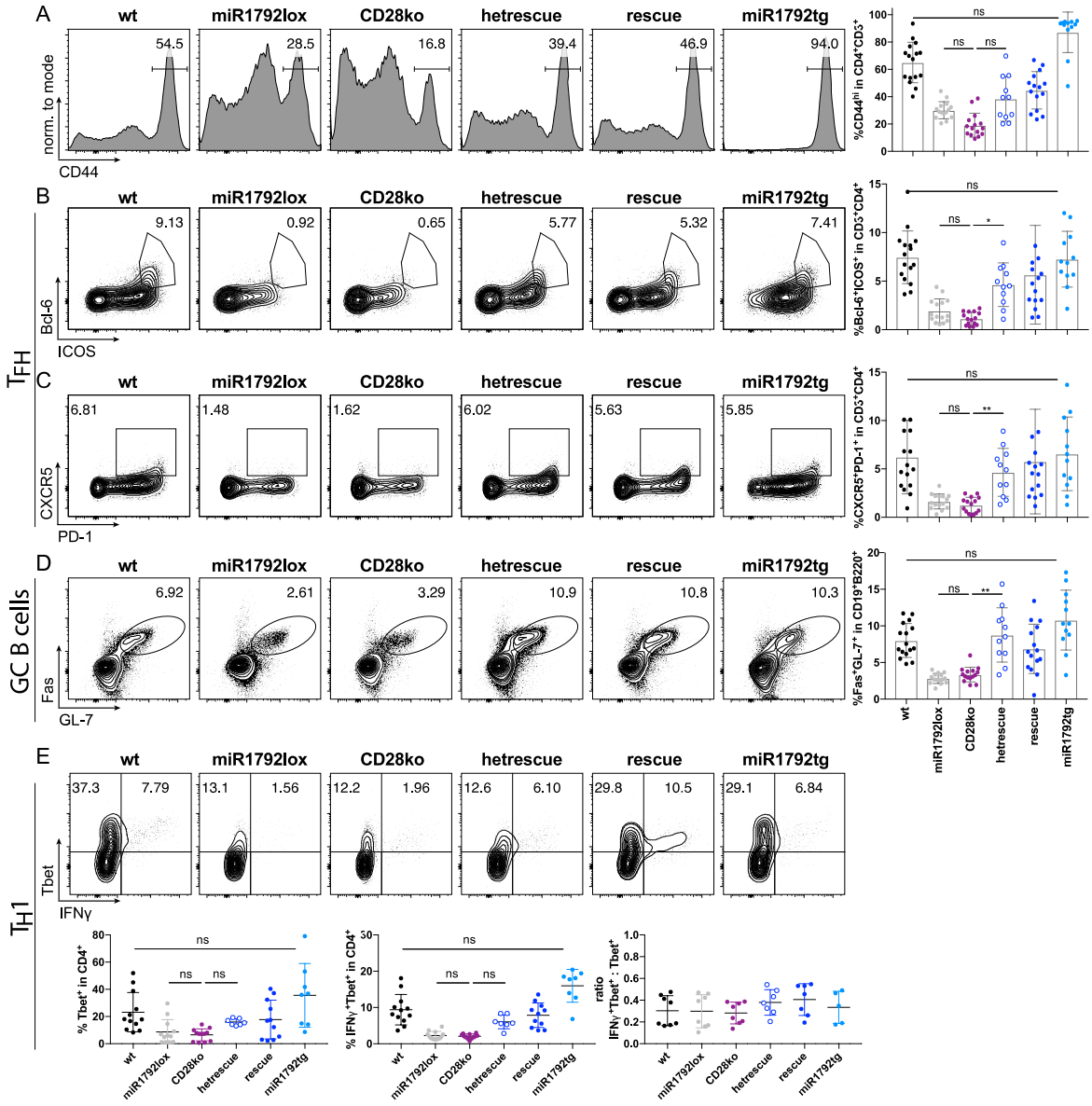

Figure 25. T_{FH} and T_H1 differentiation after LCMV Armstrong infection in wt, miR1792lox, CD28ko, hetrescue, rescue and miR1792tg mice

*six to eight weeks old mice were infected with $2*10^5$ PFU LCMV Armstrong i.p. and spleens were analyzed at day eight post infection. wt (black, left), miR1792lox (grey, second from left), CD28ko (purple, third from left), CD28ko with only one allele transgenic miR-17~92 expression= hetrescue (dark blue empty circles, third from right), CD28ko with homozygous transgenic miR-17~92 expression= rescue (dark blue, second from right), miR1792tg (light blue, right). Error bars represent mean ±SD, Dunn's multiple comparison test, p values: ns=not significant, *<0.05, **<0.002. Data represent four independent experiments (two for restimulation) with four mice per group. A) representative histograms of CD44 expression gated on viable $CD3^+CD4^+$ cells, gate shows $CD44^{hi}$ population. right: data summary of $\%CD44^{hi}$ population. T_{FH} population was stained with Bcl-6, ICOS, CXCR5 and PD-1, pre-gating on viable $CD4^+CD3^+$ cells. B) representative contour plots of T_{FH} markers Bcl-6 and ICOS, gate shows $Bcl6^+ICOS^+$ population. C) representative contour plots of T_{FH} markers CXCR5 and PD-1, gate shows $CXCR5^+PD\text{-}1^+$*

population. D) GC B cells were stained with Fas and GL7, pre-gating on viable CD19⁺B220⁺ cells. Left: representative contour plots of Fas and GL7 expression, gate shows Fas⁺GL7⁺ population. E) T_H1 response was addressed with restimulation of total splenocytes with GP-64 and BFA for four hours. Pre-gating on viable CD3⁺CD4⁺ cells. Top: representative contour plots of Tbet and IFNγ expression, bottom left: percentage of Tbet⁺ cells (top quadrants in the plots), bottom middle: percentage of Tbet⁺IFNγ⁺ (top right quadrants of the plots) bottom right: ratio of Tbet⁺IFNγ⁺ to total Tbet⁺ cells.

6.2.4. Transgenic miR-17~92 expression rescue effect is CD4⁺ T cell intrinsic

Due to the nature of T cell development, also the CD8⁺ T cells in our rescue mice express the miR-17~92 transgene, which raised the question if our rescue effect was actually CD4⁺ T cell intrinsic. This was unlikely since CD28 signaling was shown to be dispensable for CD8⁺ T cells during LCMV infection [268], however, we performed adoptive cell transfer experiments to exclude any external influence. For this, we crossed the B6.CD4cre.Rosa26^{lox}STOP^{lox}CAG-miR-17~92.CD28ko strain additionally to SMARTA TCR transgenic mice. This mouse line expresses an MHC class II restricted TCR with specificity for LCMV-GP, which consists of Vα2/Vβ8.3. We isolated naïve CD4⁺ T cells from SMARTA⁺wt, SMARTA⁺CD28ko, and SMARTA⁺rescue mice and adoptively transferred them into CD28ko host mice. Two days later the recipient mice were infected with LCMV Armstrong, and their mesenteric LN, peripheral LN and spleen were analyzed eight days post infection. Since our donor- and recipient strain express the same congenic markers, we decided to stain for Vα2⁺Vβ8.3⁺ CD4⁺ T cells to identify the donor cells. However, this has the caveat that also recipient cells will be contained in the gate that naturally express this combination of α- and β TCR chain and might expand upon LCMV infection. Therefore, we included a non-transferred mouse to display the intrinsic Vα2⁺Vβ8.3⁺ population, which is shown as dotted line in the plots. The cell-intrinsic Vα2⁺Vβ8.3⁺ population was negligibly small in comparison to mice receiving donor cells. In peripheral LN, we found less CD28ko Vα2⁺Vβ8.3⁺ CD4⁺ T cells as compared to wt (Figure 26A). This was rescued by transgenic miR-17~92 expression in percentage and also absolute numbers (%Vα2⁺Vβ8.3⁺ in wt 57.9±10.0%, CD28ko 1.9±0.9%, rescue 26.4±12.9%, total number in wt $3.2*10^6±1.9*10^6$, CD28ko $9.3*10^4±3.1*10^4$, rescue $8.4*10^5±5.0*10^5$). We found a similar pattern in spleen (%Vα2⁺Vβ8.3⁺ in wt 63.4±10.1%, CD28ko 2.2±1.6%, rescue 19.2±8.6%, total number

in wt $1.3*10^7 \pm 6.34*10^6$, CD28ko $9.9*10^4 \pm 4.8*10^4$, rescue $2.7*10^6 \pm 1.2*10^6$) and mesenteric LN (%Vα2$^+$Vβ8.3$^+$ in wt 29.7±2.5%, CD28ko 2.1±1.4%, rescue 12.7±4.9%, total number in wt $1.9*10^6 \pm 8.9*10^5$, CD28ko $1.6*10^5 \pm 9.4*10^4$, rescue $6.8*10^5 \pm 1.7*10^5$) (Figure 26B and C) as in the peripheral LN. The presence of less Vα2$^+$Vβ8.3$^+$ CD28ko cells suggested that CD28ko donor cells either had a proliferation- or a survival defect, which could be rescued by miR-17~92 expression. This goes in line with previously published literature showing the importance of miR-17~92 for survival and proliferation of T cells [134, 208].

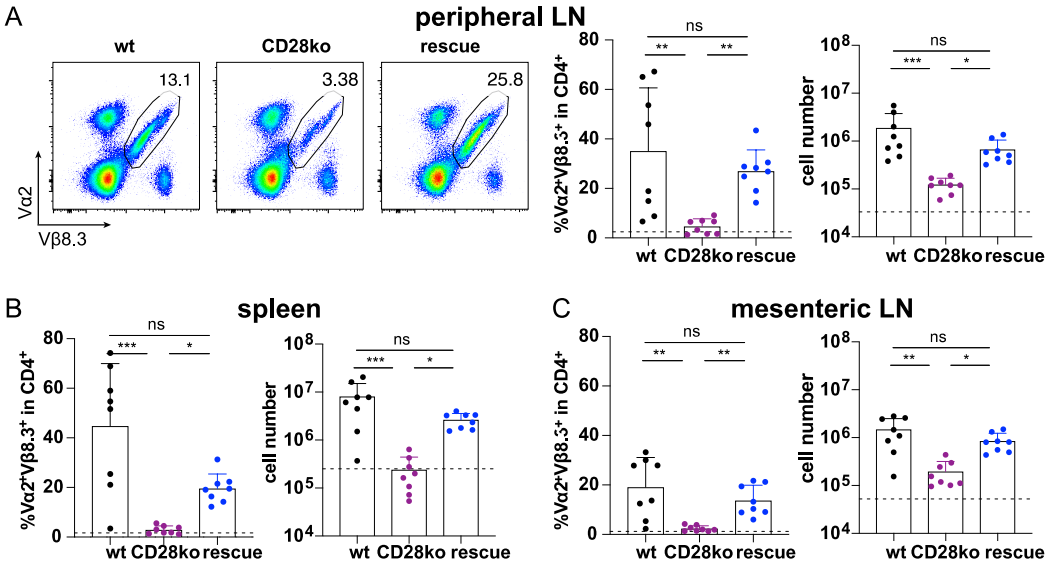

Figure 26. Less CD28ko Vα2$^+$Vβ8.3$^+$ CD4$^+$ T cells are found in recipient mice.

*Naïve SMARTA$^+$ CD4$^+$ T cells from six weeks old donor mice were transferred into CD28ko hosts i.v.. These were infected at day two post transfer with $2*10^5$ PFU LCMV Armstrong i.p.. peripheral LN (A), spleen (B) and mesenteric LN (C) were analyzed at day eight post infection. Pre-gating on viability, CD3 and CD4. Donor groups wt (black, left), CD28ko (purple, middle), CD28ko with transgenic miR-17~92 expression= rescue (dark blue). Dotted line indicates non-transferred control. Error bars represent mean ±SD, Dunn's multiple comparison test, p values: ns=not significant, *<0.05, **<0.002, ***<0.0002. Data represent two independent experiments with four mice per group.*

Since our previous experiments had shown a defect in CD44 upregulation in CD28ko cells *in vitro* (see Figure 17B) as well as *in vivo* (see Figure 22), we hypothesized that proliferation might not be the only defect that CD28ko donor cells have in this system. We stained viable CD4$^+$Vα2$^+$Vβ8.3$^+$ cells of peripheral LN for their CD44 expression (Figure 27A), and found that CD28ko Vα2$^+$Vβ8.3$^+$ cells expressed less CD44 as

compared to wt Vα2⁺Vβ8.3⁺ cells, which could be rescued by transgenic miR-17~92 expression in percentage and also total numbers (%CD44^{hi} in wt 98.7±0.2 %, CD28ko 55.9±14.7%, rescue 96.15±2.2%, total number in wt $3.2*10^6±1.9*10^6$, CD28ko $5.4*10^4±2.8*10^4$, rescue $8.1*10^5±5.0*10^5$). Again, this pattern was found in peripheral LN, but also in spleen (%CD44^{hi} in wt 97.6±0.5 %, CD28ko 59.9±22.0%, rescue 94.8±1.8%, total number in wt $1.3*10^7±6.1*10^6$, CD28ko $5.9*10^4±3.3*10^4$, rescue $2.6*10^6±1.2*10^6$) (Figure 27B) and mesenteric LN (%CD44^{hi} in wt 96.8±0.3 %, CD28ko 52.2±20.0%, rescue 92.9±2.3%, total number in wt $1.8*10^6±8.6*10^5$, CD28ko $9.8*10^4±9.8*10^4$, rescue $6.3*10^5±1.8*10^5$) (Figure 27C). This suggested that there are not only fewer donor CD28ko cells present, they are also not as activated as their wt or rescue counterparts. Thus, these data unequivocally demonstrate that the rescue effect was cell intrinsic.

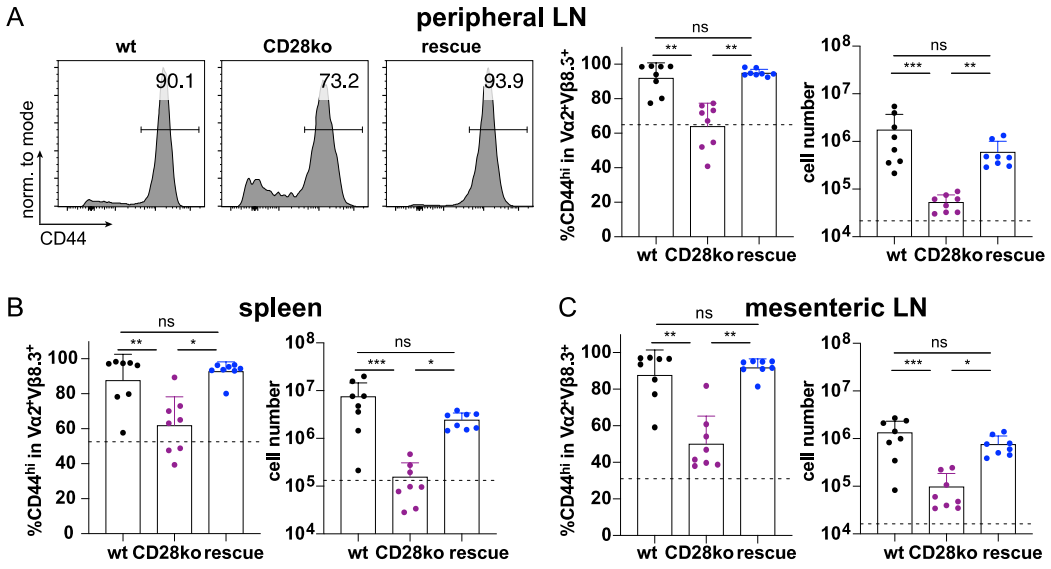

Figure 27. CD28ko Vα2⁺Vβ8.3⁺ CD4⁺ T cells express less CD44

*Naïve SMARTA⁺ CD4⁺ T cells from six weeks old donor mice were transferred into CD28ko hosts i.v.. These were infected at day two post transfer with $2*10^5$ PFU LCMV Armstrong i.p.. peripheral LN (A), spleen (B) and mesenteric LN (C). Pre-gating on viability, CD3 and CD4, Vα2⁺/Vβ8.3⁺ (Figure 26). Donor groups wt (black, left), CD28ko (purple, middle), CD28ko with transgenic miR-17~92 expression= rescue (dark blue). Dotted line indicates non-transferred control. Error bars represent mean ±SD, Dunn's multiple comparison test, p values: ns=not significant, *<0.05, **<0.002, ***<0.0002. Data represent two independent experiments with four mice per group.*

6.3. Molecular mechanism of the rescue effect

6.3.1. miR-17~92 expression shapes the transcriptome during T cell activation

We observed a strong effect of miR-17~92 expression on the T cell activation process. Therefore, we set out to determine the target genes of the miRNA cluster mediating this effect. Multiple targets for each member of the cluster were previously identified and validated (see section 3.2.3.3). Of note, limitation in expression of a target gene to one allele often led to a partial rescue of the corresponding miRNA knockout, e.g. Rorα limitation in miR1792lox cells during T_{FH} differentiation [134]. However, each of these publications investigated a different time point, in different context and a different T cell subset, so that these targets might not necessarily be relevant for our setting. Moreover, there might be additional, so far unknown target genes that mediate the rescue effect. Importantly, this does not exclude that previously reported target genes are also repressed in our system, since miRNAs are known to act on multiple target genes simultaneously. We stimulated naïve $CD4^+$ T cells from miR1792lox, wt and miR1792tg mice for 24h or 48h and isolated total RNA for sequencing. A PCA (Figure 28A) showed that the highest proportion of variance was caused by the process of activation itself (principal component 1 (PC1), explaining 80.3% of the variance). The second PC separated the activation time points 24h and 48h (PC2 9.5% of the variance), and the third PC separated the three genotypes (PC3, 3.6% of the variance, Figure 28B). The transcriptome of naïve miR1792lox and wt cells was very similar (largely overlapping in the PCA plot, even on PC3), and only 40 genes were down- and 75 upregulated in the comparison between miR1792tg to wt (at 1% FDR, also see Figure 28C, top block). This was consistent with our *in vitro* experimental data, and suggests that the cluster is functionally less relevant for naïve cells. At 24h post activation, 216 genes were down- and 262 upregulated in the direct comparison of miR1792tg vs. miR1792lox cells (Figure 28C, middle block). At 48h, the total number of differentially expressed genes between miR1792tg and miR1792lox increased to 625 down- and 459 upregulated, and the relative changes in expression of the genes (more intense red- or blue shading) that had already been differentially expressed at 24h were increased. Direct targets of the miRNA cluster are expected to get down-

regulated in their expression upon miRNA targeting (negative correlation of miRNA expression and target). A positive correlation of miRNA with gene expression suggests that these genes are indirectly regulated, e.g. genes whose expression is regulated by an inhibitor which is targeted by miR-17~92. From this first analysis we concluded that differences in miR-17~92 expression during activation shape the transcriptome of CD4$^+$ T cells. Our next aim was therefore to further characterize these differences in transcriptome and possibly define a mechanism which mediates these differences.

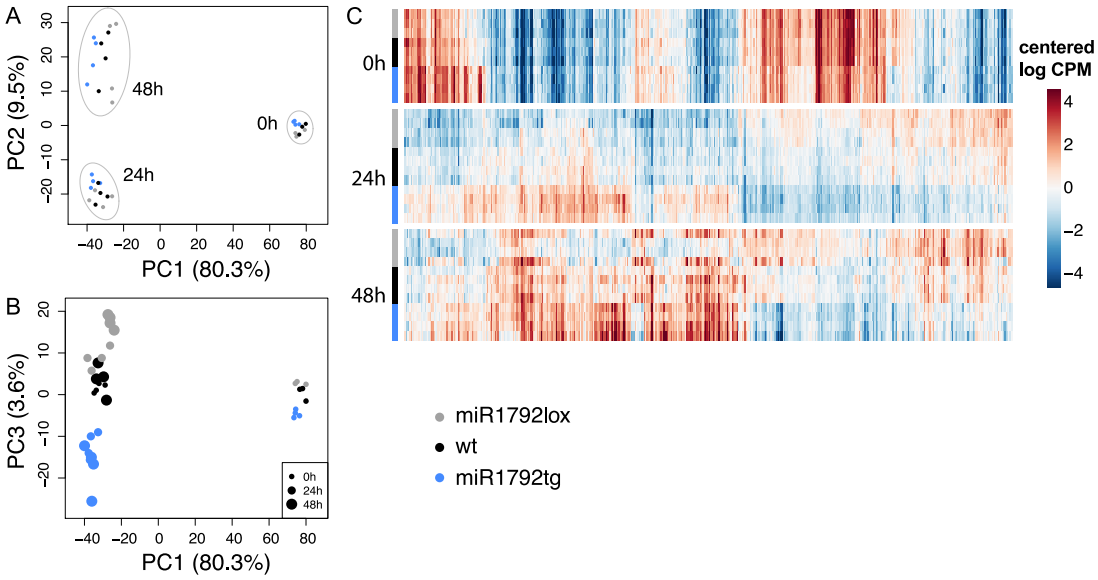

Figure 28. Differences in the transcriptome between miR1792lox, wt and miR1792tg cells

Naïve CD4$^+$ T cells from miR1792lox (grey), miR1792tg (light blue) or cre negative littermates (wt, black) were activated for 0, 24h and 48h. Total RNA was extracted for bulk RNA-sequencing.

A) *and B) PCA analysis based on the top 25% most variable genes of the dataset. Dot size in the lower plot corresponds to time point. C) Heatmap of the gene set defined as abs(log2FC)>1 & FDR<0.01 in the miR1792tg vs. miR1792lox comparison at 24h. The heatmap displays the centered log of read counts per million read mapped (CPM), with blue indicating lower and red indicating higher expression. Top block: naïve samples, Middle: 24h activated cells, Bottom: 48h activated cells*

6.3.2. Cytokine and TF expression of different T_H subsets are promoted by miR-17~92 expression

We performed gene set enrichment analysis (GSEA) with our RNA-sequencing data in order to find pathways of genes that are regulated by miR-17~92 expression. We found an enrichment of gene sets that were associated with cytokine expression (Table 2) in the top 25 most significantly enriched gene sets. Considering our *in vitro*

data (see also section 6.2.2), we then plotted known lineage-defining TF and cytokine genes of T_H subsets that were rescued by transgenic miR-17~92 expression and found that T_H1 as well as T_H2 and T_H17 cytokine expression was increased in miR1792tg cells (Figure 29). This argued that miR-17~92 controls a master regulatory pathway that is relevant for the differentiation of all of these T_H subsets. One pathway that matches these criteria is the calcineurin-NFAT axis [128], and indeed, most of these genes had a binding site for NFAT in their promoter region. We therefore aimed for defining a list of *bona fide* target genes, and within this list finding candidate genes that might negatively regulate an inhibitor of the NFAT pathway.

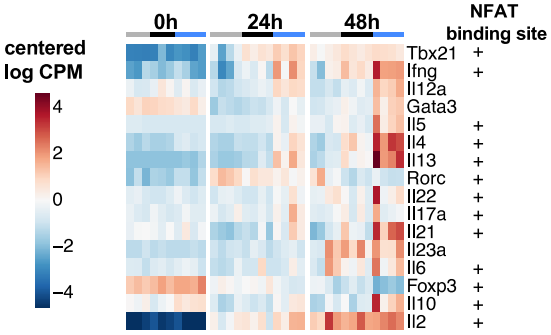

Figure 29. Expression of lineage defining TFs and cytokines in different T_H subsets are promoted by increased miR-17~92 expression.

miR1792lox (grey), wt (cre negative, black) and miR1792tg (blue) CD4$^+$ T cells are compared at time points 0 (left), 24h (middle) and 48h (right) after activation in their expression of selected lineage defining cytokine and TF expression of T_H1, T_H2, T_H17 and T_{reg} lineages. + indicate which of these genes are bound by NFAT in their promoter region [128]

Table 2. Gene set enrichment analysis: Top 25

The Top 25 most significant "curated gene sets" from KEGG/Biocarta/Reactome in the comparison miR1792tg vs. miR1792lox. Shown in yellow are the gene sets associated with cytokine expression

GeneSet	NGenes	Direction	absLog2FC	PValue	FDR
KEGG_ALLOGRAFT_REJECTION	38	Up	0.86425538	1.16E-08	2.30E-05
KEGG_TYPE_I_DIABETES_MELLITUS	39	Up	0.85594368	2.09E-08	2.76E-05
REACTOME_INTERFERON_GAMMA_SIGNALING	62	Up	0.69694524	1.69E-07	0.000133
BIOCARTA_CYTOKINE_PATHWAY	16	Up	1.35985987	3.74E-07	0.000184
KEGG_GRAFT_VERSUS_HOST_DISEASE	37	Up	0.79390884	3.46E-07	0.000184
BIOCARTA_INFLAM_PATHWAY	19	Up	1.22709045	7.06E-07	0.000279
KEGG_AUTOIMMUNE_THYROID_DISEASE	39	Up	0.72565543	3.30E-06	0.000817
KEGG_JAK_STAT_SIGNALING_PATHWAY	112	Up	0.58631266	6.05E-06	0.001331
REACTOME_ER_PHAGOSOME_PATHWAY	64	Up	0.31851723	6.77E-06	0.001412
BIOCARTA_NKT_PATHWAY	26	Up	0.97921623	1.01E-05	0.001737
REACTOME_ANTIGEN_PRESENTATION_FOLDING_ASSEMBLY_AND_PEPTIDE_LOADING_OF_CLASS_I_	28	Up	0.52146072	9.74E-06	0.001737
KEGG_ASTHMA	17	Up	1.00355911	1.47E-05	0.002426
REACTOME_INTERFERON_SIGNALING	138	Up	0.46903952	1.66E-05	0.002625
BIOCARTA_TH1TH2_PATHWAY	16	Up	1.15363531	2.03E-05	0.003088
KEGG_VALINE_LEUCINE_AND_ISOLEUCINE_DEGRADATION	42	Down	0.33811971	2.13E-05	0.003126
KEGG_FATTY_ACID_METABOLISM	37	Down	0.30681536	2.25E-05	0.003182
REACTOME_ANTIGEN_PROCESSING_CROSS_PRESENTATION	75	Up	0.29790777	2.65E-05	0.003623
KEGG_CYTOKINE_CYTOKINE_RECEPTOR_INTERACTION	157	Up	0.62556163	3.55E-05	0.004603
REACTOME_ENDOSOMAL_VACUOLAR_PATHWAY	16	Up	0.66794746	4.10E-05	0.004978
KEGG_METABOLISM_OF_XENOBIOTICS_BY_CYTOCHROME_P450	26	Down	0.61994646	0.000135	0.01215
KEGG_ASCORBATE_AND_ALDARATE_METABOLISM	12	Down	0.45219979	0.000152	0.01285
BIOCARTA_DC_PATHWAY	18	Up	1.05610989	0.000155	0.01286
REACTOME_CYTOKINE_SIGNALING_IN_IMMUNE_SYSTEM	236	Up	0.43153582	0.000173	0.0135
REACTOME_HOST_INTERACTIONS_OF_HIV_FACTORS	121	Up	0.27154151	0.000173	0.0135
BIOCARTA_CTL_PATHWAY	21	Up	0.67928008	0.000201	0.0148

6.3.3. Identification of bona fide canonical miR-17~92 targets

To identify the *bona fide* canonical target genes of the miR-17~92 cluster, we focused on the 24h time point because it was more likely to reflect primary effects of the miRNA cluster targeting. As opposed to this, changes in gene expression at 48h might also result from changes in the 24h time point as indirect effects. In the 24h data set, we wanted to specifically look at genes whose mRNA 3'UTR are bound by Ago2, i.e., genes that are targeted for degradation by the RISC complex after being bound by a microRNA (see section 3.2.2) at the moment of harvest. The High-throughput sequencing of RNA isolated by crosslinking immunoprecipitation (HITS CLIP) technique provides exactly this kind of biochemical evidence since a specific protein [269], in this case Ago2, is used for immunoprecipitation of the RNA of interest prior to sequencing. For our analysis, we took advantage of an Ago2-HITS CLIP (AHC) RNA sequencing data set from collaborators in Mark Ansel's group at the University of California, San Francisco.

We defined the following criteria for *bona fide* target genes:

a) conserved seed match for at least one member of the miRNA cluster, according to the miRNA targets database TargetScan [270].
b) Coverage of more than 5 reads in the AHC data (AHC>5)

The subsetting of genes with AHC and TargetScan reduced the list of in total 12'625 genes that were detected in the sequencing to several hundred potential target genes per seed family, i.e. 532 for the miR-17 seed family, 98 for the miR-18 seed family, 488 for the miR-19 seed family and 379 for the miR-92 seed family (Figure 30). Of note, with the above criteria we might miss some genuine target genes. For example, we exclude the non-canonical targets detected in the Ago2-HITS CLIP, namely those without seed match to one of the cluster members. These are also target genes, but we mainly aim at strongly enriching our candidate list for *bona fide* canonical target genes.

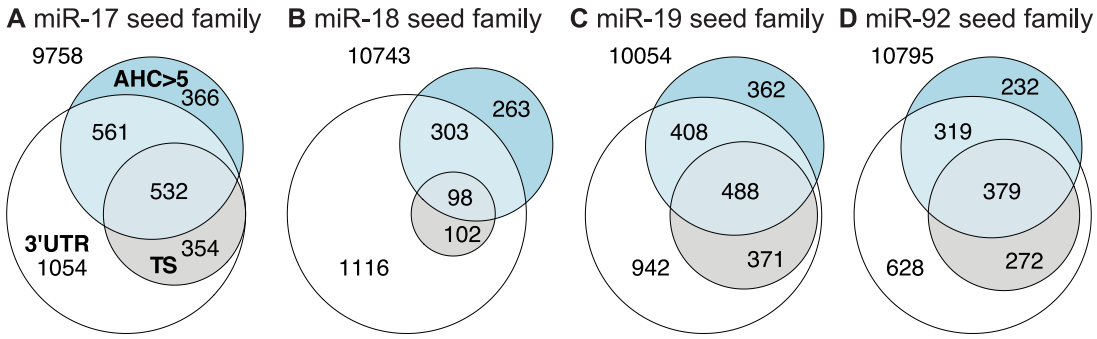

Figure 30. Venn diagrams illustrating the criteria used to identify canonical target genes of each seed family of the miR-17~92 cluster.

Number outside circles: genes that do not fulfill any of the criteria, white circle: genes with a seed match in their 3' UTR, grey circle: genes with a conserved binding site according to TargetScan (TS), blue circle: genes that showed a coverage of more than 5 reads in the AHC. Of note, non-canonical targets are likely present among genes without seed match (darkest part of blue circle).

We used cumulative distribution function (CDF) plots to verify whether we enrich for canonical target genes (Figure 31). For each seed family (see section 3.2.3.1), we visualize the distribution of logFC in comparisons across genotypes (miR1792lox vs. wt and miR1792tg vs. wt) for genes with a conserved seed sequence according to TargetScan (red curve) as well as the combination of the AHC and TargetScan criteria (blue curve), relative to genes without seed match and less than five AHC reads (black curve). We furthermore included miR-21 as a negative control, a miRNA which is induced upon T cell activation [271] independently from miR-17~92 and therefore its target genes should not display expression differences across genotypes (Figure 31A). If we enrich for real targets with these criteria, we expect the gene set to shift in the distribution of logFC towards higher FC in the miR1792lox vs. wt comparison and lower FC in the miR1792tg vs. wt comparison. We looked at all four seed families (see section 3.2.3.1) separately: for the miR-17 seed family, there was no clear shift in the distribution of logFC from the comparison between naïve miR1792lox and wt cells for putative target gene sets (red and blue curves), relative to the control genes (black curve). However, we observed reduced log2FC in miR1792tg vs wt naïve and activated samples, and increased log2FC in activated miR1792lox and wt cells (Figure 31B). A similar, but weaker shifting was observed in the miR-19 (Figure 31D) and miR-92 (Figure 31E) seed families. Of note, for the target genes of miR-18 (Figure 31C), the shift was overall minor. Considering also the relatively low number of genes identified

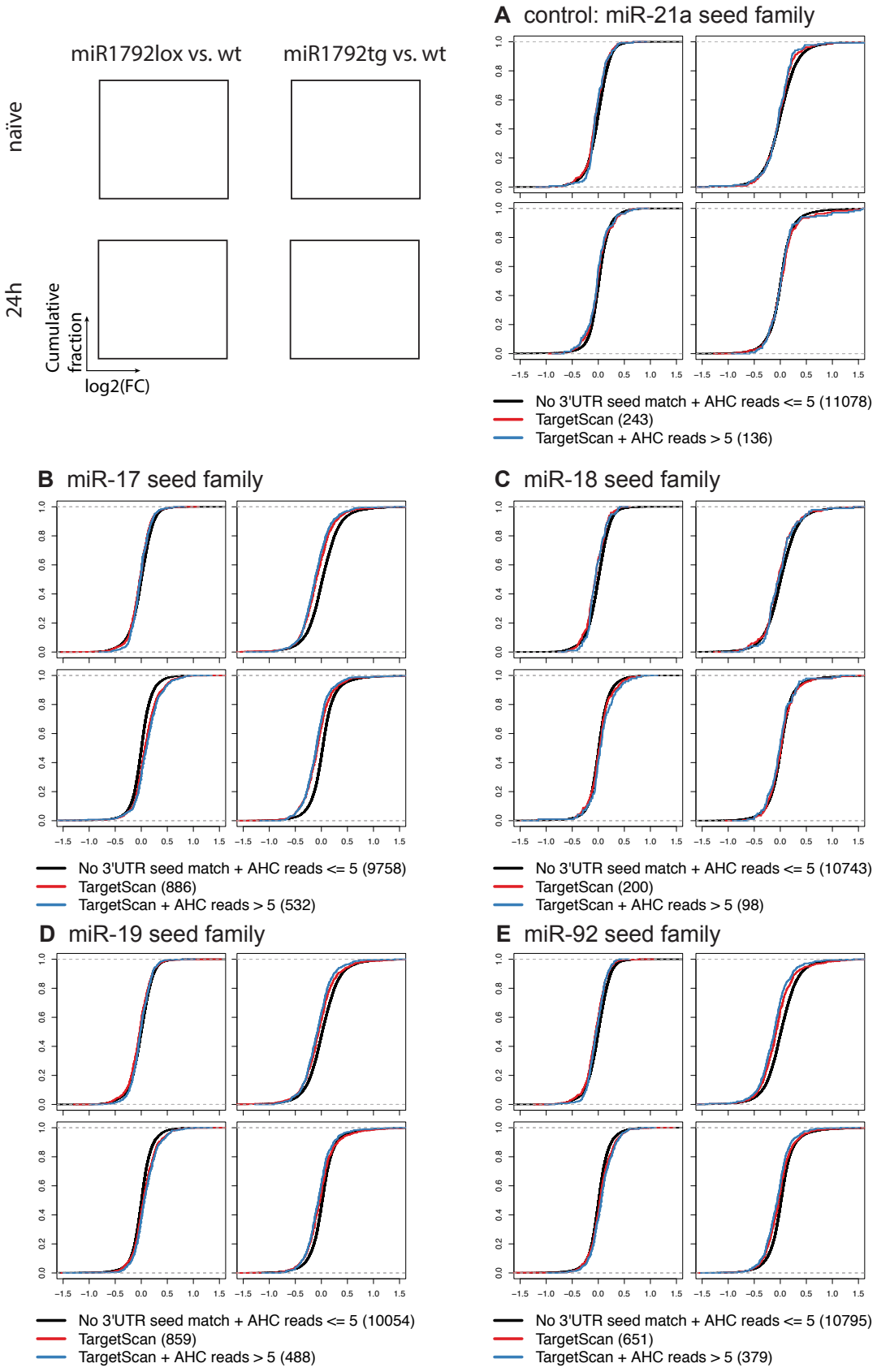

Figure 31. Up- and downregulation of canonical targets of different seed families of the miR-17~92 cluster.

Genes of distinct seed families of miR-17~92 show similar behavior, except for the miR-18 seed family. miR-21a was used as a control miRNA. black curve: all genes of our data set that do not have a seed match and showed five or less AHC reads, red: subset of genes that has a seed sequence for the indicated seed family, blue: subset of genes that has a seed sequence for the indicated seed family plus did also show more than five reads in the AHC

with our selection criteria, this might indicate that miR-18 has no or only few target genes in this setting. Additionally, the processing of the different members of the miRNA might be time- and context dependent, which had also been reported before [237]. Importantly, for the target genes of miR-21a (Figure 31A), we did not observe any shift. From this analysis we concluded that our criteria did enrich for canonical target genes of different miRNAs of the miR-17~92 cluster, and that many of them are differentially expressed in this setting.

Thus, to reduce the candidate list further for experimental validation, we included additional criteria like the exon-intron split analysis (EISA, [272]). This was especially important because of differences in transcriptional and post-transcriptional regulation: changes in transcriptional activity will be reflected by a change in intron as well as exon expression due to an increase in pre-mRNA, which is mostly nuclear RNA. In contrast to this, genes which are post-transcriptionally repressed by miRNAs should change their exon expression. Therefore, the log2FC in introns and exons is plotted (illustrated as an example for miR-17 seed family in Figure 32) to visualize which genes

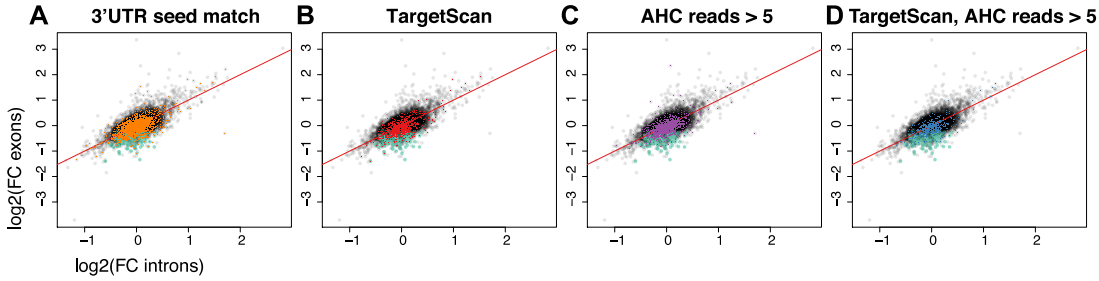

Figure 32. Illustration of the intronic vs exonic expression fold change criteria

Illustration shows the comparison of 24h activated miR1792tg vs wt cells, focused on miR-17 seed family. Bona fide target genes should only change at exonic level, indicating that the mature, spliced mRNA is changed in abundance (shift down in comparison to the red diagonal). A) 3'UTR seed match genes have a miR-17 seed family seed sequence (orange dots), B) TargetScan genes have a conserved miR-17 seed family seed sequence (red dots), C) AHC reads > 5 genes showed more than 5 reads in the AHC (purple dots), D) TargetScan + AHC reads > 5 match both of the latter two criteria (blue dots). Green dots mark the genes that are differentially expressed

change post-transcriptionally only [272] (shift down in this example, since we look at the comparison miR1792tg vs. wt in 24h activated cells).

Additionally, we wanted to focus on genes which are significantly differentially expressed in the absence of miR-17~92 as well as in the overexpressing cells in comparison to wt. For direct targets, the expression should be increased in miR1792lox, but decreased in miR1792tg cells. This results in the following three additional criteria for *bona fide* canonical targets:

c) differential expression (FDR < 0.01) in both lox vs. wt and tg vs. wt comparisons at 24h,

d) log2FC > 0 in lox vs. wt and log2FC < 0 in tg vs. wt comparisons at 24h,

e) no differential expression of introns (see Figure 32) (FDR >= 0.01) in both lox vs. wt and tg vs. wt comparisons at 24h.

With these criteria we result in the final canonical target candidate gene list of 125 genes shown in Table 3. Of note, this list includes targets of all four seed families, and some candidates are targeted by multiple miRNAs of the cluster.

Table 3. List of bona fide canonical target candidate genes

ENTREZID	SYMBOL	GENENAME	Seed family
11308	*Abi1*	abl-interactor 1	miR-17
11566	*Adss*	adenylosuccinate synthetase, non muscle	miR-19
11798	*Xiap*	X-linked inhibitor of apoptosis	miR-17
12380	*Cast*	calpastatin	miR-19
12753	*Clock*	circadian locomotor output cycles kaput	miR-17, miR-19
14007	*Celf2*	CUGBP, Elav-like family member 2	miR-17
14055	*Ezh1*	enhancer of zeste 1 polycomb repressive complex 2 subunit	miR-17
16451	*Jak1*	Janus kinase 1	miR-17
17113	*M6pr*	mannose-6-phosphate receptor, cation dependent	miR-17
17764	*Mtf1*	metal response element binding transcription factor 1	miR-92
18020	*Nfatc2ip*	nuclear factor of activated T cells, cytoplasmic, calcineurin dependent 2 interacting protein	miR-92
19338	*Rab33b*	RAB33B, member RAS oncogene family	miR-19
19344	*Rab5b*	RAB5B, member RAS oncogene family	miR-17, miR-19
19357	*Rad21*	RAD21 cohesin complex component	miR-17, miR-92
20238	*Atxn1*	ataxin 1	miR-17, miR-19, miR-92
20499	*Slc12a7*	solute carrier family 12, member 7	miR-17
20544	*Slc9a1*	solute carrier family 9 (sodium/hydrogen exchanger), member 1	miR-19, miR-92
21813	*Tgfbr2*	transforming growth factor, β receptor II	miR-17, miR-19
21815	*Tgif1*	TGFB-induced factor homeobox 1	miR-19, miR-92
22388	*Wdr1*	WD repeat domain 1	miR-19

27999	*Fam3c*	family with sequence similarity 3, member C	miR-17
29864	*Rnf11*	ring finger protein 11	miR-19
30934	*Tor1b*	torsin family 1, member B	miR-17, miR-19
50789	*Fbxl3*	F-box and leucine-rich repeat protein 3	miR-17
52592	*Brms1l*	breast cancer metastasis-suppressor 1-like	miR-17
52609	*Cbx7*	chromobox 7	miR-19
52635	*Esyt2*	extended synaptotagmin-like protein 2	miR-92
52864	*Slx4*	SLX4 structure-specific endonuclease subunit homolog (S. cerevisiae)	miR-17
53902	*RCAN3*	regulator of calcineurin 3	miR-17
54484	*Mkrn1*	makorin, ring finger protein, 1	miR-17
54650	*Sfmbt1*	Scm-like with four mbt domains 1	miR-17
56174	*Nagk*	N-acetylglucosamine kinase	miR-17, miR-92
56613	*Rps6ka4*	ribosomal protein S6 kinase, polypeptide 4	miR-92
57431	*Dnajc4*	DnaJ heat shock protein family (Hsp40) member C4	miR-17
58205	*Pdcd1lg2*	programmed cell death 1 ligand 2	miR-17
58244	*Stx6*	syntaxin 6	miR-19
66505	*Zmynd11*	zinc finger, MYND domain containing 11	miR-17, miR-19
67121	*Mastl*	microtubule associated serine/threonine kinase-like	miR-19
67229	*Prpf18*	pre-mRNA processing factor 18	miR-17, miR-18
67276	*Eri1*	exoribonuclease 1	miR-17
67894	*Fam45a*	family with sequence similarity 45, member A	miR-19
68465	*Adipor2*	adiponectin receptor 2	miR-92
68520	*Zfyve21*	zinc finger, FYVE domain containing 21	miR-19
68801	*Elovl5*	ELOVL family member 5, elongation of long chain fatty acids (yeast)	miR-92
69046	*Isca1*	iron-sulfur cluster assembly 1	miR-17
69470	*Tmem127*	transmembrane protein 127	miR-17
69721	*Nkiras1*	NFKB inhibitor interacting Ras-like protein 1	miR-19
70186	*Fam162a*	family with sequence similarity 162, member A	miR-19
70510	*Rnf167*	ring finger protein 167	miR-19
70533	*Btf3l4*	basic transcription factor 3-like 4	miR-17, miR-19, miR-92
70797	*Ankib1*	ankyrin repeat and IBR domain containing 1	miR-19, miR-92
70827	*Trak2*	trafficking protein, kinesin binding 2	miR-17, miR-92
71063	*Zfp597*	zinc finger protein 597	miR-17
71704	*Arhgef3*	Rho guanine nucleotide exchange factor (GEF) 3	miR-17
71819	*Kif23*	kinesin family member 23	miR-17
71929	*Tmem123*	transmembrane protein 123	miR-17, miR-19
73389	*Hbp1*	high mobility group box transcription factor 1	miR-17, miR-19, miR-92
73469	*Rnf38*	ring finger protein 38	miR-17
74114	*Crot*	carnitine O-octanoyltransferase	miR-19
74256	*Cyld*	CYLD lysine 63 deubiquitinase	miR-17
74360	*Cep57*	centrosomal protein 57	miR-19, miR-92
74769	*Pik3cb*	phosphatidylinositol-4,5-bisphosphate 3-kinase catalytic subunit β	miR-19
74868	*Tmem65*	transmembrane protein 65	miR-17
75221	*Dpp3*	dipeptidylpeptidase 3	miR-17, miR-18, miR-19
75580	*Zbtb4*	zinc finger and BTB domain containing 4	miR-92
75627	*Snapc1*	small nuclear RNA activating complex, polypeptide 1	miR-17, miR-19

76089	*Rapgef2*	Rap guanine nucleotide exchange factor (GEF) 2	miR-92
76740	*Efr3a*	EFR3 homolog A	miR-17
76763	*Mospd2*	motile sperm domain containing 2	miR-17
77644	*C330007P06Rik*	RIKEN cDNA C330007P06 gene	miR-17
77975	*Tmem50b*	transmembrane protein 50B	miR-18, miR-19
78334	*Cdk19*	cyclin-dependent kinase 19	miR-92
80517	*Herpud2*	HERPUD family member 2	miR-17
83924	*Gpr137b*	G protein-coupled receptor 137B	miR-17, miR-92
98193	*Dcaf8*	DDB1 and CUL4 associated factor 8	miR-17
98396	*Slc41a1*	solute carrier family 41, member 1	miR-17, miR-19
100201	*Tmem64*	transmembrane protein 64	miR-92
100383	*Bsdc1*	BSD domain containing 1	miR-17
102595	*Plekho2*	pleckstrin homology domain containing, family O member 2	miR-19
104625	*Cnot6*	CCR4-NOT transcription complex, subunit 6	miR-17
108645	*Mat2b*	methionine adenosyltransferase II, β	miR-19
108767	*Pnrc1*	proline-rich nuclear receptor coactivator 1	miR-17
109161	*Ube2q2*	ubiquitin-conjugating enzyme E2Q family member 2	miR-17
109168	*Atl3*	atlastin GTPase 3	miR-19
170459	*Stard4*	StAR-related lipid transfer (START) domain containing 4	miR-17
170719	*Oxr1*	oxidation resistance 1	miR-92
170740	*Zfp287*	zinc finger protein 287	miR-17, miR-19
192292	*Nrbp1*	nuclear receptor binding protein 1	miR-17, miR-92
213056	*Fam126b*	family with sequence similarity 126, member B	miR-17, miR-19
214897	*Csnk1g1*	casein kinase 1, γ 1	miR-17
215751	*Ginm1*	glycoprotein integral membrane 1	miR-17
216001	*Micu1*	mitochondrial calcium uptake 1	miR-19
216527	*Ccm2*	cerebral cavernous malformation 2	miR-17, miR-92
216558	*Ugp2*	UDP-glucose pyrophosphorylase 2	miR-92
216742	*Fnip1*	folliculin interacting protein 1	miR-92
217946	*Cdca7l*	cell division cycle associated 7 like	miR-17, miR-92
218503	*Fcho2*	FCH domain only 2	miR-17
218699	*Pxk*	PX domain containing serine/threonine kinase	miR-19
223918	*Spryd3*	SPRY domain containing 3	miR-19
224703	*March2*	membrane-associated ring finger (C3HC4) 2	miR-17
225995	*D030056L22Rik*	RIKEN cDNA D030056L22 gene	miR-19
226757	*Wdr26*	WD repeat domain 26	miR-17, miR-19
228359	*Arhgap1*	Rho GTPase activating protein 1	miR-19
229521	*Syt11*	synaptotagmin XI	miR-92
231070	*Insig1*	insulin induced gene 1	miR-17, miR-19
231464	*Cnot6l*	CCR4-NOT transcription complex, subunit 6-like	miR-92
231570	*A830010M20Rik*	RIKEN cDNA A830010M20 gene	miR-17, miR-19
231986	*Jazf1*	JAZF zinc finger 1	miR-19
232196	*C87436*	expressed sequence C87436	miR-18
232430	*Crebl2*	cAMP responsive element binding protein-like 2	miR-17
233765	*Plekha7*	pleckstrin homology domain containing, family A member 7	miR-17
234094	*Arhgef10*	Rho guanine nucleotide exchange factor (GEF) 10	miR-17, miR-19
236511	*Ago1*	argonaute RISC catalytic subunit 1	miR-17, miR-18, miR-19
238673	*Zfp367*	zinc finger protein 367	miR-92
240055	*Neurl1b*	neuralized E3 ubiquitin protein ligase 1B	miR-17

242960	*Fbxl5*	F-box and leucine-rich repeat protein 5	miR-17, miR-92
244650	*Phlpp2*	PH domain and leucine rich repeat protein phosphatase 2	miR-19
266781	*Snx17*	sorting nexin 17	miR-92
319263	*Pcmtd1*	protein-L-isoaspartate (D-aspartate) O-methyltransferase domain containing 1	miR-19
319701	*Fbxo48*	F-box protein 48	miR-17
320191	*Hook3*	hook microtubule tethering protein 3	miR-17, miR-92
330401	*Tmcc1*	transmembrane and coiled coil domains 1	miR-92
338366	*Mia3*	melanoma inhibitory activity 3	miR-17, miR-92
353047	*Plekhm1*	pleckstrin homology domain containing, family M (with RUN domain) member 1	miR-17
433667	*Ankrd13c*	ankyrin repeat domain 13c	miR-19
100504663	*Atg14*	autophagy related 14	miR-17

Within this list, we find known target genes of miR-17~92 like *Phlpp2*, *Tgfbr2* and *Zbtb4F*. These genes have been validated by others and serve as a positive control for our analysis.

6.3.4. Exogenous miR-17~92 expression partially rescues the transcriptome of CD28ko cells

Since we observed a rather strong rescue effect on different aspects of T cell activation and differentiation (see section 6.2), we wondered if this rescue was only phenotypical or if the transgenic miR-17~92 expression might also rescue the transcriptome of CD28ko cells. Following this hypothesis, we isolated RNA from naïve and 24h activated $CD4^+$ T cells from CD28ko, wt, rescue, miR1792tg and miR1792lox mice to perform RNA sequencing again. In a PCA analysis, most of the variance was again explained by T cell activation (PC1 (90.7%)). PC2 (2.4%) separated the different genotypes, a pattern that was more apparent in activated samples, and while the miR1792lox, wt and miR1792tg genotypes did not separate clearly, the CD28ko samples were very different from the others. This was expected, since CD28 co-stimulation is known to have profound effects on the transcriptome during early T cell activation [273]. Strikingly, the overexpression of miR-17~92 in CD28ko cells partially rescued the transcriptome so that the rescue samples were more similar to miR1792lox/wt/miR1792tg (Figure 33). According to our hypothesis that miR-17~92 promotes T cell activation, we expect “two extremes of activation”: the “super activated” miR1792tg cells and the “improperly activated” CD28ko cells. This was confirmed by this PCA analysis: miR1792tg were the most different from CD28ko samples.

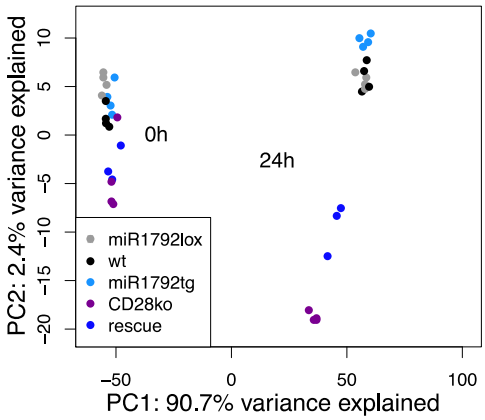

Figure 33. Exogenous miR-17~92 expression partially rescues CD28ko transcriptome during CD4⁺ T cell activation

Naïve CD4⁺ T cells from miR1792lox (grey), miR1792tg (light blue), cre negative littermates (wt, black), CD28ko (purple), and rescue cells (dark blue) were activated for 24h, total RNA was extracted for bulk sequencing. PCA analysis was based on the 25% most variable genes of the dataset.

The PCA analysis however suggested that the transcriptome differences between CD28ko and wt samples can only partially be rescued by forced miR-17~92 expression, at least until this time point in this context. We hypothesized that the rescued part of the transcriptome was including miR-17~92 targets and investigated our dataset like before (Figure 30 and Figure 31): We verified the log FC shifts in the comparisons across genotypes in activated cells for gene subsets with conserved binding sites according to TargetScan and with AHC data coverage. Additionally, we added in this analysis the list of *bona fide* canonical target genes that we had defined in the previous section as a new subset (green curve in Figure 34; these genes are by definition regulated by miR-17~92 expression). Similar to the shift towards increased FC in miR1792lox vs. wt (Figure 31), the FC of the same genes were also shifted to increased FC in CD28ko vs. wt (Figure 34, top row). This suggests that the genes that are repressed by miR-17~92 and therefore up-regulated upon miR-17~92 inactivation in activated cells were also up-regulated in CD28-deficient cells during activation. This shift mostly was reversed with transgenic expression of miR-17~92 in rescue cells (Figure 34, bottom row). Even more, the expression of the most relevant putative target genes (Table 3, green curve in Figure 34) was over compensated, so that the FC became even negative. From this analysis we concluded that a fraction of genes that are differentially expressed in the CD28ko transcriptome is regulated by miR-17~92.

Therefore, the exogenous expression of miR-17~92 led to a partial rescue of the CD28ko transcriptome in rescue cells.

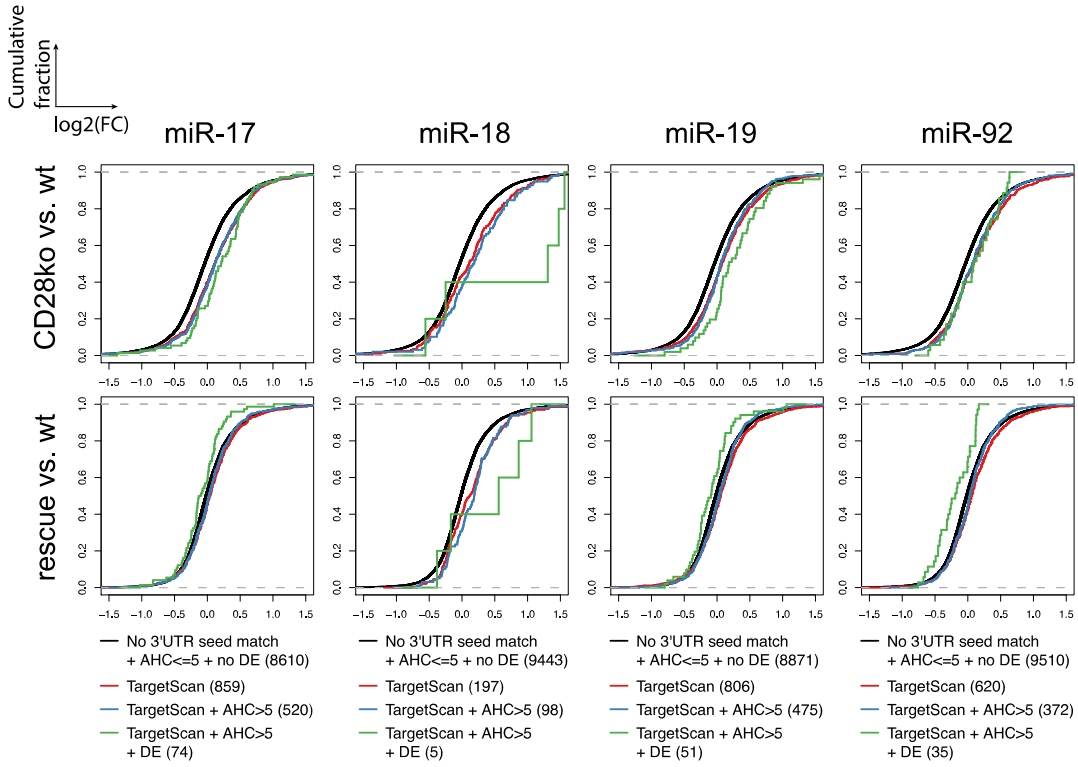

Figure 34. Bona fide canonical targets of miR-17~92 are also regulated by CD28

Genome-wide transcriptome analysis, presented as the log2 value of the gene-expression ratio for each gene versus the cumulative fraction of all log2 ratios. Shown are the contrasts between activated samples separated by seed family, top row: CD28ko vs wt comparison, bottom row: rescue vs wt comparison. black curve: genes that do not have a seed match, five or less AHC reads, and no differential expression in the first RNA sequencing. red: genes with a conserved binding site for the indicated seed family, blue: genes with a conserved binding site for the indicated seed family and more than five reads in the AHC, green: genes with a conserved binding site for the indicated seed family, more than five reads in the AHC and differential expression in the first RNA sequencing data set

6.3.5. Target gene RCAN3 expression is dependent on CD28 or miR-17~92 expression

Since cytokine expression was promoted by increased miR-17~92 expression (Figure 29), and NFAT is a common regulator of most of these, we searched in our target gene list (Table 3) for candidates that might negatively regulate the calcineurin-NFAT pathway. One such candidate gene is Regulator of calcineurin 3 (*RCAN3*), which was reported to interact with and thereby inhibit calcineurin [112].

We used published HITS-CLIP data [274] to investigate if the 3'UTR of our selected target candidate gene *RCAN3* in this setting. The activation conditions of this published data set were not exactly the same as in our situation (longer activation), however they should still be within acceptable range of difference. The visualization showed that there are multiple binding sites for different miRNAs in the 3'UTR of *RCAN3*, though only the miR-17 binding site was occupied by Ago2 at the moment of sequencing (Figure 35), suggesting that this is a true target gene.

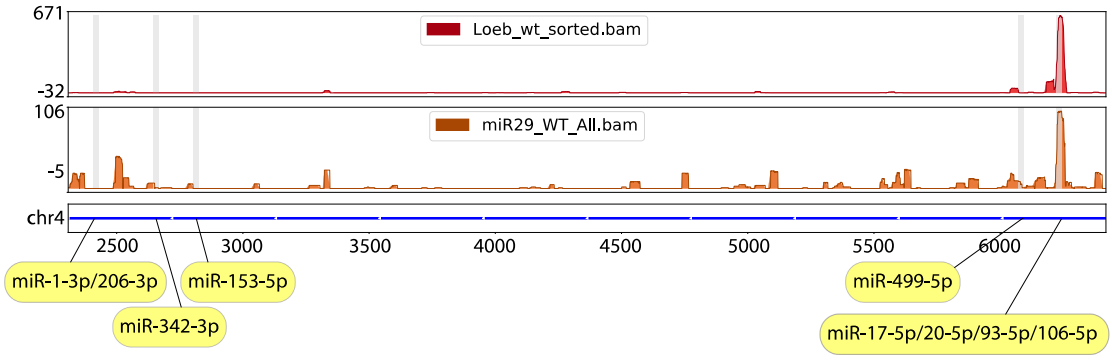

Figure 35. Visualization of RCAN3 3'UTR: AHC track.
Binding sites of Ago2 in 3'UTR of RCAN3 detected by HITS-CLIP (orange and red peaks), yellow flags and grey bars indicate potential binding sites for miRNA

The second RNA sequencing dataset showed a ~0.5-fold in expression of *RCAN3* RNA in CD28ko cells in comparison to wt. We then performed qPCR on RNA that we extracted from 24h activated miR1792lox, wt and miR1792tg cells to validate the sequencing results. *RCAN3* mRNA expression was ~1.5-fold increased in miR1792lox as compared to wt cells, and ~0.6-fold reduced in miR1792tg as compared to wt (Figure 36A).

The regulation of the mRNA is the first important aspect of target validation, but the translation into protein is of even greater importance. We therefore set out to test if RCAN3 protein abundance is also regulated. Since no antibody for FACS and no good antibody for WesternBlot was available for RCAN3, we performed targeted proteomics in order to address protein expression. RCAN3 protein expression was ~2-fold increased in CD28ko and miR1792lox cells in comparison to wt, which was reduced by transgenic miR-17~92 expression in the rescue cells (Figure 36B). However, even if RNA expression in miR1792tg cells was decreased in comparison to

wt cells, protein was not significantly changed (normalized protein abundance in CD28ko 0.85±0.07, miR1792lox 1.03±0.09, rescue 0.60±0.13, wt 0.42±0.10 and miR1792tg 0.33±0.16). From this data, we concluded that *RCAN3* RNA as well as protein expression is regulated by CD28 and miR-17~92.

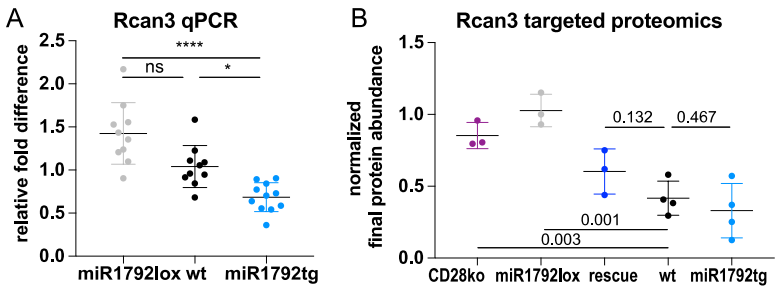

Figure 36. RCAN3 mRNA and protein is elevated in CD28ko, and reduced in rescue cells
*A) RCAN3 RNA expression detected with qPCR 24h after activation, shown is the fold change to wt from three independent experiments. miR1792lox (grey), wt (black), miR1792tg (light blue). mRNA expression was normalized to 18S ribosomal RNA. Error bars represent mean ±SD, Dunn's multiple comparison test, p values: ns=not significant, *<0.05 ****<0.0001 B) RCAN3 protein abundance measured by targeted proteomics 24h after activation. CD28ko (purple), miR1792lox (grey), rescue (dark blue), and miR1792tg (light blue) are compared to wt (black). Numbers indicate p values from T-test*

6.3.6. Sensitivity to Cyclosporin A is increased in CD28 deficient cells and rescued by transgenic miR-17~92 expression

Our data on *RCAN3* RNA and protein expression suggested the hypothesis that one so far unknown way of how miR-17~92 acts in T cell activation might be the regulation of calcineurin and NFAT via the inhibition of a cell-intrinsic calcineurin repressor, RCAN3. We hypothesized that increased RCAN3 expression in CD28ko cells might increase the sensitivity of the cells to the chemical calcineurin inhibitor CsA. To test this hypothesis, we activated wt, CD28ko and rescue $CD4^+$ T cells in the presence of increasing concentrations of CsA for 48h. As already shown in Figure 17, all genotypes reached similar percentages of $CD25^+CD69^+$ expression. With increasing CsA concentrations, CD28ko cells showed reduced percentages of $CD25^+CD69^+$ expression in comparison to wt already at a concentration 6.25ng/ml (Figure 37A). Wt cells only reacted at a 4-fold higher concentration, while rescue cells were even more resistant than wt cells. The failure of early activation marker upregulation went in hand with

differences in cell size: at 6.25ng/ml CsA, CD28ko cells were almost not blasting at all, wt cells were blasting, and rescue cells looked normal, which is shown as FSC-A in Figure 37B. This indicated a higher sensitivity to CsA for CD28ko cells, which could be rescued by transgenic miR-17~92 expression.

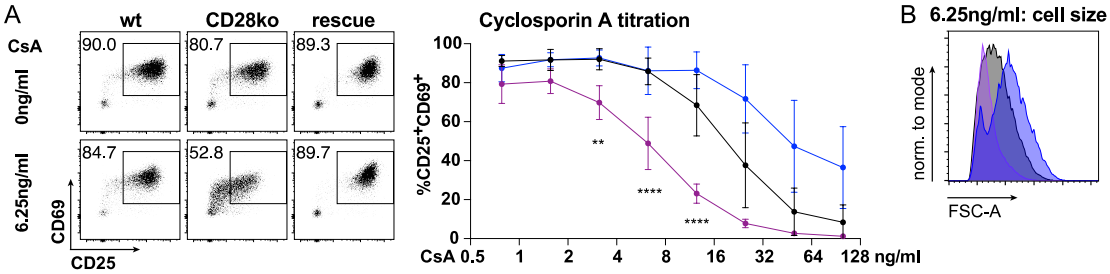

Figure 37. CD28ko cells react more sensitively to CsA treatment, and rescue cells are more resistant

*wt (black), CD28ko (purple) and rescue (dark blue) cells were activated for 48h in the presence of increasing concentrations of Cyclosporin A (CsA) as indicated and stained for their expression of CD25 and CD69. A) left: representative plots of CD25/CD69 expression in viable $CD4^+$ T cells activated for 48h with no or 6.25ng/ml CsA. right: percentage of the $CD25^+CD69^+$ population as gated on the left. Shown are two independent experiments, error bars represent means ±SD. Tukey's multiple comparison, p values: **<0.002, ****<0.0001 refer to the difference between CD28ko and wt. B) Representative example of the influence of 6.25ng/ml CsA on blasting (FSC-A of the lymphocyte gate) of viable $CD4^+$ cells.*

The main mode of action of calcineurin inhibitors is to prevent nuclear localization of NFAT by inhibition of the phosphatase activity of calcineurin [275]. We therefore investigated nuclear localization of NFATc2 by ImageStream: again, $CD4^+$ T cells were activated in the presence of 6.25ng/ml CsA. The acquisition showed small cells with most of the NFATc2 signal in the cytoplasm (Figure 38A, top row) and big cells in which the NFATc2 signal co-localized with the DAPI signal (Figure 38A, bottom row). The histogram of the similarity dilate, a value used to score co-localization of signals, indicates that at a concentration of 6.25ng/ml CsA in culture, CD28ko cells show less nuclear localization of NFATc2 as compared to wt and rescue cells (Figure 38B).

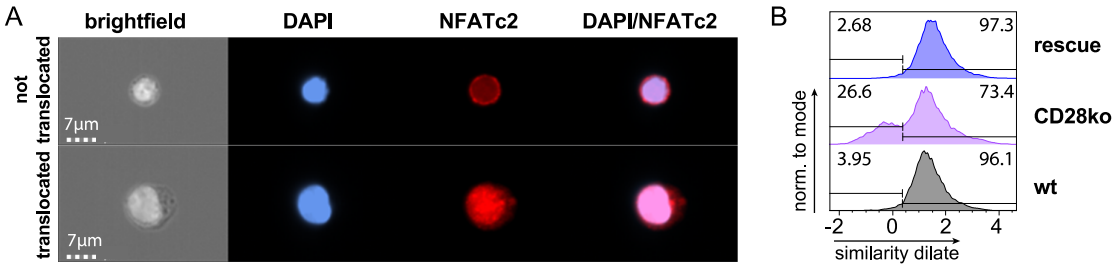

Figure 38. NFATc2 nuclear translocation is reduced in CD28ko cells and rescued by exogenous miR-17~92 expression

48h activated CD4$^+$ T cells with 6.25ng/ml Cyclosporin A, stained for DAPI (blue) and NFATc2 (red).

A) Examples of ImageStream acquisition images for not translocated (top) and translocated (bottom) NFAT in a CD28ko sample. B) ImageStream data: histogram of the similarity dilate for each sample, indicative of the co-localization of NFATc2 and DAPI signal, gates indicate the translocated population (high similarity dilate) and the non-translocated population (low similarity dilate)

With this, we concluded that CD28ko cells are more sensitive to CsA as compared to wt cells, which is rescued by transgenic miR-17~92 expression in CD28ko cells. We suggest that this happens via a so far unknown mechanism, which is the promotion of calcineurin activity via regulation of the natural calcineurin inhibitor RCAN3. As this is an essential aspect of immune suppression, our work suggests new possibilities for immunosuppressive medication but also cellular immune therapies.

7. Discussion

The importance of miR-17~92 expression for the function of $CD4^+$ T cells has been established by independent research groups for different T_H subsets and models [134, 208, 216, 234-237, 240]. Although some of these reports are in contrast to each other, a few key effects of miR-17~92 expression have been agreed on [227], which are mainly the amplification of cytokine expression as well as promotion of proliferation. Based on our own findings and published data [208] we hypothesized that overexpression of miR-17~92, which is normally induced with CD28 co-stimulation [215], might compensate for the co-stimulatory signal given by this receptor. Thus, we elucidated if transgenic miR-17~92 expression compensates for CD28 signaling in $CD4^+$ T cell activation *in vitro* and *in vivo*. This concept was also suggested by Benhamou et al. [276] who could show that activation of B cells partially depends on PI3K activity, which is initiated by the co-stimulatory signal given by CD19 in this case. Similar to CD28ko T cells, CD19ko B cells are deficient in activation, proliferation and differentiation. Benhamou et al. showed that the artificial expression of miR-17~92 in B cells can partially compensate for CD19 deficiency [41]. Moreover, the authors investigated the role of a known miR-17~92 target, *PTEN* [277], which restricts the CD19-PI3K axis. They demonstrate an autostimulatory axis of c-Myc/miR-17~92/PTEN which regulates PI3K mediated positive and negative selection. However, other pathways than PI3K or other targets remain obscure in this publication. *PTEN* was also shown to be an important miR-17~92 target in T cells, though Baumjohann et al. showed that limitation of *PTEN* expression to one allele alone could not restore the phenotype of miR1792lox mice in T_{FH} differentiation [134], which strongly suggests that other targets must be regulated in this setting as well. Many different targets for all members of the miR-17~92 cluster have been validated so far [227, 228]. We identify a new list of *bona fide* canonical target genes in our setting, which are not only regulated by miR-17~92 but also by CD28 expression. Importantly, by showing that the overexpression of miR-17~92 rescued the expression of these genes, we also provide evidence that the rescue is not only a phenotypic effect, but also manifested in the transcriptome and most likely mediated by *bona fide* canonical targets. This

demonstrates that during activation of $CD4^+$ T cells with CD28 co-stimulation, which is known to induce the expression of genes, also the repression of genes is essential.

We searched for pathways other than PI3K that are regulated by miR-17~92 during $CD4^+$ T cell activation, and found that also calcineurin-NFAT axis is promoted by miR-17~92 expression. We suggest a new target for miR-17, which is the cell-intrinsic calcineurin inhibitor RCAN3 [112]. Repression of RCAN3 by miR-17 increases calcineurin activity, consequently leading to increased NFAT activity, with marked consequences for cell fate.

7.1. miR-17~92 expression promotes $CD4^+$ T cell activation

Baumjohann et al. showed that reduced miR-17~92 expression decreases proliferation *in vitro* [134], while Xiao et al. showed increased proliferation due to miR-17~92 overexpression [231]. Moreover, previous literature suggests that also cytokine expression is decreased in the absence of miR-17~92 expression, and increased in the case of miR-17~92 overexpression [231].

Here, we show that IL-2 production and secretion as well as proliferation are proportional to miR-17~92 expression. Of note, differences in miR1792lox vs wt as well as miR1792tg vs wt are relatively small, which reflects the general problem of subtle changes in miRNA studies. Usually, large number of samples are required to reach significant differences [278]. This is also partially caused by the paralogue clusters whose expression is unchanged in these mouse models, and their function which is partially redundant to miR-17~92 [192, 218]. From these experiments, we concluded that IL-2 production and proliferation is promoted by miR-17~92 expression. These findings are in accordance with previously published literature.

$CD4^+$ T cell activation results in major changes in the $CD4^+$ T cell's metabolism regarding glucose uptake and glycolytic activity. MiR-17~92 is involved in the regulation of c-Myc, which is an important regulator of metabolism [279]. Interestingly, we found increased glucose uptake in naïve miR1792tg $CD4^+$ T cells, but no difference in mitochondria stress tests. This suggests that glucose uptake is promoted by miR-17~92 expression, however it is not metabolized by glycolysis or oxidative phosphorylation. This shows that naïve miR1792tg $CD4^+$ T cells metabolically do not resemble more activated cells, which contradicts the hypothesis that

transgenic miR-17~92 expression leads to some kind of metabolic checkpoint passage. We could probably argue that this is expected since miR-17~92 expression is usually only induced during $CD4^+$ T cell activation [215] and target genes might not be expressed in the naïve setting. In activated $CD4^+$ T cells, miR-17~92 expression correlates with metabolic activity. However, we suppose that this results from higher activation the more miRNA cluster is expressed as suggested already by our previous experiments.

In order to get a deeper insight into the metabolic phenotype of activated $CD4^+$ T cell cells of different miR-17~92 expression, we performed a metabolomics analysis on activated $CD4^+$ T cell lysates. There we found only eight metabolites which were differentially abundant in the direct comparison of miR1792tg to miR1792lox cells. Moreover, these metabolites belonged to distinct pathways and FC were just above cut-off, which raised the question if the detected differences are biologically relevant. We investigated our RNA sequencing results for the same pathways, which did not reveal patterns of pathways being repressed or promoted by miR-17~92 expression. With these results we could not confirm, nor neglect, the hypothesis of metabolic checkpoint allowance by miR-17~92 expression during $CD4^+$ T cell activation.

From this first part of the thesis, we concluded that miR-17~92 expression directly correlates with $CD4^+$ T cell activation, including IL-2 production as well as proliferation and metabolic activity. Notably, the differences relative to wt in these experiments were sometimes subtle, which provokes the question of biological significance. Blevins et al. suggested that the role of miRNAs is more the regulation of cell-to-cell variability than active meaningful changes in cell phenotype [186]. Thus, upregulation of miR-17~92 expression regulates genes which are also upregulated during activation in feedback loops. However, the significance of the differences introduced by miRNAs have been extensively debated in the past (reviewed e.g. in [278]): with the regulation of genes close to specific threshold levels, miRNAs might, even if introducing only small changes in target gene expression, also mediate important on-off switches. Since $CD4^+$ T cell activation is a very dynamic process of parallel changes in expression of surface molecules as well as intracellular proteins, we hypothesized that miR-17~92 is a key player in CD28 dependent activation.

7.2. Exogenous miR-17~92 expression rescues CD28 deficiency

7.2.1. Exogenous miR-17~92 expression compensates for CD28 signal during in vitro activation

Different key aspects of $CD4^+$ T cell activation were shown to be regulated by CD28 as well as miR-17~92 expression. Xiao et al. showed that miR1792tg cells proliferate better than wt cells when stimulated with αCD3 alone [231]. Therefore, we expected from our B6.CD4cre.Rosa26^{lox}STOP^{lox}CAG-miR-17~92.CD28ko (rescue) mouse model that proliferation and other aspects of $CD4^+$ T cell activation are restored by exogenous miR-17~92 expression. We found that IL-2 production in rescue cells was not only rescued to the wt amount, but even higher as compared to wt cells. One explanation for this supraphysiologic rescue might be that with transgenic expression, more miR-17~92 expression is achieved than during activation of wt cells. Since miR-17~92 was shown to promote PI3K dependent pathways, the PI3K dependent aspect of IL-2 production, which is IL-2 transcription [162], might be over-compensated. Moreover, this assay was performed with PMA/Iono stimulation. Iono initiates Ca^{2+} influx [280] while PMA acts on Ras [281], both resulting in increased IL-2 production. Thus, we might look at Ca^{2+} dependent pathways that could be promoted by transgenic miR-17~92 expression.

As expected from the literature [231], proliferation and blasting was rescued by transgenic miR-17~92 expression. More surprising to us was that all genotypes induced CD25 and CD69 expression: CD25 was previously shown to be CD28 dependent [282] while CD69 was not [117]. Investigation of the MFI revealed that CD69 is actually unchanged, while CD25 MFI depends on CD28 or miR-17~92 expression. One explanation for this might be that exogenous IL-2 was present in the culture, which might lead to CD25 induction [283]. The differences that we observe in MFI might then originate from autocrine IL-2 stimulation. The differences in $CD44^{hi}CD62L^{lo}$ populations were expected since we had shown in previous experiments that activation is rescued by exogenous miR-17~92 expression. However, defects in CD44 expression of CD28ko cells had not been described before.

These experiments demonstrated that exogenous miR-17~92 expression can indeed compensate for CD28 signaling during *in vitro* activation of $CD4^+$ T cells in terms of IL-2 production, proliferation and surface marker upregulation similar to what Benhamou et al. had reported for CD19 deficient B cells.

7.2.2. Exogenous miR-17~92 expression compensates for CD28 deficiency during in vitro differentiation

After encountering an antigen in a specific context (e.g. cytokine milieu) during an infection, the $CD4^+$ T cell fate changes according to extracellular signals. The networks of master regulators, STAT proteins and cytokines in T_H differentiation are complex: Lineage fates influence each other by repression of TFs or interaction between master regulators. However, these networks are also partially redundant, with the consequence that differentiation is possible even if single players of the networks are absent [284]. For example, Usui et al. reported that Tbet is not absolutely essential for IFNγ production as long as IL-4 signals are blocked [285]. miRNAs were shown to influence differentiation of subsets e.g. by targeting TFs [134], therefore we expected an influence on differentiation of rescue cells as well.

We observed that T_H1 differentiation was delayed for Tbet production in CD28ko cells and rescued by exogenous miR-17~92 expression. IFNγ production was massively increased by exogenous miR-17~92 expression, which might be explained by the fact that STAT5, a signaling molecule downstream of IL-2R, regulates IFNγ locus availability [94, 286], and we showed that IL-2 production is increased with miR-17~92 expression. In this case, on one hand cell-intrinsic IL-2 production might promote IFNγ production in rescue cells, but additionally reduced expression of CD25 in CD28ko cells as seen in previous experiments might reduce signaling from IL-2 contained in the culture.

Rorγt expression was impaired in CD28ko cells as compared to wt during T_H17 differentiation, and exogenous miR-17~92 expression led to a rescue, even though with different kinetics in Rorγt induction as compared to wt. Moreover, miR1792tg cells even expressed less Rorγt than wt at 24h post induction, while later on miR1792tg and wt were indistinguishable. IL-17A production was reduced in CD28ko

cells, and only partially rescued by exogenous miR-17~92 expression. MiR1792tg cells also were delayed in their IL-17A production as compared to wt.

The data for CD28ko cells looks like contrast to published literature which showed that CD28 co-stimulation actually inhibits *in vitro* generation of IL-17A producing cells [165]. Of note, Bouguermouh et al. stain their cells at day four or five (other than our experiments which end on day three) after six hours of PMA/Iono restimulation. Moreover, in their publication most of the experiments were conducted without the addition of neutralizing antibodies for IL-2 and IFNγ. However, the authors also include one experiment where they added these antibodies, with the result that IL-17A production was similar between CD28ko and wt cells. They therefore claim that CD28 inhibits T_H17 differentiation by promoting IL-2 and IFNγ. This means that this publication is actually not necessarily in contrast to our experiments, since we included neutralizing antibodies in our culture, and we observed a delay in IL-17A expression induction in CD28ko cells. The data on rescue and miR1792tg cells argues for a complex network of regulatory mechanisms which are partially influenced by miR-17~92 in a timing-dependent manner. One possible explanation for this phenotype might be that not all members of the miR-17~92 cluster promote the same differentiation processes: Montoya et al. showed that miR-18a has an inhibitory effect on T_H17 development [237], while miR-17 family members promoted cytokine production. This indicates that different T_H17 inhibitory- and promoting mechanisms are happening at the same time and sequentially after each other in this setting, resulting in a mixed, timing-dependent phenotype. Additionally, the Montoya et al. show that during T_H17 differentiation, not all members of the cluster are regulated or processed to the same extent, resulting in differential expression of different cluster members. This suggests that during differentiation, timing of individual miRNA expression is very important, target mRNAs might be upregulated early and get repressed later, which would explain why miR1792tg cells are first delayed in Rorγt induction but later on produce more IL-17A than wt. Our observation at 24h suggests that excess miR-17~92 expression is inhibitory for T_H17 differentiation in early stages (which is consistent with the findings from Montoya at al.). However, at a later time point, the miR-17~92 is needed to some extent since miR-17~92 expression does rescue parts of the CD28ko phenotype. Of note, this is not necessarily in contrast to

what Montoya et al. showed, since they investigated day 3.5 post differentiation, which might be regulated by a different interplay of miRNAs and targets again.

Surprisingly, we observed reduced differentiation into iTreg cells in CD28ko cells and complete rescue by exogenous miR-17~92 expression. This was unexpected because so far, miR-17~92 was reported to inhibit iT_{reg} differentiation [208]. Several differences in the experimental procedure might explain for this discrepancy: first of all, the time point of harvest by Jiang et al. was at day six (other than day one to three in our experiment). Second, they only used 50U/ml of IL-2 during their culture, which is 5-fold less than what we use for iT_{reg} differentiation. Additionally, the amount of αCD28/αCD3, which is not indicated in their publication, might change the relevance of miR-17~92 cluster expression during the experiment [134]. Moreover, strong CD28 signals were shown to inhibit Foxp3 induction [287]. Assuming that miR-17~92 amplifies CD28 signaling, co-stimulation with higher concentrations than in our setting might therefore lead to different experimental outcomes.

Of note, at 72h post induction also viability was impaired in CD28ko samples of T_H17 and iT_{reg} differentiation, which was expected from the literature since CD28 was shown to induce pro-survival gene B-cell lymphoma-extra large (*Bcl-$_{XL}$*)[288]. Interestingly, exogenous miR-17~92 partially rescued viability during *in vitro* differentiation. To look into this, we used our second RNA sequencing set, for which we had extracted RNA from 24h activated wt, CD28ko, rescue, miR1792tg and miR1792lox cells (see section 6.3.4). Of note, other than the *in vitro* differentiation, these cells are only activated but not skewed into a specific subset. We confirmed with RNA sequencing data that *Bcl-$_{XL}$* expression is indeed reduced in CD28ko as compared to wt during $CD4^+$ T cell activation, but partially rescued upon exogenous miR-17~92 expression, which fits previous literature showing a beneficial effect of miR-17~92 expression on survival [208]. However, miR1792tg cells showed similar viability as wt cells, and *Bcl-$_{XL}$* expression is similar. This suggests that an expression threshold of *Bcl-$_{XL}$* might be achieved by natural miR-17~92 induction in activated wt cells, so that additional miR-17~92 from the transgene does not further increase *Bcl-$_{XL}$* expression.

Overall, these *in vitro* differentiation assays led to the conclusion that also for complex processes like T_H subset differentiation, exogenous miR-17~92 expression rescues

CD28 deficiency. Of note, the extent of rescue is time- and subset dependent, but in all subsets a rescue could be observed. This suggests that different targets are regulating processes of $CD4^+$ T cell differentiation, and all of them have their individual contribution, which emphasizes the need for the identification of miR-17~92 targets. Moreover, since all subsets were affected, this also implied that there might be targets that are common among distinct T_H subsets

7.2.3. Exogenous miR-17~92 expression rescues CD28 deficiency in $CD4^+$ T cells in vivo

The importance of CD28 as well as miR-17~92 expression for T_{FH} and germinal center differentiation has been established [134, 140, 216]. Additionally, CD44 was shown to positively correlate with miR-17~92 expression during acute viral infection [134, 216]. Similar to our *in vitro* results and in accordance to this literature, CD44 is reduced in CD28ko cells as compared to wt, and rescued upon exogenous miR-17~92 expression. If CD44 is a "side-effect" or active contributor to the enhanced activation cannot be decided at this point: CD44 cannot induce proliferation of $CD4^+$ T cells, but it was reported to promote Lck and Fyn, suggesting an influence on T cell activation [289, 290].

As expected from the literature, T_{FH} ($CD3^+CD4^+CXCR5^+Bcl\text{-}6^+ICOS^+PD\text{-}1^+$) and GC B cells ($CD19^+B220^+Fas^+GL7^+$) are reduced in CD28ko as compared to wt mice [140] in our experiments. Exogenous miR-17~92 expression restored both T_{FH} as well as GC populations. The development of GC B cells suggests for a functional T_{FH} differentiation. This raises the question whether miR-17~92 consequently also rescues the functionality of GC B cells. Additional experiments to test this would be to investigate the antibody repertoire for isotype switch and specificity, as well as cytokine secretion, e.g. IL-21. Especially, we report a strong effect of miR-17~92 expression on ICOS as well as PD-1 induction. This could be interpreted as a direct consequence of CD28 signaling independent from T_{FH} differentiation, since ICOS expression is induced on $CD4^+$ T cells via CD28 dependent and independent pathways [149, 159]. DiToro et al. recently showed that those $CD4^+$ T cells which produce IL-2 after activation induce Bcl-6 expression and give rise to T_{FH} cells, while non-producers

are not able to differentiate to T_{FH} [291]. Moreover, they reported that the most significantly enhanced gene sets in IL-2 producers were those of Myc and E2F family of TFs. This is especially interesting because these TFs are known to be involved in auto-regulatory loops with miR-17~92 [224, 225, 230], which might suggest that these cells express miR-17~92, promoting IL-2. This might represent another, so far unknown possibility of how miR-17~92 contributes to increased T_{FH} differentiation. DiToro et al. further propose that their phenotype results from thresholds in T cell activation, with stronger activation leading to IL-2 production and T_{FH} differentiation. Considering this literature, we suggest that (among other effects, like e.g. the targeting of Rorα [134]) miR-17~92 enhances T cell activation with cell-intrinsic IL-2 production, which allows wt, miR1792tg and rescue cells to acquire T_{FH} phenotype, and accordingly reduces T_{FH} differentiation in CD28ko and miR1792lox.

Other than in our *in vitro* experiments, IFNγ production was not overcompensated in the rescue cells as compared to CD28ko cells, which might be due to the more physiologic differentiation conditions *in vivo*, or the different time point that we investigate in this experiment. Similar to the *in vitro* data, also *in vivo* we can speculate that reduced IL-2 production in CD28ko mice leads to reduced IFNγ production. Moreover, for T_H1 differentiation, we assume that CD44 upregulation in wt and rescue cells might enhance differentiation in this setting, since Baaten et al. reported that CD44 expression promoted T_H1 effector cell survival [292].

Overall, we concluded from our experiments that also *in vivo*, exogenous miR-17~92 expression compensates for CD28 deficiency in terms of T_{FH} and T_H1 differentiation.

7.2.4. Exogenous miR-17~92 expression rescue effect is CD4$^+$ T cell intrinsic

One caveat of our rescue mouse model is that CD4cre expression might lead to side effects in cell populations other than CD4$^+$ T cells, raising the question if the rescue effect that we observed in our *in vivo* experiments was CD4$^+$ T cell intrinsic. We found fewer Vα2$^+$Vβ8.3$^+$ CD28ko cells in all investigated organs after adoptive transfer of SMARTA$^+$ cells with subsequent LCMV infection. Importantly, the population was rescued by exogenous miR-17~92 expression. Again, in addition to the cell-intrinsic

proliferation defect which we showed in previous experiments, this effect might be mediated by IL-2: IL-2 production in recipient CD28ko mice is reduced [162], so that IL-2 produced by donor cells is needed for proper expansion. Since our *in vitro* experiments showed that IL-2 production is reduced in CD28ko but rescued by exogenous miR-17~92 expression, we propose that expansion might also be reduced due to low IL-2 abundance in CD28ko recipients. Moreover, $V\alpha2^+V\beta8.3^+$ CD28ko cells were reduced in their CD44 expression as compared to wt, which was fully rescued by exogenous miR-17~92 expression. This argues that not only expansion, but also activation is diminished in CD28ko cells. Again, further experiments will be interesting to elucidate if CD44 expression is actually a consequence or a precondition for T cell differentiation at this point, and also if this is a direct or an indirect effect of miR-17~92 expression. Possible experiments to test this would be the use of CD44 blocking antibodies or, in a more laborious approach, CD44 gene targeting.

So far, we concluded from these transfer experiments that the rescue effect of miR-17~92 expression was $CD4^+$ T cell intrinsic. Moreover, as mentioned in the previous section, effects on IL-2 production could explain for some, but not all of the results. We could test this by the addition of IL-2 blocking antibodies or IL-2 injections. However, we set priority on elucidating if the rescue was phenotypic or actually mediated in the transcriptome, which on one hand might show how IL-2 is regulated by miR-17~92 but on the other hand also reveal additional pathways.

7.3. Molecular mechanism of the rescue effect

Many targets for miR-17~92 have been described and validated so far, among them *PTEN* [218, 232], *Klf2* [242], *TGFβRII* [208] and *PHLPP2* [216]. Some of them might also contribute to our phenotype, explaining for the effect of miR-17~92 on T cell activation. Most likely, multiple targets cooperate in their function, resulting in a complex network of parallel processes to synergistically amplify activation. Clearly, PI3K is established as a pathway that is promoted by miR-17~92 e.g. through repression of *PTEN*. However, the possibility remained that there are still unknown targets that regulate other pathways, which were not detected in previous screenings e.g. due to different experimental setup.

We show that miR-17~92 expression shapes the transcriptome during $CD4^+$ T cell activation. Importantly, changes start at 24h post activation and possibly have secondary effects so that even more genes are differentially expressed at 48h. With GSEA we detected that cytokines are promoted by miR-17~92, which in principle was known before [208, 231, 234, 235]. However, what has not been addressed before is that different cytokines can be promoted by one common pathway, which is the calcineurin-NFAT axis [128]. Of note, differences in IL-2 mRNA expression at 24h or 48h are not striking in this heatmap. This might be reasoned by different regulatory mechanisms of IL-2 production as previously mentioned, but also in different experimental conditions: ELISA at 48h was measured from culture supernatants without the addition of exogenous IL-2 at the beginning, so that intrinsic IL-2 production by each cell type might result in auto-stimulatory loops, which then amplified the differences.

7.3.1. Identification of miR-17~92 bona fide canonical target genes during activation

We used stringent criteria to identify *bona fide* canonical target genes in our list of thousands of genes which were identified by RNA sequencing. This came at the cost of excluding target genes that might be relevant in some “unconventional” way. For example, with this analysis we excluded so-called non-canonical miRNA targets: the TargetScan criteria only allows conserved perfect seed matches. However, miRNAs

were shown to also bind to RNA with bulges and wobbles, thus non-perfect seed matches. Moreover, the targeting can happen also outside the 3'UTR and in a RISC-independent manner [293]. Thus, our data set theoretically allows also for the identification of non-canonical targets, however we prioritized the canonical targets. With contrasts between activated miR1792lox and wt as well as miR1792tg and wt, we show that RISC-bound genes from each seed family are increased in their FC in the absence of miR-17~92, and also decreased in FC in miR-17~92 overexpression. Notably, distinct miRNA seed families show slightly different behavior: while miR-17 seed family members shift very clearly, the shift is less pronounced in miR-18, miR-19 and miR-92 seed families. Different explanations might account for this phenotype. First of all, the regulation of miRNA targets is context dependent so that one seed family or miRNA might be more important in a specific setting as compared to a different miRNA of the same cluster. Second, there might be less genes expressed that are targeted by a specific seed family in this setting. Third, the efficiency of targeting (i.e. resulting in a change in expression of the targeted gene) also depends on the target abundance: Mukherji et al. showed that low abundant targets can be 2-fold suppressed effectively with only one miRNA binding site, and seven binding sites reduce the target 10-fold. However, if the target is highly expressed, no matter if one or seven binding sites were present, only a 2-fold reduction was achieved [187]. With this, we can clearly say that miRNAs set thresholds in gene expression, which enables them on one hand to mediate on-off switch of genes at low target expression but also fine-tuning at high target expression. Additionally, the individual members of miR-17~92 might be differentially regulated, resulting in different abundance and consequently differential regulation of the specific target genes [216, 237]. The contrasts of naïve cells were not shifted for the miR1792lox vs. wt. We might speculate from this data that miR-17~92 expression is not essential in naïve $CD4^+$ T cells, which would also fit the fact that the cluster expression is only induced upon CD28 co-stimulation [215]. Alternatively, since the literature suggests redundancy for some targets, paralogue clusters might compensate for miR-17~92 function in the naïve setting [24]. Other than suggested by PCA, the CDF plot for the contrast between naïve miR1792tg and wt cells shows a shift for miR-17, miR-19 and miR-92 family members, indicating that some target genes are differentially expressed in naïve $CD4^+$ T cells as

well. However, we focus on the analysis of genes that are differentially expressed during activation. The difference between CDF plot and PCA might originate from less restrictions in the PCA: the CDF plots focus on genes which are also detected in the AHC.

Some more targets might be excluded with the EISA criterium: if a gene is regulated transcriptionally as well as post-transcriptionally, it is also excluded from our analysis. Moreover, genes that are targeted by miRNAs from paralogue clusters might not be contained in our list, since redundant function might prevent changes in the miR1792lox vs. wt situation, while there might be a significant change in the miR1792tg vs wt contrast.

Any gene in the list of 125 canonical *bona fide* target genes might contribute to the rescue phenotype. However, this does not imply that the changes in expression of these genes introduced by miRNA in this setting are actually biologically relevant. As mentioned previously, small changes at threshold expression level might have a bigger impact as compared to larger changes at higher expression. Importantly, some of these genes also harbor multiple seed sequences for different family members, which also opens possibilities for multiple regulatory mechanisms that depending on the abundance of individual miRNAs. Another effect that we do not cover in this project is the possibility of selective avoidance, which is the shortening of the 3'UTR during activation and proliferation, leading to the loss of miRNA binding sites and therefore escape of repression in ongoing activation. In our *bona fide* canonical target gene list we find known and validated target genes like *TGFβRII* [208] and *PHLPP2* [216], which serve as positive controls for our analysis. Of note, we do not expect all of the "typical" target genes in this list since timing and experimental conditions might be different from the settings in which they were published. However, the question remained if the transcriptome of CD28ko cells was rescued by exogenous miR-17~92 expression as well, and if the genes that we identified as *bona fide* canonical target genes might actively contribute to the rescue.

7.3.2. Exogenous miR-17~92 expression partially rescues the transcriptome of CD28ko cells

CD28 was shown to be an essential contributor to shaping the transcriptome during $CD4^+$ T cell activation [273]. We confirmed these data and additionally demonstrate that exogenous miR-17~92 expression partially rescues the transcriptome of CD28ko cells. Furthermore, even if miR1792lox cells phenocopied CD28ko cells in $CD4^+$ T cell activation, their transcriptome was markedly different. Following our hypothesis that exogenous miR-17~92 expression amplifies CD28-dependent $CD4^+$ T cell activation, we note that miR1792tg cells (most activated) showed the biggest difference to CD28ko (least activated) cells. Importantly, the *bona fide* canonical target genes that we identified with the previous RNA sequencing data set were also dysregulated in the CD28ko vs. wt contrast, which argues that these genes are regulated by CD28 as well as miR-17~92. The contrast of rescue vs. wt samples shows that the same genes are also rescued in their expression FC by exogenous miR-17~92 expression. This confirms that these target genes actually do mediate the rescue that we observe phenotypically also in the transcriptome. Of note, the miR-18 seed family again shows a milder phenotype, indicating that genes which are targeted by this family are not fully rescued by exogenous miR-17~92 expression. Like before, differential expression of individual miRNAs and timing might account for this difference. Moreover, miR-18 has been reported to antagonize the function of other miR-17~92 family members [237], which might also be the case in this setting. Since also in our target gene list we only find five genes that are targeted by a miR-18 seed family member, most likely target genes of miR-18 are not as relevant in this setting as targets of other seed families.

Most importantly, we conclude from this dataset that not only the CD28 signaling dependent induction of transcription contributes to $CD4^+$ T cell activation, but also the repression of genes which is mediated by miR-17~92. This concept resembles of T_H differentiation which depends on the careful co-regulation of distinct effectors [121].

7.3.3. Target gene RCAN3 expression is dependent on CD28 or miR-17~92 expression

As mentioned previously, the NFAT pathway is an interesting candidate to investigate for target genes since it is one common factor promoting cytokines of different T_H subsets [128]. Increased NFAT activity might also explain increased expression of ICOS: an elegant study performed by Tan et al. investigated different TCR and CD28 dependent signaling molecules for their potential to induce ICOS expression. Using selective chemical inhibitors, the authors found that Fyn promotes ICOS expression via NFATc2, while MEK and Erk also induce ICOS in an independent pathway [149]. Within our list of 125 *bona fide* canonical target genes, we identified *RCAN3*, a regulator of calcineurin activity, as a target gene that might influence T cell activation by regulating NFAT. Among all different miRNA binding sites in the 3'UTR of *RCAN3*, only the miR-17-5p/20-5p/93-5p/106-5p site was bound to Ago2, indicating that this is the only active miRNA target site in this setting. qPCR confirms that *RCAN3* mRNA is negatively correlated with miR-17~92 expression. Interestingly, RCAN3 protein abundance was increased in CD28ko and miR1792lox while wt, rescue and miR1792tg cells were comparable in their expression. This suggests that differences in mRNA abundance due to miRNA targeting translate into protein. However, it also indicates that a certain miR-17~92 expression threshold is sufficient to repress *RCAN3*. In αCD3/αCD28 activated wt cells, this is reached by natural miR-17~92 induction while exogenous miR-17~92 in rescue cells reduces RCAN3 expression.

The gold standard for the ultimate validation of RCAN3 would be the interruption of the miR-17~92-RCAN3-calcineurin/NFAT pathway. Distinct approaches for this are possible, from the complete RCAN3ko to mutations in the calcineurin interaction motif or mutation of the miRNA target site. Canaider et al. successfully knocked out RCAN3 expression in HUVEC cells using small interfering RNA (siRNA) [294], which reduced proliferation. We attempted to do the same in primary $CD4^+$ T cells, however in our setting we could not measure an impact of RCAN3 siRNA on any of our parameters. Nevertheless, it was unclear if the experimental set up was suitable for our case, since $CD4^+$ T cells need to get activated before they can be electroporated. This suggests the use of gene editing to reach a more robust knockdown, which allows

for resting the cells before analysis. Different targeting strategies are possible for the gene editing approach. Importantly, several publications [294, 295] have shown that Exon 1 of *RCAN3* can be non-coding, making it unattractive for gene editing purposes. We rather suggest to target the region harboring the CIC motif within Exon 5, which was found to be the interacting domain for calcineurin [112]. Preliminary results suggest that editing efficiency of 50-60% can be achieved in this locus. Further experiments will show if these mutations have any biological effect, e.g. increase IL-2 production.

Another approach is the mutation of the miR-17 seed sequence of *RCAN3* to investigate the functional importance of this miRNA:mRNA interaction [278, 296]. For this, we suggest to use rescue cells and target their miR-17 seed sequence in the *RCAN3* 3'UTR. This should reduce the *RCAN3* targeting, and abolish the rescue affect. However, also this experiment will need careful optimization: with the use of classical Cas9 derived from *S.pyogenes*, we are dependent on the abundance of the protospacer adjacent motif (PAM) sequence NGG directly downstream of the target locus [297, 298], which will induce a double strand break in the DNA 4bp upstream of the PAM. The challenge at this point is that the seed sequence is only 8nt in length, and the PAMs around this seed allow only double strand breaks right after and before the seed. Since disruption of the seed or deletion is needed, this suggests the use of a multiplexing approach, introducing two double strand breaks at both sides of the seed, with the chance of recombination without the seed. However, this might result in a mild phenotype: due to redundancy of miRNA function, the phenotypic consequences of a single miRNA:target disruption can be very minor [299].

Over all, these experiments to knock out *RCAN3* are possible but will need careful optimization and control of the experimental setup. So far, we suggest that *RCAN3* is most likely targeted by miR-17, leading to differences in mRNA and protein expression depending on CD28 and/or miR-17~92 expression.

7.3.4. Exogenous miR-17~92 expression decreases sensitivity to Cyclosporin A

The activity of calcineurin leads to NFAT de-phosphorylation, translocation to the nucleus [51] and initiation of transcriptional activation. Therefore, the consequences of increased (or decreased) RCAN3 expression are crucial for $CD4^+$ T cell activation and differentiation. Current immunosuppressive drugs like CsA and FK506 target $CD4^+$ T cell activation by inhibition of the enzymatic activity of calcineurin [300]. This leads to a very efficient inhibition of the NFAT pathway and T cell activation, however it comes at the cost of severe side effects [301]. We hypothesized that manipulation of a natural calcineurin inhibitor like RCAN3 with miR-17~92 modifies the sensitivity to CsA. Indeed, we demonstrate that CD28ko cells react more sensitively to CsA than wt and rescue cells, which was also manifested in decreased nuclear localization of NFAT. CD28 so far had only been shown to be essential for nuclear localization of NFκB [162], and it had been demonstrated before that NFAT dependent transcription of IL-2 was abolished by CsA [302, 303]. Surprisingly, nuclear localization of NFAT in CD28ko was only partially reduced in low concentrations of CsA. However, this seemed to be sufficient to reduce activation.

Usually, cytokines bind to their corresponding receptors which signal via STAT proteins to initiate transcription of TFs and cytokines, which then act in a feedback loop [125, 284, 285, 304]. We suggest that this loop is interrupted in CD28ko cells through increased RCAN3 expression, resulting in decreased NFAT nuclear localization and reduced cytokine production. With exogenous miR-17~92 expression, leading to targeting and repression of RCAN3, NFAT activity is increased, cytokine expression is promoted and the loop is at least partially restored.

These experiments indicate that miR-17~92 and CD28 expression are contributing factors to CsA responsiveness. We propose that this effect is mediated by RCAN3 repression, which consequently promotes calcineurin activity. This discovery bears great potential for development of new therapeutic approaches in immunosuppression as will be discussed in the next section.

7.4. Relevance and future perspective

The relevance of CD28 for immune therapy is diverse. On one hand, it has been shown to be essential for the efficacy of PD-1 checkpoint blockade [147, 148] and immune suppression [305] but also lately in the development of chimeric antigen receptor (CAR) T cells, intracellular CD28 signaling domains have been shown to be crucial for function [306]. The role of miR-17~92 in the context of CD28 that we demonstrated in this thesis therefore bears great potential for the development of new therapies.

However, the translation of our findings in mice to human is delicate and will need detailed investigation. The exact translation of miRNA findings from mouse to human is usually difficult. Expression of targets, miRNAs and conservation has to be verified [192, 307]. miR-17~92 is highly conserved between mice and humans, has been shown to be expressed in human $CD4^+$ T cells, and it was demonstrated to be important for the human $CD4^+$ T cell function (see section 3.2.3.4). For example, in Jurkat cells, an immortalized cell line of human T lymphocytes, transgenic expression of miR-17~92 led to increased IL-2 production [308]. We therefore expect that the role for miR-17~92 in CD28 dependent co-stimulation of human $CD4^+$ T cells is similarly important as in murine $CD4^+$ T cells, although this still has to be investigated. The expression of target gene *RCAN3* is a separate question. Interestingly, more than 20 (theoretical) splice variants of this protein were reported so far, however some of them in tissue and context dependent manner [309]. It will therefore be crucial to determine which RCAN3 variant is present, if the variant is changed upon activation, and if miR-17 also suppresses RCAN3 in human $CD4^+$ T cells. Moreover, assuming that this will be the case, the sensitivity to calcineurin inhibitors need to be investigated.

The calcineurin inhibitors FK506 (Tacrolimus) and CsA have been used for treatment in the field of organ transplantation for more than 30 years [54]. Both of them share their pharmacodynamic property of inhibition of calcineurin [310]. However, even if great success in terms of prevention of organ rejection are reached with these calcineurin inhibitors, it comes at the cost of nephrotoxicity [311] as well as neurotoxicity [312]. The two inhibitors differ in their detailed toxicity profile, however both of them induce severe side effects. Even if many attempts for therapy improvement have been taken in the last years, the complete avoidance of calcineurin

inhibitors comes with significantly higher risk of rejection and/or graft loss [54]. With our results showing that miR-17~92 promoting calcineurin-NFAT, we identify a new potential target for calcineurin inhibition. The idea of promoting RCAN3 activity instead of inhibiting calcineurin was already proposed when the molecule was described to inhibit calcineurin activity [112]. We suggest to target the miRNA which targets RCAN3 for immune modulation: through interfering with miR-17 expression, the natural inhibition of calcineurin by RCAN3 might be enhanced. Several mechanisms of how targeting of miRNAs could be achieved in patients have been suggested [313, 314], e.g. miRNA sponges, antisense oligonucleotides and small molecule inhibitors. The first miRNA drug, which is miravirsen targeting miR-122 in Hepatitis C treatment, is currently in clinical trials [315, 316]. Thus, targeting of miRNAs in patients seems possible, though careful investigation and monitoring of potential new side effects will be crucial.

Another possibility for application would be the exploitation of increased resistance to calcineurin inhibitors due to exogenous miR-17~92 expression. This is especially interesting in the case of transplantation of engineered cells, e.g. CAR T cells, to immunosuppressed patients. Transgenic expression of miR-17~92 in CAR T cells was already shown to augment proliferation, IFNγ and targeting efficacy [317]. In addition to the beneficial effect of miR-17~92 expression leading to “more activation”, we expect to achieve resistance to ongoing immunosuppressive medication, paving the way for CAR T cell therapy in organ transplant recipients.

Next to the potential of RCAN3 and NFAT as new targets of miR-17~92, our data also provide the potential for further research. It will be interesting to look into our *bona fide* canonical target gene list and elucidate their role in T cell activation. For this, the use of focused candidate gene deletion with CRISPR/Cas9 is the most promising. Furthermore, as already mentioned, we restrict our analysis to canonical targets, while non-canonical targets might be important for $CD4^+$ T cell activation as well.

After all, we provide strong evidence that miR-17~92 not only promotes PI3K pathway via *PTEN* repression [218, 232] but also promotes NFAT pathway via RCAN3 targeting. It is important to keep in mind that rather the combination of pathways than a single target finally result in the rescue of CD28ko cells. We therefore suggest to also

investigate combinations of gene deletions to address their cooperative role and synergistic effects during $CD4^+$ T cell activation in the future.

8. Conclusion and model

In the present thesis project, we showed that

1. miR-17~92 is an important modulator of CD28 co-stimulation
2. exogenous miR-17~92 expression can rescue CD28 deficiency *in vitro* and *in vivo*
3. *bona fide* canonical target genes are regulated by miR-17~92 and CD28, and the rescue effect is mediated at transcriptome level
4. not only induction of expression, but also repression of genes is important during CD28 co-stimulation
5. miR-17~92 promotes calcineurin/NFAT most likely by repressing calcineurin inhibitor *RCAN3*, with modulates sensitivity to calcineurin inhibitors

Our results are surprising regarding the fact that other than conventional TFs, miRNAs are often seen as fine tuners of expression rather than master regulators of gene expression [299]. Importantly, we show that miR-17~92 is an essential contributor to CD28 co-stimulation, which possibly results from the sum of different targets and pathways regulated by miR-17~92, of which so far only the PI3K pathway has been known. We show that also the NFAT pathway is regulated by miR-17~92, most likely by targeting *RCAN3*. This leads to increased expression of NFAT-induced genes, e.g. cytokines as illustrated in Figure 39.

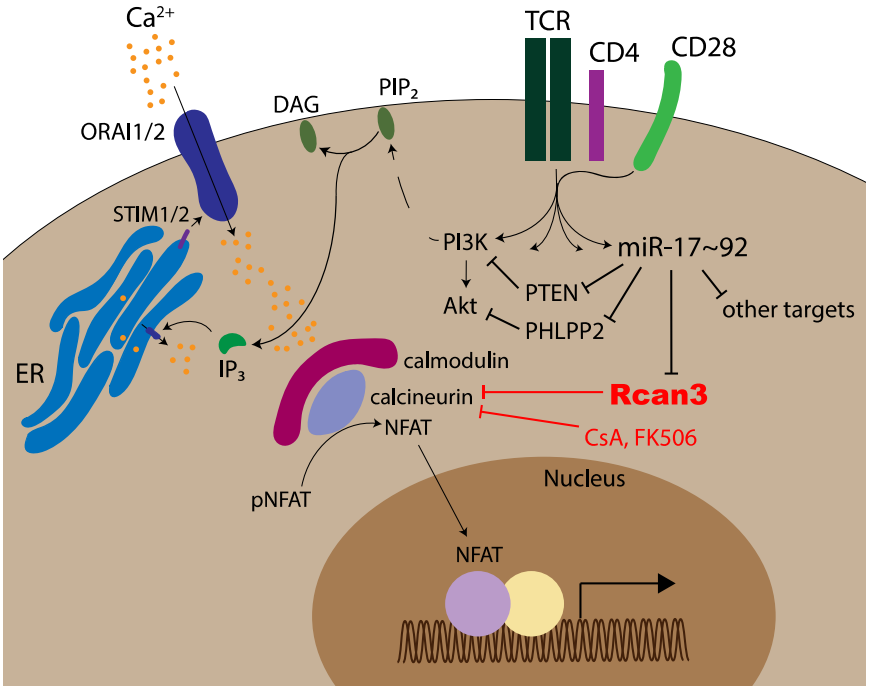

Figure 39. Suggested model for miR-17~92 influence on NFAT pathway

$CD4^+$ T cell activation with CD28 co-stimulation initiates many different processes, among which is the activation of PI3K, recruitment of PLCγ and cleavage of PIP_2 to DAG and IP_3. IP_3 binds to Ca^{2+} channels in the ER membrane, releasing Ca^{2+} from the ER stores. This is sensed by STIM1/2, which therefore interact with ORAI1/2. These change their conformation, allowing Ca^{2+} influx and activation of calcineurin. Calcineurin de-phosphorylates NFAT, which translocates to the nucleus where it dimerizes with other factors to initiate transcription. Calcineurin is inhibited by immunosuppressive drugs like CsA and FK506. miR-17~92 is also induced with CD28 co-stimulation and regulates different targets, e.g. PTEN and PHLPP2 which in turn are inhibitors of the PI3K pathway. We newly suggest RCAN3 as a target for miR-17~92, which is a natural inhibitor of calcineurin. Thereby, miR-17~92 indirectly promotes NFAT activity and T cell activation.

9. Disclosure

A patent application related to these findings was filed.

10. References

1. Bretscher, P. and M. Cohn, *A theory of self-nonself discrimination.* Science, 1970. **169**(3950): p. 1042-9.
2. Lafferty, K.J. and A.J. Cunningham, *A new analysis of allogeneic interactions.* Aust J Exp Biol Med Sci, 1975. **53**(1): p. 27-42.
3. Schwartz, R.H., et al., *T-cell clonal anergy.* Cold Spring Harb Symp Quant Biol, 1989. **54 Pt 2**: p. 605-10.
4. Jenkins, M.K., et al., *Inhibition of antigen-specific proliferation of type 1 murine T cell clones after stimulation with immobilized anti-CD3 monoclonal antibody.* J Immunol, 1990. **144**(1): p. 16-22.
5. June, C.H., et al., *The B7 and CD28 receptor families.* Immunol Today, 1994. **15**(7): p. 321-31.
6. Truitt, K.E., C.M. Hicks, and J.B. Imboden, *Stimulation of CD28 triggers an association between CD28 and phosphatidylinositol 3-kinase in Jurkat T cells.* J Exp Med, 1994. **179**(3): p. 1071-6.
7. Prasad, K.V., et al., *T-cell antigen CD28 interacts with the lipid kinase phosphatidylinositol 3-kinase by a cytoplasmic Tyr(P)-Met-Xaa-Met motif.* Proc Natl Acad Sci U S A, 1994. **91**(7): p. 2834-8.
8. August, A. and B. Dupont, *CD28 of T lymphocytes associates with phosphatidylinositol 3-kinase.* Int Immunol, 1994. **6**(5): p. 769-74.
9. Kapeller, R. and L.C. Cantley, *Phosphatidylinositol 3-kinase.* Bioessays, 1994. **16**(8): p. 565-76.
10. Meuer, S.C., et al., *Clonotypic structures involved in antigen-specific human T cell function. Relationship to the T3 molecular complex.* J Exp Med, 1983. **157**(2): p. 705-19.
11. Reinherz, E.L., S.C. Meuer, and S.F. Schlossman, *The Delineation of Antigen Receptors on Human Lymphocytes-T.* Immunology Today, 1983. **4**(1): p. 5-8.
12. Reth, M., *Antigen Receptor Tail Clue.* Nature, 1989. **338**(6214): p. 383-384.
13. Baker, P.E., S. Gillis, and K.A. Smith, *Monoclonal Cytolytic T-Cell Lines.* Journal of Experimental Medicine, 1979. **149**(1): p. 273-278.
14. Chu, K. and D.R. Littman, *Requirement for kinase activity of CD4-associated p56lck in antibody-triggered T cell signal transduction.* J Biol Chem, 1994. **269**(39): p. 24095-101.
15. D'Oro, U. and J.D. Ashwell, *Cutting edge: The CD45 tyrosine phosphatase is an inhibitor of Lck activity in thymocytes.* Journal of Immunology, 1999. **162**(4): p. 1879-1883.
16. Bergman, M., et al., *The Human P50(Csk) Tyrosine Kinase Phosphorylates P56(Lck) at Tyr-505 and down Regulates Its Catalytic Activity.* Embo Journal, 1992. **11**(8): p. 2919-2924.
17. Pelosi, M., et al., *Tyrosine 319 in the interdomain B of ZAP-70 is a binding site for the Src homology 2 domain of Lck.* Journal of Biological Chemistry, 1999. **274**(20): p. 14229-14237.
18. Au-Yeung, B.B., et al., *The structure, regulation, and function of ZAP-70.* Immunol Rev, 2009. **228**(1): p. 41-57.
19. Zhang, W., et al., *LAT: the ZAP-70 tyrosine kinase substrate that links T cell receptor to cellular activation.* Cell, 1998. **92**(1): p. 83-92.
20. Okkenhaug, K. and B. Vanhaesebroeck, *PI3K in lymphocyte development, differentiation and activation.* Nat Rev Immunol, 2003. **3**(4): p. 317-30.
21. Raab, M., et al., *p56Lck and p59Fyn regulate CD28 binding to phosphatidylinositol 3-kinase, growth factor receptor-bound protein GRB-2, and T cell-specific protein-tyrosine kinase ITK: implications for T-cell costimulation.* Proc Natl Acad Sci U S A, 1995. **92**(19): p. 8891-5.
22. Auger, K.R., et al., *Phosphatidylinositol 3-Kinase and Its Novel Product, Phosphatidyl-Inositol 3-Phosphate, Are Present in Saccharomyces-Cerevisiae.* Journal of Biological Chemistry, 1989. **264**(34): p. 20181-20184.
23. Thompson, C.B., et al., *CD28 activation pathway regulates the production of multiple T-cell-derived lymphokines/cytokines.* Proc Natl Acad Sci U S A, 1989. **86**(4): p. 1333-7.
24. Acuto, O. and F. Michel, *CD28-mediated co-stimulation: a quantitative support for TCR signalling.* Nat Rev Immunol, 2003. **3**(12): p. 939-51.
25. Williamson, J.R., *Inositol Trisphosphate and Diacylglycerol as Intracellular Second Messengers.* Federation Proceedings, 1985. **44**(3): p. R9-R9.
26. Downward, J., et al., *Stimulation of p21ras upon T-cell activation.* Nature, 1990. **346**(6286): p. 719-23.

27. Roskoski, R., Jr., *ERK1/2 MAP kinases: structure, function, and regulation.* Pharmacol Res, 2012. **66**(2): p. 105-43.
28. Jain, J., et al., *Nuclear factor of activated T cells contains Fos and Jun.* Nature, 1992. **356**(6372): p. 801-4.
29. Lin, X., et al., *Protein kinase C-theta participates in NF-kappa B activation induced by CD3-CD28 costimulation through selective activation of I kappa B kinase beta.* Molecular and Cellular Biology, 2000. **20**(8): p. 2933-2940.
30. Mor, A., M.L. Dustin, and M.R. Philips, *Small GTPases and LFA-1 reciprocally modulate adhesion and signaling.* Immunol Rev, 2007. **218**: p. 114-25.
31. Menasche, G., et al., *RIAM links the ADAP/SKAP-55 signaling module to Rap1, facilitating T-cell-receptor-mediated integrin activation.* Molecular and Cellular Biology, 2007. **27**(11): p. 4070-4081.
32. Ma, Q., et al., *Activation-induced conformational changes in the I domain region of lymphocyte function-associated antigen 1.* J Biol Chem, 2002. **277**(12): p. 10638-41.
33. Burkhardt, J.K., E. Carrizosa, and M.H. Shaffer, *The actin cytoskeleton in T cell activation.* Annu Rev Immunol, 2008. **26**: p. 233-59.
34. Abe, K., et al., *Vav2 is an activator of Cdc42, Rac1, and RhoA.* Journal of Biological Chemistry, 2000. **275**(14): p. 10141-10149.
35. Pearce, E.L., *Metabolism in T cell activation and differentiation.* Curr Opin Immunol, 2010. **22**(3): p. 314-20.
36. Kane, L.P. and A. Weiss, *The PI-3 kinase/Akt pathway and T cell activation: pleiotropic pathways downstream of PIP3.* Immunol Rev, 2003. **192**: p. 7-20.
37. Frauwirth, K.A., et al., *The CD28 signaling pathway regulates glucose metabolism.* Immunity, 2002. **16**(6): p. 769-77.
38. Gamper, C.J. and J.D. Powell, *All PI3Kinase signaling is not mTOR: dissecting mTOR-dependent and independent signaling pathways in T cells.* Front Immunol, 2012. **3**: p. 312.
39. Imboden, J.B. and J.D. Stobo, *Transmembrane signalling by the T cell antigen receptor. Perturbation of the T3-antigen receptor complex generates inositol phosphates and releases calcium ions from intracellular stores.* J Exp Med, 1985. **161**(3): p. 446-56.
40. Feske, S., *Calcium signalling in lymphocyte activation and disease.* Nat Rev Immunol, 2007. **7**(9): p. 690-702.
41. Stathopulos, P.B., et al., *Structural and mechanistic insights into STIM1-mediated initiation of store-operated calcium entry.* Cell, 2008. **135**(1): p. 110-22.
42. Hogan, P.G., R.S. Lewis, and A. Rao, *Molecular basis of calcium signaling in lymphocytes: STIM and ORAI.* Annu Rev Immunol, 2010. **28**: p. 491-533.
43. Liou, J., et al., *STIM is a Ca2+ sensor essential for Ca2+-store-depletion-triggered Ca2+ influx.* Curr Biol, 2005. **15**(13): p. 1235-41.
44. Muik, M., et al., *Dynamic coupling of the putative coiled-coil domain of ORAI1 with STIM1 mediates ORAI1 channel activation.* J Biol Chem, 2008. **283**(12): p. 8014-22.
45. Li, Z., et al., *Mapping the interacting domains of STIM1 and Orai1 in Ca2+ release-activated Ca2+ channel activation.* J Biol Chem, 2007. **282**(40): p. 29448-56.
46. Feske, S., et al., *A mutation in Orai1 causes immune deficiency by abrogating CRAC channel function.* Nature, 2006. **441**(7090): p. 179-85.
47. Vaeth, M., et al., *ORAI2 modulates store-operated calcium entry and T cell-mediated immunity.* Nat Commun, 2017. **8**: p. 14714.
48. Prakriya, M., et al., *Orai1 is an essential pore subunit of the CRAC channel.* Nature, 2006. **443**(7108): p. 230-3.
49. Putney, J.W., Jr., *A model for receptor-regulated calcium entry.* Cell Calcium, 1986. **7**(1): p. 1-12.
50. Shaw, P.J. and S. Feske, *Physiological and pathophysiological functions of SOCE in the immune system.* Front Biosci (Elite Ed), 2012. **4**: p. 2253-68.
51. Jain, J., et al., *The T-cell transcription factor NFATp is a substrate for calcineurin and interacts with Fos and Jun.* Nature, 1993. **365**(6444): p. 352-5.
52. Liu, J., et al., *Calcineurin is a common target of cyclophilin-cyclosporin A and FKBP-FK506 complexes.* Cell, 1991. **66**(4): p. 807-15.
53. Loh, C., et al., *Calcineurin binds the transcription factor NFAT1 and reversibly regulates its activity.* J Biol Chem, 1996. **271**(18): p. 10884-91.

54. Azzi, J.R., M.H. Sayegh, and S.G. Mallat, *Calcineurin inhibitors: 40 years later, can't live without.* J Immunol, 2013. **191**(12): p. 5785-91.
55. Desvignes, L., et al., *STIM1 controls T cell-mediated immune regulation and inflammation in chronic infection.* J Clin Invest, 2015. **125**(6): p. 2347-62.
56. Oh-Hora, M., et al., *Dual functions for the endoplasmic reticulum calcium sensors STIM1 and STIM2 in T cell activation and tolerance.* Nat Immunol, 2008. **9**(4): p. 432-43.
57. Shaw, J.P., et al., *Identification of a putative regulator of early T cell activation genes.* Science, 1988. **241**(4862): p. 202-5.
58. Flanagan, W.M., et al., *Nuclear association of a T-cell transcription factor blocked by FK-506 and cyclosporin A.* Nature, 1991. **352**(6338): p. 803-7.
59. Crist, S.A., D.L. Sprague, and T.L. Ratliff, *Nuclear factor of activated T cells (NFAT) mediates CD154 expression in megakaryocytes.* Blood, 2008. **111**(7): p. 3553-61.
60. Zanoni, I., et al., *CD14 regulates the dendritic cell life cycle after LPS exposure through NFAT activation.* Nature, 2009. **460**(7252): p. 264-8.
61. Shukla, U., et al., *Tyrosine phosphorylation of 3BP2 regulates B cell receptor-mediated activation of NFAT.* J Biol Chem, 2009. **284**(49): p. 33719-28.
62. Muller, M.R., et al., *Requirement for balanced Ca/NFAT signaling in hematopoietic and embryonic development.* Proc Natl Acad Sci U S A, 2009. **106**(17): p. 7034-9.
63. Heit, J.J., et al., *Calcineurin/NFAT signalling regulates pancreatic beta-cell growth and function.* Nature, 2006. **443**(7109): p. 345-9.
64. Negishi-Koga, T. and H. Takayanagi, *Ca2+-NFATc1 signaling is an essential axis of osteoclast differentiation.* Immunol Rev, 2009. **231**(1): p. 241-56.
65. Northrop, J.P., et al., *NF-AT components define a family of transcription factors targeted in T-cell activation.* Nature, 1994. **369**(6480): p. 497-502.
66. Hoey, T., et al., *Isolation of two new members of the NF-AT gene family and functional characterization of the NF-AT proteins.* Immunity, 1995. **2**(5): p. 461-72.
67. Lopez-Rodriguez, C., et al., *NFAT5, a constitutively nuclear NFAT protein that does not cooperate with Fos and Jun.* Proc Natl Acad Sci U S A, 1999. **96**(13): p. 7214-9.
68. Macian, F., *NFAT proteins: key regulators of T-cell development and function.* Nat Rev Immunol, 2005. **5**(6): p. 472-84.
69. Klee, C.B., H. Ren, and X. Wang, *Regulation of the calmodulin-stimulated protein phosphatase, calcineurin.* J Biol Chem, 1998. **273**(22): p. 13367-70.
70. Muller, M.R. and A. Rao, *NFAT, immunity and cancer: a transcription factor comes of age.* Nat Rev Immunol, 2010. **10**(9): p. 645-56.
71. Luo, C., et al., *Recombinant NFAT1 (NFATp) is regulated by calcineurin in T cells and mediates transcription of several cytokine genes.* Mol Cell Biol, 1996. **16**(7): p. 3955-66.
72. Garcia-Cozar, F.J., et al., *Two-site interaction of nuclear factor of activated T cells with activated calcineurin.* J Biol Chem, 1998. **273**(37): p. 23877-83.
73. Shaw, K.T., et al., *Immunosuppressive drugs prevent a rapid dephosphorylation of transcription factor NFAT1 in stimulated immune cells.* Proc Natl Acad Sci U S A, 1995. **92**(24): p. 11205-9.
74. Okamura, H., et al., *Concerted dephosphorylation of the transcription factor NFAT1 induces a conformational switch that regulates transcriptional activity.* Mol Cell, 2000. **6**(3): p. 539-50.
75. Chen, L., et al., *Structure of the DNA-binding domains from NFAT, Fos and Jun bound specifically to DNA.* Nature, 1998. **392**(6671): p. 42-8.
76. Graef, I.A., et al., *Evolutionary relationships among Rel domains indicate functional diversification by recombination.* Proc Natl Acad Sci U S A, 2001. **98**(10): p. 5740-5.
77. Macian, F., C. Lopez-Rodriguez, and A. Rao, *Partners in transcription: NFAT and AP-1.* Oncogene, 2001. **20**(19): p. 2476-89.
78. Mognol, G.P., et al., *Cell cycle and apoptosis regulation by NFAT transcription factors: new roles for an old player.* Cell Death Dis, 2016. **7**: p. e2199.
79. Kim, H.P. and W.J. Leonard, *The basis for TCR-mediated regulation of the IL-2 receptor alpha chain gene: role of widely separated regulatory elements.* EMBO J, 2002. **21**(12): p. 3051-9.
80. van Rietschoten, J.G., et al., *Silencer activity of NFATc2 in the interleukin-12 receptor beta 2 proximal promoter in human T helper cells.* J Biol Chem, 2001. **276**(37): p. 34509-16.
81. Macian, F., C. Garcia-Rodriguez, and A. Rao, *Gene expression elicited by NFAT in the presence or absence of cooperative recruitment of Fos and Jun.* EMBO J, 2000. **19**(17): p. 4783-95.

82. Zhou, L. and D.R. Littman, *Transcriptional regulatory networks in Th17 cell differentiation.* Curr Opin Immunol, 2009. **21**(2): p. 146-52.
83. Tone, Y., et al., *Smad3 and NFAT cooperate to induce Foxp3 expression through its enhancer.* Nat Immunol, 2008. **9**(2): p. 194-202.
84. Bronevetsky, Y., et al., *T cell activation induces proteasomal degradation of Argonaute and rapid remodeling of the microRNA repertoire.* J Exp Med, 2013. **210**(2): p. 417-32.
85. Torgerson, T.R., et al., *FOXP3 inhibits activation-induced NFAT2 expression in T cells thereby limiting effector cytokine expression.* J Immunol, 2009. **183**(2): p. 907-15.
86. Yang, T.T. and C.W. Chow, *Transcription cooperation by NFAT.C/EBP composite enhancer complex.* J Biol Chem, 2003. **278**(18): p. 15874-85.
87. Yang, X.Y., et al., *Activation of human T lymphocytes is inhibited by peroxisome proliferator-activated receptor gamma (PPARgamma) agonists. PPARgamma co-association with transcription factor NFAT.* J Biol Chem, 2000. **275**(7): p. 4541-4.
88. Ho, I.C., et al., *The proto-oncogene c-maf is responsible for tissue-specific expression of interleukin-4.* Cell, 1996. **85**(7): p. 973-83.
89. Avni, O., et al., *T(H) cell differentiation is accompanied by dynamic changes in histone acetylation of cytokine genes.* Nat Immunol, 2002. **3**(7): p. 643-51.
90. Rengarajan, J., et al., *Interferon regulatory factor 4 (IRF4) interacts with NFATc2 to modulate interleukin 4 gene expression.* J Exp Med, 2002. **195**(8): p. 1003-12.
91. Lee, D.U., et al., *A distal enhancer in the interferon-gamma (IFN-gamma) locus revealed by genome sequence comparison.* J Biol Chem, 2004. **279**(6): p. 4802-10.
92. Decker, E.L., et al., *Early growth response proteins (EGR) and nuclear factors of activated T cells (NFAT) form heterodimers and regulate proinflammatory cytokine gene expression.* Nucleic Acids Res, 2003. **31**(3): p. 911-21.
93. Youn, H.D., T.A. Chatila, and J.O. Liu, *Integration of calcineurin and MEF2 signals by the coactivator p300 during T-cell apoptosis.* EMBO J, 2000. **19**(16): p. 4323-31.
94. Ansel, K.M., et al., *Deletion of a conserved Il4 silencer impairs T helper type 1-mediated immunity.* Nat Immunol, 2004. **5**(12): p. 1251-9.
95. Vaeth, M., et al., *Store-Operated Ca(2+) Entry Controls Clonal Expansion of T Cells through Metabolic Reprogramming.* Immunity, 2017. **47**(4): p. 664-679 e6.
96. Feske, S., et al., *Gene regulation mediated by calcium signals in T lymphocytes.* Nat Immunol, 2001. **2**(4): p. 316-24.
97. Macian, F., et al., *Transcriptional mechanisms underlying lymphocyte tolerance.* Cell, 2002. **109**(6): p. 719-31.
98. Heissmeyer, V. and A. Rao, *E3 ligases in T cell anergy--turning immune responses into tolerance.* Sci STKE, 2004. **2004**(241): p. pe29.
99. Gauld, S.B., et al., *Maintenance of B cell anergy requires constant antigen receptor occupancy and signaling.* Nat Immunol, 2005. **6**(11): p. 1160-7.
100. Parry, R.V., et al., *Ligation of the T cell co-stimulatory receptor CD28 activates the serine-threonine protein kinase protein kinase B.* Eur J Immunol, 1997. **27**(10): p. 2495-501.
101. Beals, C.R., et al., *Nuclear export of NF-ATc enhanced by glycogen synthase kinase-3.* Science, 1997. **275**(5308): p. 1930-4.
102. Okamura, H., et al., *A conserved docking motif for CK1 binding controls the nuclear localization of NFAT1.* Mol Cell Biol, 2004. **24**(10): p. 4184-95.
103. Chow, C.W., et al., *Nuclear accumulation of NFAT4 opposed by the JNK signal transduction pathway.* Science, 1997. **278**(5343): p. 1638-41.
104. Chow, C.W., et al., *c-Jun NH(2)-terminal kinase inhibits targeting of the protein phosphatase calcineurin to NFATc1.* Mol Cell Biol, 2000. **20**(14): p. 5227-34.
105. Cross, D.A., et al., *Inhibition of glycogen synthase kinase-3 by insulin mediated by protein kinase B.* Nature, 1995. **378**(6559): p. 785-9.
106. Diehn, M., et al., *Genomic expression programs and the integration of the CD28 costimulatory signal in T cell activation.* Proc Natl Acad Sci U S A, 2002. **99**(18): p. 11796-801.
107. Hogan, P.G., et al., *Transcriptional regulation by calcium, calcineurin, and NFAT.* Genes Dev, 2003. **17**(18): p. 2205-32.
108. Sun, L., et al., *Cabin 1, a negative regulator for calcineurin signaling in T lymphocytes.* Immunity, 1998. **8**(6): p. 703-11.

109. Klauck, T.M., et al., *Coordination of three signaling enzymes by AKAP79, a mammalian scaffold protein.* Science, 1996. **271**(5255): p. 1589-92.
110. Kashishian, A., et al., *AKAP79 inhibits calcineurin through a site distinct from the immunophilin-binding region.* J Biol Chem, 1998. **273**(42): p. 27412-9.
111. Rothermel, B., et al., *A protein encoded within the Down syndrome critical region is enriched in striated muscles and inhibits calcineurin signaling.* J Biol Chem, 2000. **275**(12): p. 8719-25.
112. Mulero, M.C., et al., *RCAN3, a novel calcineurin inhibitor that down-regulates NFAT-dependent cytokine gene expression.* Biochim Biophys Acta, 2007. **1773**(3): p. 330-41.
113. Esau, C., et al., *Deletion of calcineurin and myocyte enhancer factor 2 (MEF2) binding domain of Cabin1 results in enhanced cytokine gene expression in T cells.* J Exp Med, 2001. **194**(10): p. 1449-59.
114. Mulero, M.C., et al., *Inhibiting the calcineurin-NFAT (nuclear factor of activated T cells) signaling pathway with a regulator of calcineurin-derived peptide without affecting general calcineurin phosphatase activity.* J Biol Chem, 2009. **284**(14): p. 9394-401.
115. Strippoli, P., et al., *A new gene family including DSCR1 (Down Syndrome Candidate Region 1) and ZAKI-4: characterization from yeast to human and identification of DSCR1-like 2, a novel human member (DSCR1L2).* Genomics, 2000. **64**(3): p. 252-63.
116. Shay, T. and J. Kang, *Immunological Genome Project and systems immunology.* Trends Immunol, 2013. **34**(12): p. 602-9.
117. Testi, R., J.H. Phillips, and L.L. Lanier, *Leu 23 induction as an early marker of functional CD3/T cell antigen receptor triggering. Requirement for receptor cross-linking, prolonged elevation of intracellular [Ca++] and stimulation of protein kinase C.* J Immunol, 1989. **142**(6): p. 1854-60.
118. Pure, E. and C.A. Cuff, *A crucial role for CD44 in inflammation.* Trends Mol Med, 2001. **7**(5): p. 213-21.
119. Ansel, K.M., D.U. Lee, and A. Rao, *An epigenetic view of helper T cell differentiation.* Nat Immunol, 2003. **4**(7): p. 616-23.
120. Ansel, K.M., et al., *Regulation of Th2 differentiation and Il4 locus accessibility.* Annu Rev Immunol, 2006. **24**: p. 607-56.
121. O'Shea, J.J. and W.E. Paul, *Mechanisms underlying lineage commitment and plasticity of helper CD4+ T cells.* Science, 2010. **327**(5969): p. 1098-102.
122. Monney, L., et al., *Th1-specific cell surface protein Tim-3 regulates macrophage activation and severity of an autoimmune disease.* Nature, 2002. **415**(6871): p. 536-41.
123. Szabo, S.J., et al., *A novel transcription factor, T-bet, directs Th1 lineage commitment.* Cell, 2000. **100**(6): p. 655-69.
124. Szabo, S.J., et al., *Distinct effects of T-bet in TH1 lineage commitment and IFN-gamma production in CD4 and CD8 T cells.* Science, 2002. **295**(5553): p. 338-42.
125. Lighvani, A.A., et al., *T-bet is rapidly induced by interferon-gamma in lymphoid and myeloid cells.* Proceedings of the National Academy of Sciences of the United States of America, 2001. **98**(26): p. 15137-15142.
126. Afkarian, M., et al., *T-bet is a STAT1-induced regulator of IL-12R expression in naive CD4+ T cells.* Nat Immunol, 2002. **3**(6): p. 549-57.
127. Schulz, E.G., et al., *Sequential polarization and imprinting of type 1 T helper lymphocytes by interferon-gamma and interleukin-12.* Immunity, 2009. **30**(5): p. 673-83.
128. Hermann-Kleiter, N. and G. Baier, *NFAT pulls the strings during CD4+ T helper cell effector functions.* Blood, 2010. **115**(15): p. 2989-97.
129. Miller, J.F. and G.F. Mitchell, *Cell to cell interaction in the immune response.* Transplant Proc, 1969. **1**(1): p. 535-8.
130. Nurieva, R.I., et al., *Bcl6 mediates the development of T follicular helper cells.* Science, 2009. **325**(5943): p. 1001-5.
131. Crotty, S., *Follicular helper CD4 T cells (TFH).* Annu Rev Immunol, 2011. **29**: p. 621-63.
132. Johnston, R.J., et al., *Bcl6 and Blimp-1 are reciprocal and antagonistic regulators of T follicular helper cell differentiation.* Science, 2009. **325**(5943): p. 1006-10.
133. Yu, D., et al., *The transcriptional repressor Bcl-6 directs T follicular helper cell lineage commitment.* Immunity, 2009. **31**(3): p. 457-68.
134. Baumjohann, D., et al., *The microRNA cluster miR-17 approximately 92 promotes TFH cell differentiation and represses subset-inappropriate gene expression.* Nat Immunol, 2013. **14**(8): p. 840-8.

135. von Herrath, M. and J.L. Whitton, *Animal models using lymphocytic choriomeningitis virus.* Curr Protoc Immunol, 2001. **Chapter 19**: p. Unit 19 10.
136. Chen, L. and D.B. Flies, *Molecular mechanisms of T cell co-stimulation and co-inhibition.* Nat Rev Immunol, 2013. **13**(4): p. 227-42.
137. Rudd, C.E. and H. Schneider, *Unifying concepts in CD28, ICOS and CTLA4 co-receptor signalling.* Nat Rev Immunol, 2003. **3**(7): p. 544-56.
138. Waterhouse, P., et al., *Lymphoproliferative disorders with early lethality in mice deficient in Ctla-4.* Science, 1995. **270**(5238): p. 985-8.
139. Tivol, E.A., et al., *Loss of CTLA-4 leads to massive lymphoproliferation and fatal multiorgan tissue destruction, revealing a critical negative regulatory role of CTLA-4.* Immunity, 1995. **3**(5): p. 541-7.
140. Wang, C.J., et al., *CTLA-4 controls follicular helper T-cell differentiation by regulating the strength of CD28 engagement.* Proc Natl Acad Sci U S A, 2015. **112**(2): p. 524-9.
141. Walunas, T.L., et al., *CTLA-4 can function as a negative regulator of T cell activation.* Immunity, 1994. **1**(5): p. 405-13.
142. Linsley, P.S., et al., *Immunosuppression in vivo by a soluble form of the CTLA-4 T cell activation molecule.* Science, 1992. **257**(5071): p. 792-5.
143. Freeman, G.J., et al., *Engagement of the PD-1 immunoinhibitory receptor by a novel B7 family member leads to negative regulation of lymphocyte activation.* J Exp Med, 2000. **192**(7): p. 1027-34.
144. Riley, J.L., *PD-1 signaling in primary T cells.* Immunol Rev, 2009. **229**(1): p. 114-25.
145. Nishimura, H., et al., *Immunological studies on PD-1 deficient mice: implication of PD-1 as a negative regulator for B cell responses.* Int Immunol, 1998. **10**(10): p. 1563-72.
146. Iwai, Y., et al., *Involvement of PD-L1 on tumor cells in the escape from host immune system and tumor immunotherapy by PD-L1 blockade.* Proc Natl Acad Sci U S A, 2002. **99**(19): p. 12293-7.
147. Hui, E., et al., *T cell costimulatory receptor CD28 is a primary target for PD-1-mediated inhibition.* Science, 2017. **355**(6332): p. 1428-1433.
148. Kamphorst, A.O., et al., *Rescue of exhausted CD8 T cells by PD-1-targeted therapies is CD28-dependent.* Science, 2017. **355**(6332): p. 1423-1427.
149. Tan, A.H., S.C. Wong, and K.P. Lam, *Regulation of mouse inducible costimulator (ICOS) expression by Fyn-NFATc2 and ERK signaling in T cells.* J Biol Chem, 2006. **281**(39): p. 28666-78.
150. Weber, J.P., et al., *ICOS maintains the T follicular helper cell phenotype by down-regulating Kruppel-like factor 2.* J Exp Med, 2015. **212**(2): p. 217-33.
151. Bossaller, L., et al., *ICOS deficiency is associated with a severe reduction of CXCR5+CD4 germinal center Th cells.* J Immunol, 2006. **177**(7): p. 4927-32.
152. Green, J.M., et al., *Absence of B7-dependent responses in CD28-deficient mice.* Immunity, 1994. **1**(6): p. 501-8.
153. Rudd, C.E., A. Taylor, and H. Schneider, *CD28 and CTLA-4 coreceptor expression and signal transduction.* Immunol Rev, 2009. **229**(1): p. 12-26.
154. Dodson, L.F., et al., *Targeted knock-in mice expressing mutations of CD28 reveal an essential pathway for costimulation.* Mol Cell Biol, 2009. **29**(13): p. 3710-21.
155. Harada, Y., et al., *Critical requirement for the membrane-proximal cytosolic tyrosine residue for CD28-mediated costimulation in vivo.* J Immunol, 2001. **166**(6): p. 3797-803.
156. Rohr, J., et al., *Recurrent activating mutations of CD28 in peripheral T-cell lymphomas.* Leukemia, 2016. **30**(5): p. 1062-70.
157. Shahinian, A., et al., *Differential T cell costimulatory requirements in CD28-deficient mice.* Science, 1993. **261**(5121): p. 609-12.
158. Ferguson, S.E., et al., *CD28 is required for germinal center formation.* J Immunol, 1996. **156**(12): p. 4576-81.
159. Linterman, M.A., et al., *CD28 expression is required after T cell priming for helper T cell responses and protective immunity to infection.* Elife, 2014. **3**.
160. King, C.L., et al., *CD28-deficient mice generate an impaired Th2 response to Schistosoma mansoni infection.* Eur J Immunol, 1996. **26**(10): p. 2448-55.
161. Guo, F., et al., *CD28 controls differentiation of regulatory T cells from naive CD4 T cells.* J Immunol, 2008. **181**(4): p. 2285-91.

162. Sanchez-Lockhart, M., et al., *Cutting edge: CD28-mediated transcriptional and posttranscriptional regulation of IL-2 expression are controlled through different signaling pathways.* J Immunol, 2004. **173**(12): p. 7120-4.
163. Zhang, R., et al., *An obligate cell-intrinsic function for CD28 in Tregs.* J Clin Invest, 2013. **123**(2): p. 580-93.
164. Zhang, R., et al., *Requirement for CD28 in Effector Regulatory T Cell Differentiation, CCR6 Induction, and Skin Homing.* J Immunol, 2015. **195**(9): p. 4154-61.
165. Bouguermouh, S., et al., *CD28 co-stimulation down regulates Th17 development.* PLoS One, 2009. **4**(3): p. e5087.
166. Pearce, E.L. and E.J. Pearce, *Metabolic pathways in immune cell activation and quiescence.* Immunity, 2013. **38**(4): p. 633-43.
167. Hough, K.P., D.A. Chisolm, and A.S. Weinmann, *Transcriptional regulation of T cell metabolism.* Mol Immunol, 2015.
168. Frauwirth, K.A. and C.B. Thompson, *Regulation of T lymphocyte metabolism.* J Immunol, 2004. **172**(8): p. 4661-5.
169. Macintyre, A.N., et al., *The glucose transporter Glut1 is selectively essential for CD4 T cell activation and effector function.* Cell Metab, 2014. **20**(1): p. 61-72.
170. Jacobs, S.R., et al., *Glucose uptake is limiting in T cell activation and requires CD28-mediated Akt-dependent and independent pathways.* J Immunol, 2008. **180**(7): p. 4476-86.
171. Wang, R.N., et al., *The Transcription Factor Myc Controls Metabolic Reprogramming upon T Lymphocyte Activation.* Immunity, 2011. **35**(6): p. 871-882.
172. Fox, C.J., P.S. Hammerman, and C.B. Thompson, *Fuel feeds function: energy metabolism and the T-cell response.* Nat Rev Immunol, 2005. **5**(11): p. 844-52.
173. Geiger, R., et al., *L-Arginine Modulates T Cell Metabolism and Enhances Survival and Anti-tumor Activity.* Cell, 2016. **167**(3): p. 829-842 e13.
174. Carr, E.L., et al., *Glutamine uptake and metabolism are coordinately regulated by ERK/MAPK during T lymphocyte activation.* J Immunol, 2010. **185**(2): p. 1037-44.
175. Powell, J.D., et al., *Regulation of immune responses by mTOR.* Annu Rev Immunol, 2012. **30**: p. 39-68.
176. Slack, M., T. Wang, and R. Wang, *T cell metabolic reprogramming and plasticity.* Mol Immunol, 2015.
177. Dang, E.V., et al., *Control of T(H)17/T(reg) balance by hypoxia-inducible factor 1.* Cell, 2011. **146**(5): p. 772-84.
178. Phan, A.T. and A.W. Goldrath, *Hypoxia-inducible factors regulate T cell metabolism and function.* Mol Immunol, 2015.
179. Doedens, A.L., et al., *Hypoxia-inducible factors enhance the effector responses of CD8(+) T cells to persistent antigen.* Nat Immunol, 2013. **14**(11): p. 1173-82.
180. Nakamura, H., et al., *TCR engagement increases hypoxia-inducible factor-1 alpha protein synthesis via rapamycin-sensitive pathway under hypoxic conditions in human peripheral T cells.* J Immunol, 2005. **174**(12): p. 7592-9.
181. Ambros, V., *The functions of animal microRNAs.* Nature, 2004. **431**(7006): p. 350-5.
182. Bartel, D.P., *MicroRNAs: genomics, biogenesis, mechanism, and function.* Cell, 2004. **116**(2): p. 281-97.
183. Rodriguez, A., et al., *Identification of mammalian microRNA host genes and transcription units.* Genome Res, 2004. **14**(10A): p. 1902-10.
184. Concepcion, C.P., C. Bonetti, and A. Ventura, *The microRNA-17-92 family of microRNA clusters in development and disease.* Cancer J, 2012. **18**(3): p. 262-7.
185. Song, G. and L. Wang, *MiR-433 and miR-127 arise from independent overlapping primary transcripts encoded by the miR-433-127 locus.* PLoS One, 2008. **3**(10): p. e3574.
186. Blevins, R., et al., *microRNAs regulate cell-to-cell variability of endogenous target gene expression in developing mouse thymocytes.* PLoS Genet, 2015. **11**(2): p. e1005020.
187. Mukherji, S., et al., *MicroRNAs can generate thresholds in target gene expression.* Nat Genet, 2011. **43**(9): p. 854-9.
188. Lee, Y., et al., *MicroRNA genes are transcribed by RNA polymerase II.* EMBO J, 2004. **23**(20): p. 4051-60.
189. Cai, X., C.H. Hagedorn, and B.R. Cullen, *Human microRNAs are processed from capped, polyadenylated transcripts that can also function as mRNAs.* RNA, 2004. **10**(12): p. 1957-66.

190. Gregory, R.I., et al., *The Microprocessor complex mediates the genesis of microRNAs.* Nature, 2004. **432**(7014): p. 235-40.
191. Hutvagner, G., et al., *A cellular function for the RNA-interference enzyme Dicer in the maturation of the let-7 small temporal RNA.* Science, 2001. **293**(5531): p. 834-8.
192. Baumjohann, D. and K.M. Ansel, *MicroRNA-mediated regulation of T helper cell differentiation and plasticity.* Nat Rev Immunol, 2013. **13**(9): p. 666-78.
193. Kim, V.N., *MicroRNA biogenesis: coordinated cropping and dicing.* Nat Rev Mol Cell Biol, 2005. **6**(5): p. 376-85.
194. Baek, D., et al., *The impact of microRNAs on protein output.* Nature, 2008. **455**(7209): p. 64-71.
195. Selbach, M., et al., *Widespread changes in protein synthesis induced by microRNAs.* Nature, 2008. **455**(7209): p. 58-63.
196. Su, H., et al., *Mammalian hyperplastic discs homolog EDD regulates miRNA-mediated gene silencing.* Mol Cell, 2011. **43**(1): p. 97-109.
197. Krek, A., et al., *Combinatorial microRNA target predictions.* Nat Genet, 2005. **37**(5): p. 495-500.
198. Friedman, R.C., et al., *Most mammalian mRNAs are conserved targets of microRNAs.* Genome Res, 2009. **19**(1): p. 92-105.
199. Kloosterman, W.P., et al., *Substrate requirements for let-7 function in the developing zebrafish embryo.* Nucleic Acids Res, 2004. **32**(21): p. 6284-91.
200. Xia, Z., et al., *Molecular dynamics simulations of Ago silencing complexes reveal a large repertoire of admissible 'seed-less' targets.* Sci Rep, 2012. **2**: p. 569.
201. Lal, A., et al., *miR-24 Inhibits cell proliferation by targeting E2F2, MYC, and other cell-cycle genes via binding to "seedless" 3'UTR microRNA recognition elements.* Mol Cell, 2009. **35**(5): p. 610-25.
202. Vella, L.A., R.S. Herati, and E.J. Wherry, *CD4(+) T Cell Differentiation in Chronic Viral Infections: The Tfh Perspective.* Trends Mol Med, 2017. **23**(12): p. 1072-1087.
203. Ha, M. and V.N. Kim, *Regulation of microRNA biogenesis.* Nat Rev Mol Cell Biol, 2014. **15**(8): p. 509-24.
204. Hu, H.Y., et al., *Sequence features associated with microRNA strand selection in humans and flies.* BMC Genomics, 2009. **10**: p. 413.
205. Chong, M.M., et al., *Canonical and alternate functions of the microRNA biogenesis machinery.* Genes Dev, 2010. **24**(17): p. 1951-60.
206. Babiarz, J.E., et al., *Mouse ES cells express endogenous shRNAs, siRNAs, and other Microprocessor-independent, Dicer-dependent small RNAs.* Genes Dev, 2008. **22**(20): p. 2773-85.
207. Siomi, H. and M.C. Siomi, *Posttranscriptional regulation of microRNA biogenesis in animals.* Mol Cell, 2010. **38**(3): p. 323-32.
208. Jiang, S., et al., *Molecular dissection of the miR-17-92 cluster's critical dual roles in promoting Th1 responses and preventing inducible Treg differentiation.* Blood, 2011. **118**(20): p. 5487-97.
209. Cobb, B.S., et al., *A role for Dicer in immune regulation.* J Exp Med, 2006. **203**(11): p. 2519-27.
210. Chong, M.M., et al., *The RNAseIII enzyme Drosha is critical in T cells for preventing lethal inflammatory disease.* J Exp Med, 2008. **205**(9): p. 2005-17.
211. Cobb, B.S., et al., *T cell lineage choice and differentiation in the absence of the RNase III enzyme Dicer.* J Exp Med, 2005. **201**(9): p. 1367-73.
212. Muljo, S.A., *Aberrant T cell differentiation in the absence of Dicer.* Journal of Experimental Medicine, 2005. **202**(2): p. 261-269.
213. Zhou, X., et al., *Selective miRNA disruption in T reg cells leads to uncontrolled autoimmunity.* J Exp Med, 2008. **205**(9): p. 1983-91.
214. Jeker, L.T., et al., *DGCR8-mediated production of canonical microRNAs is critical for regulatory T cell function and stability.* PLoS One, 2013. **8**(5): p. e66282.
215. de Kouchkovsky, D., et al., *microRNA-17-92 regulates IL-10 production by regulatory T cells and control of experimental autoimmune encephalomyelitis.* J Immunol, 2013. **191**(4): p. 1594-605.
216. Kang, S.G., et al., *MicroRNAs of the miR-17 approximately 92 family are critical regulators of T(FH) differentiation.* Nat Immunol, 2013. **14**(8): p. 849-57.
217. Ota, A., et al., *Identification and characterization of a novel gene, C13orf25, as a target for 13q31-q32 amplification in malignant lymphoma.* Cancer Res, 2004. **64**(9): p. 3087-95.

218. Ventura, A., et al., *Targeted deletion reveals essential and overlapping functions of the miR-17 through 92 family of miRNA clusters.* Cell, 2008. **132**(5): p. 875-86.
219. Houbaviy, H.B., M.F. Murray, and P.A. Sharp, *Embryonic stem cell-specific MicroRNAs.* Dev Cell, 2003. **5**(2): p. 351-8.
220. Tanzer, A. and P.F. Stadler, *Molecular evolution of a microRNA cluster.* J Mol Biol, 2004. **339**(2): p. 327-35.
221. Xiao, C. and K. Rajewsky, *MicroRNA control in the immune system: basic principles.* Cell, 2009. **136**(1): p. 26-36.
222. Han, Y.C., et al., *An allelic series of miR-17 approximately 92-mutant mice uncovers functional specialization and cooperation among members of a microRNA polycistron.* Nat Genet, 2015.
223. He, L., et al., *A microRNA polycistron as a potential human oncogene.* Nature, 2005. **435**(7043): p. 828-833.
224. Mu, P., et al., *Genetic dissection of the miR-17~92 cluster of microRNAs in Myc-induced B-cell lymphomas.* Genes Dev, 2009. **23**(24): p. 2806-11.
225. O'Donnell, K.A., et al., *c-Myc-regulated microRNAs modulate E2F1 expression.* Nature, 2005. **435**(7043): p. 839-43.
226. Izreig, S., et al., *The miR-17 approximately 92 microRNA Cluster Is a Global Regulator of Tumor Metabolism.* Cell Rep, 2016. **16**(7): p. 1915-28.
227. Mogilyansky, E. and I. Rigoutsos, *The miR-17/92 cluster: a comprehensive update on its genomics, genetics, functions and increasingly important and numerous roles in health and disease.* Cell Death Differ, 2013. **20**(12): p. 1603-14.
228. Baumjohann, D., *Diverse functions of miR-17-92 cluster microRNAs in T helper cells.* Cancer Lett, 2018. **423**: p. 147-152.
229. Gerstein, M.B., et al., *Architecture of the human regulatory network derived from ENCODE data.* Nature, 2012. **489**(7414): p. 91-100.
230. Woods, K., J.M. Thomson, and S.M. Hammond, *Direct regulation of an oncogenic micro-RNA cluster by E2F transcription factors.* J Biol Chem, 2007. **282**(4): p. 2130-4.
231. Xiao, C., et al., *Lymphoproliferative disease and autoimmunity in mice with increased miR-17-92 expression in lymphocytes.* Nat Immunol, 2008. **9**(4): p. 405-14.
232. Buckler, J.L., et al., *Cutting edge: T cell requirement for CD28 costimulation is due to negative regulation of TCR signals by PTEN.* J Immunol, 2006. **177**(7): p. 4262-6.
233. Wu, T., et al., *Cutting Edge: miR-17-92 Is Required for Both CD4 Th1 and T Follicular Helper Cell Responses during Viral Infection.* J Immunol, 2015. **195**(6): p. 2515-9.
234. Simpson, L.J., et al., *A microRNA upregulated in asthma airway T cells promotes TH2 cytokine production.* Nat Immunol, 2014. **15**(12): p. 1162-70.
235. Liu, S.Q., et al., *miR-17-92 cluster targets phosphatase and tensin homology and Ikaros Family Zinc Finger 4 to promote TH17-mediated inflammation.* J Biol Chem, 2014. **289**(18): p. 12446-56.
236. Zhu, E., et al., *miR-20b suppresses Th17 differentiation and the pathogenesis of experimental autoimmune encephalomyelitis by targeting RORgammat and STAT3.* J Immunol, 2014. **192**(12): p. 5599-609.
237. Montoya, M.M., et al., *A Distinct Inhibitory Function for miR-18a in Th17 Cell Differentiation.* J Immunol, 2017. **199**(2): p. 559-569.
238. Yang, H.Y., et al., *MicroRNA-17 Modulates Regulatory T Cell Function by Targeting Co-regulators of the Foxp3 Transcription Factor.* Immunity, 2016. **45**(1): p. 83-93.
239. Wu, Y., et al., *MicroRNA-17-92 is required for T-cell and B-cell pathogenicity in chronic graft-versus-host disease in mice.* Blood, 2018. **131**(17): p. 1974-1986.
240. Jeker, L.T. and J.A. Bluestone, *MicroRNA regulation of T-cell differentiation and function.* Immunol Rev, 2013. **253**(1): p. 65-81.
241. de Pontual, L., et al., *Germline deletion of the miR-17 approximately 92 cluster causes skeletal and growth defects in humans.* Nat Genet, 2011. **43**(10): p. 1026-30.
242. Serr, I., et al., *miRNA92a targets KLF2 and the phosphatase PTEN signaling to promote human T follicular helper precursors in T1D islet autoimmunity.* Proc Natl Acad Sci U S A, 2016. **113**(43): p. E6659-E6668.
243. Lee, P.P., et al., *A critical role for Dnmt1 and DNA methylation in T cell development, function, and survival.* Immunity, 2001. **15**(5): p. 763-74.

244. Oxenius, A., et al., *Virus-specific MHC class II-restricted TCR-transgenic mice: effects on humoral and cellular immune responses after viral infection.* European Journal of Immunology, 1998. **28**(1): p. 390-400.
245. Vigne, S., et al., *IL-36R ligands are potent regulators of dendritic and T cells.* Blood, 2011. **118**(22): p. 5813-23.
246. Barrat, F.J., et al., *In vitro generation of interleukin 10-producing regulatory CD4(+) T cells is induced by immunosuppressive drugs and inhibited by T helper type 1 (Th1)- and Th2-inducing cytokines.* J Exp Med, 2002. **195**(5): p. 603-16.
247. Chen, W.J., et al., *Conversion of peripheral CD4(+)CD25(-) naive T cells to CD4(+)CD25(+) regulatory T cells by TGF-beta induction of transcription factor Foxp3.* Journal of Experimental Medicine, 2003. **198**(12): p. 1875-1886.
248. Gubser, P.M., et al., *Rapid effector function of memory CD8+ T cells requires an immediate-early glycolytic switch.* Nat Immunol, 2013. **14**(10): p. 1064-72.
249. Dobin, A., et al., *STAR: ultrafast universal RNA-seq aligner.* Bioinformatics, 2013. **29**(1): p. 15-21.
250. Gaidatzis, D., et al., *QuasR: quantification and annotation of short reads in R.* Bioinformatics, 2015. **31**(7): p. 1130-1132.
251. Robinson, M.D., D.J. McCarthy, and G.K. Smyth, *edgeR: a Bioconductor package for differential expression analysis of digital gene expression data.* Bioinformatics, 2010. **26**(1): p. 139-140.
252. Robinson, M.D. and A. Oshlack, *A scaling normalization method for differential expression analysis of RNA-seq data.* Genome Biol, 2010. **11**(3): p. R25.
253. Wu, D. and G.K. Smyth, *Camera: a competitive gene set test accounting for inter-gene correlation.* Nucleic Acids Res, 2012. **40**(17): p. e133.
254. Subramanian, A., et al., *Gene set enrichment analysis: A knowledge-based approach for interpreting genome-wide expression profiles.* Proc Natl Acad Sci U S A, 2005. **102**(43): p. 15545-15550.
255. Kanehisa, M., et al., *KEGG: new perspectives on genomes, pathways, diseases and drugs.* Nucleic Acids Res, 2017. **45**(D1): p. D353-D361.
256. Fabregat, A., et al., *The Reactome Pathway Knowledgebase.* Nucleic Acids Res, 2018. **46**(D1): p. D649-D655.
257. Ritchie, M.E., et al., *limma powers differential expression analyses for RNA-sequencing and microarray studies.* Nucleic Acids Res, 2015. **43**(7): p. e47.
258. Shi, L.Z., et al., *HIF1alpha-dependent glycolytic pathway orchestrates a metabolic checkpoint for the differentiation of TH17 and Treg cells.* J Exp Med, 2011. **208**(7): p. 1367-76.
259. Levine, B.L., et al., *Effects of CD28 costimulation on long-term proliferation of CD4+ T cells in the absence of exogenous feeder cells.* J Immunol, 1997. **159**(12): p. 5921-30.
260. Kim, H.P., J. Imbert, and W.J. Leonard, *Both integrated and differential regulation of components of the IL-2/IL-2 receptor system.* Cytokine & Growth Factor Reviews, 2006. **17**(5): p. 349-366.
261. Li, Y., et al., *MYC through miR-17-92 suppresses specific target genes to maintain survival, autonomous proliferation, and a neoplastic state.* Cancer Cell, 2014. **26**(2): p. 262-72.
262. Wherry, E.J., et al., *Viral persistence alters CD8 T-cell immunodominance and tissue distribution and results in distinct stages of functional impairment.* J Virol, 2003. **77**(8): p. 4911-27.
263. Oxenius, A., et al., *Presentation of endogenous viral proteins in association with major histocompatibility complex class II: on the role of intracellular compartmentalization, invariant chain and the TAP transporter system.* Eur J Immunol, 1995. **25**(12): p. 3402-11.
264. Wolint, P., et al., *Immediate cytotoxicity but not degranulation distinguishes effector and memory subsets of CD8+ T cells.* J Exp Med, 2004. **199**(7): p. 925-36.
265. Hutloff, A., et al., *ICOS is an inducible T-cell co-stimulator structurally and functionally related to CD28.* Nature, 1999. **397**(6716): p. 263-6.
266. Rekik, R., et al., *PD-1 induction through TCR activation is partially regulated by endogenous TGF-beta.* Cellular & Molecular Immunology, 2015. **12**(5): p. 648-649.
267. Kagi, D., et al., *Cytotoxicity mediated by T cells and natural killer cells is greatly impaired in perforin-deficient mice.* Nature, 1994. **369**(6475): p. 31-7.
268. Christensen, J.E., et al., *Role of CD28 co-stimulation in generation and maintenance of virus-specific T cells.* Int Immunol, 2002. **14**(7): p. 701-11.

269. Licatalosi, D.D., et al., *HITS-CLIP yields genome-wide insights into brain alternative RNA processing.* Nature, 2008. **456**(7221): p. 464-9.
270. Agarwal, V., et al., *Predicting effective microRNA target sites in mammalian mRNAs.* Elife, 2015. **4**.
271. Kim, C., et al., *Activation of miR-21-Regulated Pathways in Immune Aging Selects against Signatures Characteristic of Memory T Cells.* Cell Rep, 2018. **25**(8): p. 2148-2162 e5.
272. Gaidatzis, D., et al., *Analysis of intronic and exonic reads in RNA-seq data characterizes transcriptional and post-transcriptional regulation.* Nat Biotechnol, 2015. **33**(7): p. 722-9.
273. Martinez-Llordella, M., et al., *CD28-inducible transcription factor DEC1 is required for efficient autoreactive CD4+ T cell response.* J Exp Med, 2013. **210**(8): p. 1603-19.
274. Loeb, G.B., et al., *Transcriptome-wide miR-155 binding map reveals widespread noncanonical microRNA targeting.* Mol Cell, 2012. **48**(5): p. 760-70.
275. Kapturczak, M.H., H.U. Meier-Kriesche, and B. Kaplan, *Pharmacology of calcineurin antagonists.* Transplant Proc, 2004. **36**(2 Suppl): p. 25S-32S.
276. Benhamou, D., et al., *A c-Myc/miR17-92/Pten Axis Controls PI3K-Mediated Positive and Negative Selection in B Cell Development and Reconstitutes CD19 Deficiency.* Cell Rep, 2016. **16**(2): p. 419-31.
277. Anzelon, A.N., H. Wu, and R.C. Rickert, *Pten inactivation alters peripheral B lymphocyte fate and reconstitutes CD19 function.* Nat Immunol, 2003. **4**(3): p. 287-94.
278. Bartel, D.P., *MicroRNAs: target recognition and regulatory functions.* Cell, 2009. **136**(2): p. 215-33.
279. Morrish, F., et al., *The oncogene c-Myc coordinates regulation of metabolic networks to enable rapid cell cycle entry.* Cell Cycle, 2008. **7**(8): p. 1054-1066.
280. Roehrl, M.H.A., et al., *Selective inhibition of calcineurin-NFAT signaling by blocking protein-protein interaction with small organic molecules.* Proceedings of the National Academy of Sciences of the United States of America, 2004. **101**(20): p. 7554-7559.
281. Li, Y.Q., et al., *Regulation of lymphotoxin production by the p21(ras)-raf-MEK-ERK cascade in PHA/PMA-stimulated Jurkat cells.* Journal of Immunology, 1999. **162**(6): p. 3316-3320.
282. Ledbetter, J.A., et al., *Cd28 Ligation in T-Cell Activation - Evidence for 2 Signal Transduction Pathways.* Blood, 1990. **75**(7): p. 1531-1539.
283. Sereti, I., et al., *Interleukin 2 leads to dose-dependent expression of the alpha chain of the IL-2 receptor on CD25-negative T lymphocytes in the absence of exogenous antigenic stimulation.* Clin Immunol, 2000. **97**(3): p. 266-76.
284. Zhu, J., H. Yamane, and W.E. Paul, *Differentiation of Effector CD4 T Cell Populations*.* Annual Review of Immunology, 2010. **28**(1): p. 445-489.
285. Usui, T., et al., *T-bet regulates Th1 responses through essential effects on GATA-3 function rather than on IFNG gene acetylation and transcription.* Journal of Experimental Medicine, 2006. **203**(3): p. 755-766.
286. Shi, M., et al., *Janus-kinase-3-dependent signals induce chromatin remodeling at the Ifng locus during T helper 1 cell differentiation.* Immunity, 2008. **28**(6): p. 763-773.
287. Semple, K., et al., *Strong CD28 costimulation suppresses induction of regulatory T cells from naive precursors through Lck signaling.* Blood, 2011. **117**(11): p. 3096-103.
288. Boise, L.H., et al., *CD28 Costimulation Can Promote T Cell Survival by Enhancing the Expression of Bcl-x(L) (Reprinted from Immunity, vol 3, pg 87-98, 1995).* Journal of Immunology, 2010. **185**(7): p. 3788-3799.
289. Rozsnyay, Z., *Signaling complex formation of CD44 with src-related kinases.* Immunol Lett, 1999. **68**(1): p. 101-8.
290. Foger, N., R. Marhaba, and M. Zoller, *CD44 supports T cell proliferation and apoptosis by apposition of protein kinases.* Eur J Immunol, 2000. **30**(10): p. 2888-99.
291. DiToro, D., et al., *Differential IL-2 expression defines developmental fates of follicular versus nonfollicular helper T cells.* Science, 2018. **361**(6407).
292. Baaten, B.J., et al., *CD44 regulates survival and memory development in Th1 cells.* Immunity, 2010. **32**(1): p. 104-15.
293. Seok, H., et al., *MicroRNA Target Recognition: Insights from Transcriptome-Wide Non-Canonical Interactions.* Mol Cells, 2016. **39**(5): p. 375-81.
294. Canaider, S., et al., *Human RCAN3 gene expression and cell growth in endothelial cells.* International Journal of Molecular Medicine, 2010. **26**(6): p. 913-918.

295. Strippoli, P., et al., *The murine DSCR1-like (Down Syndrome Candidate Region 1) gene family: conserved synteny with the human orthologous genes.* Gene, 2000. **257**(2): p. 223-232.
296. Dorsett, Y., et al., *MicroRNA-155 suppresses activation-induced cytidine deaminase-mediated Myc-Igh translocation.* Immunity, 2008. **28**(5): p. 630-8.
297. Anders, C., et al., *Structural basis of PAM-dependent target DNA recognition by the Cas9 endonuclease.* Nature, 2014. **513**(7519): p. 569-+.
298. Sternberg, S.H., et al., *DNA interrogation by the CRISPR RNA-guided endonuclease Cas9.* Nature, 2014. **507**(7490): p. 62-+.
299. Vidigal, J.A. and A. Ventura, *The biological functions of miRNAs: lessons from in vivo studies.* Trends Cell Biol, 2015. **25**(3): p. 137-147.
300. Liu, J., et al., *Calcineurin Is a Common Target of Cyclophilin-Cyclosporine-a and Fkbp-Fk506 Complexes.* Cell, 1991. **66**(4): p. 807-815.
301. Martinez-Martinez, S. and J.M. Redondo, *Inhibitors of the calcineurin/NFAT pathway.* Current Medicinal Chemistry, 2004. **11**(8): p. 997-1007.
302. Ragheb, J.A., M. Deen, and R.H. Schwartz, *CD28-mediated regulation of mRNA stability requires sequences within the coding region of the IL-2 mRNA.* Journal of Immunology, 1999. **163**(1): p. 120-129.
303. Abraham, C. and J. Miller, *Molecular mechanisms of IL-2 gene regulation following costimulation through LFA-1.* Journal of Immunology, 2001. **167**(9): p. 5193-5201.
304. Afkarian, M., et al., *T-bet is a STAT1-induced regulator of IL-12R expression in naive CD4(+) T cells.* Nature Immunology, 2002. **3**(6): p. 549-557.
305. Esensten, J.H., et al., *CD28 Costimulation: From Mechanism to Therapy.* Immunity, 2016. **44**(5): p. 973-88.
306. Maher, J., et al., *Human T-lymphocyte cytotoxicity and proliferation directed by a single chimeric TCR zeta/CD28 receptor.* Nature Biotechnology, 2002. **20**(1): p. 70-75.
307. Pagani, M., et al., *Role of microRNAs and long-non-coding RNAs in CD4(+) T-cell differentiation.* Immunol Rev, 2013. **253**(1): p. 82-96.
308. Sasaki, K., et al., *miR-17-92 expression in differentiated T cells - implications for cancer immunotherapy.* J Transl Med, 2010. **8**: p. 17.
309. Facchin, F., et al., *Complexity of Bidirectional Transcription and Alternative Splicing at Human RCAN3 Locus.* Plos One, 2011. **6**(9).
310. Fruman, D.A., et al., *Calcineurin phosphatase activity in T lymphocytes is inhibited by FK 506 and cyclosporin A.* Proc Natl Acad Sci U S A, 1992. **89**(9): p. 3686-90.
311. Calne, R.Y., et al., *Cyclosporin A in patients receiving renal allografts from cadaver donors.* Lancet, 1978. **2**(8104-5): p. 1323-7.
312. Ishikura, K., et al., *Posterior reversible encephalopathy syndrome in children: its high prevalence and more extensive imaging findings.* Am J Kidney Dis, 2006. **48**(2): p. 231-8.
313. Jeker, L.T. and R. Marone, *Targeting microRNAs for immunomodulation.* Current Opinion in Pharmacology, 2015. **23**: p. 25-31.
314. Simonson, B. and S. Das, *MicroRNA Therapeutics: the Next Magic Bullet?* Mini-Reviews in Medicinal Chemistry, 2015. **15**(6): p. 467-474.
315. Lindow, M. and S. Kauppinen, *Discovering the first microRNA-targeted drug.* Journal of Cell Biology, 2012. **199**(3): p. 407-412.
316. Chakraborty, C., et al., *Therapeutic miRNA and siRNA: Moving from Bench to Clinic as Next Generation Medicine.* Molecular Therapy-Nucleic Acids, 2017. **8**: p. 132-143.
317. Ohno, M., et al., *Expression of miR-17-92 enhances anti-tumor activity of T-cells transduced with the anti-EGFRvIII chimeric antigen receptor in mice bearing human GBM xenografts.* J Immunother Cancer, 2013. **1**: p. 21.

11. Reagents

11.1. Cell culture media, buffers, solutions

item	*ingredients*	*supplier*	*Catalogue number*
$CD4^+$ T cell medium	RPMI-1640 Medium 10% FCS, 1% HEPES, 1% Sodium pyruvate, 1% non-essential amino acids, 1% Glutamax, 1% Penstrep (if cells were sorted) 0.1% 2-Mercaptoethanol	SIGMA Atlanta SIGMA Gibco Gibco Gibco Gibco Gibco	R8758-500ML S11150 H0887 11360-039 11140-050 35050-038 15140-122 31350-010
FACS buffer	PBS 2% heat-inactivated FCS For stainings, add 0.002% NaN_3	In house Milian SIGMA	See below S0750 S2002-5G
10x PBS (for 1l)	80g NaCl (1.369M) 2g KCl (0.027M) 14.4g Na_2HPO_4 * $2H_2O$ (0.08M) 2.4g KH_2PO_4 (0.018M) pH=7.4	SIGMA SIGMA SIGMA SIGMA	S3014-1KG P5405-500G 71643-1KG 5655-500G
ACK lysis buffer	8.29g NH_4Cl (0.155M) 200µl 0.5M EDTA pH=8.0 1g $NaHCO_3$ pH 7.2 (0.012M)	SIGMA SIGMA SIGMA	A9434-500G 03690-100ML S5761-500G
$NaHCO_3$	0.1M pH=8.0	SIGMA	S5761-500G
Tail lysis buffer	0.1M Tris pH 8.5 5mM EDTA 0.2% SDS 0.1M NaCl (add 1%Proteinase K)	SIGMA SIGMA SIGMA SIGMA PROMEGA	T6066-1KG 03690-100ML 75746-1KG S3014-1KG V3021
Glucose-free unbuffered RPMI	Dissolve in 1L dH2O	SIGMA	R6504-10X1L
TE buffer		Sigma	93283-100ML

11.2. Kits, reagents and further material

item	**supplier**	**Catalogue number**
Fixation/Permeabilization Concentrate	invitrogen	00-5123-43
Fixation/Permeabilization Diluent	invitrogen	00-5223-5
Permeabilization Buffer 10X	eBioscience	00-8333-56
Heparin-Na	Braun	46613
OneComp eBeads	invitrogen	01-111-42
Ethanol	Sigma-Aldrich	51976-500ML-F
Isopropanol	Sigma-Aldrich	I9516-500ML
TRI Reagent	Sigma-Aldrich	T9424-200ML
1-Bromo-3-chloropropane	Sigma-Aldrich	B9673-200ML
M-MLV Reverse Transcriptase	Sigma-Aldrich	M1302-40KU
TaqMan™ Fast Universal PCR Master Mix (2X), no AmpErase™ UNG	ThermoFisher	4364103
TaqMan Gene Expression Assays RCAN3	ThermoFisher	4351372
TaqMan Gene Expression Assays 18S	ThermoFisher	4331182
MicroAmp™ Fast Optical 96-Well Reaction Plate, 0.1 mL	ThermoFisher	4346907
EasySep naïve $CD4^+$ T cell Isolation Kit	STEMCELL	19765A
CellTAK adhesive	Corning	354241
Seahorse XFe96/XF96 FluxPak (18 cartr.)	SeahorseBiotech	PN 102416-100

Oligomycin	SIGMA	495445
FCCP	SIGMA	C2920
Rotenone	SIGMA	R8875
D-(+)-Glucose	Sigma-Aldrich	G7021
GoTaq G2 Green Master Mix	Promega	M782B
ProLong Glass Antifade Mountant	ThermoFisher	P36982
0.4µm filters	Sefar	
Syringe for i.p. BD Micro-Fine (30G, 8mm)	BD	324826
Syringe for i.v. BD Micro-Fine (29G, 12.7mm)	BD	324824
ELISA MAX mouse IL-2 set	BioLegend	431002
Nunc-Immuno™ MicroWell™ 96 well solid plates	SIGMA	M9410-1CS
Cryo embedding medium	Medite	41-3011-00
Acetone	SIGMA	534064-500ML
ELITE PAP pen	Diagnostic Biosystems	K039
Universal Agarose	Bio&Sell	BS20.46.5000
Zymol Directzol kit	ZymoResearch	R2060
96 well cell culture cluster (96 well plate)	Corning	3596
24 well cell culture cluster (24 well plate)	Corning	3526

11.3. Antibodies, dyes, cytokines, stimulants

reactive to	*clone*	*fluorochrome*	*supplier*	*Catalogue number*
Fixable Viability Dye eF780	-	eFluor 780	eBioscience	65-0865-14
2-NBDG	-	-	ThermoFisher	N13195
Cell Trace Violet (CTV)	-	-	ThermoFisher	C34557
αCD4	RM4-5 or GK1.5	various	Biolegend	various
αCD44	IM7	PerCP-Cy5.5, PE	Biolegend	103032, 103008
αCD62L	MEL-14	APC	Biolegend	104412
αCD69	H1.2F3	BV711	Biolegend	104537
αCD25	PC61	PeCy7	Biolegend	102016
αTbet	4B10	PE	Biolegend	644810
αIFNγ	XMG1.2	Alexa 488	Biolegend	505813
αIL-17a	TC11-18H10.1	PE	Biolegend	506904
αRorγt	Q31-378	PE-CF594	BD BioScience	562684
αFoxp3	FJK-16s	APC	eBioscience	17-5773-82
αFas (CD95)	Jo2	Alexa488	BD BioScience	554257
αGL-7	GL7	Alexa 488/PerCPCy5.5	Biolegend	144612, 144610
αBcl-6	K112-91	PE	BD BioScience	561522
αICOS (CD278)	C398.4A	BV510	Biolegend	313525
αCXCR5 (CD185)	SPRCL5	PE-Texas	eBioscience	145513
αPD-1 (CD279)	29F.1A12	PeCy7	Biolegend	135216
αB220	RA3-6B2	Alexa647, APC	Biolegend, Tonbo	103229, 20-0452-U100
αCD19	1D3	BV711, Alexa647	Biolegend	115555, 115522
αCD3e	145-2C11	various	Biolegend	various
αIL-2	JES6-5H4	PE	Biolegend	503808
αVα2	B20.1	APC, PacBlue	Biolegend,	127816,
αVβ8.3	1B3.3	PE	BD BioScience	553664
αCD3	2C11	Unlabeled (coating)	BioXcell	BP0001-1
αCD28	PV-1	Unlabeled (coating)	BioXcell	BE0015-5
αCD16/32	2.4G2	Unlabeled (Fc block)	BioXcell	BE0307
Phorbol 12-Myristate 13-Acetate (PMA)	-	-	Sigma	P1585
Ionomycin	-	-	Sigma	10634-1MG
Brefeldin A (BFA)	-	-	Sigma	B7651-5MG
GP-64	-	-	Neosystem	SP991567B
IL-2	-	cytokine	R&D	202-IL

αIL4	11B11	Unlabeled (blocking)	UCSF	AM039-PURE-B25
αIFNγ	XMG1.2	Unlabeled (blocking)	UCSF	AM034-PURE-B25
αIL12/23	C17.8	Unlabeled (blocking)	UCSF	AM037-PURE-B25
Retinoic acid	-	For differentiation	Sigma	R2625
rhTGFβ	-	For differentiation	R&D	P01137
IL-6		For differentiation	R&D	406ML
Cyclosporin A	-	-	Sigma	30024
Goat anti-mouse IgG1	Alexa Fluor 647		ThermoFisher	A21240
DAPI			Sigma	10236276001
IL-12		For differentiation	R&D	419ML
αNFATC2	25A10.D6.D2	biotinylated	ThermoFisher	MA1-025
TMB		Substrate for HRP	BD	555214

11.4. Primers, oligomers and plasmids

All primers were ordered from Microsynth, resuspend at a concentration of 100µM in TE buffer and stored at -80°C.

Primer name	***purpose***	***Sequence 5' => 3'***
112_LJ_CD4-cre_for	Genotyping CD4cre fwd	ACG ACC AAG TGA CAG CAA TG
113_LJ_CD4-cre_rev	Genotyping CD4cre rev	CTC GAC CAG TTT AGT TAC CC
174_CD4-cre_for	Genotyping CD4cre fwd	TTT CAC TGA AGG CGA GAG GG
175_CD4-cre_rev	Genotyping CD4cre rev	TGG CTT AAT TAG CCC CAT CCT
688_CD28ko_wtfwd	Genotyping CD28ko wt fwd	CTT TGA TTT CAG GGC AAT GG
689_CD28ko_common	Genotyping CD28ko common	TTG ACG TGC AGA TTC CAG AG
690_CD28ko_mutfwd	Genotyping CD28ko mut fwd	CCA GTC ATA GCC GAA TAG CC
106 LJ_oIMR8916_miR17-92Tg	Genotyping miR-17~92 transgene	CCA GAT GAC TAC CTA TCC TC
107 LJ_oIMR8917_miR-17-92Tg	Genotyping miR-17~92 transgene	GAG CTG CAG TGG AGT AGG CG
108 LJ_oIMR8918_miR-17-92Tg	Genotyping miR-17~92 transgene	ACC TCC CCC TGA ACC TGA AAC A
109 LJ_oIMR8919_miR-17-92Tg	Genotyping miR-17~92 transgene	CAG TTT TAC AAG GTG ATG TTC TCT G
110 LJ_oIMR8528_miR-17-92_lox	Genotyping miR-17~92 knockout	TCG AGT ATC TGA CAA TGT GG
111 LJ_oIMR8529_miR-17-92_lox	Genotyping miR-17~92 knockout	TAG CCA GAA GTT CCA AAT TGG
207 Vα2 up primer	Genotyping SMARTA by PCR	ATA AAA AGG AAG ATG GAC GAT T
208 Vα2 lower primer	Genotyping SMARTA by PCR	TGG GGC TGA CTG ATA CCG

11.5. PCR protocols

11.5.1. miR-17~92 knockout genotyping

Reagent	V/rxn
H2O	9.5
Primer 106 (10 µM)	1
Primer 107 (10 µM)	1
Primer 108 (10 µM)	1
Primer 109 (10 µM)	1
Go green Taq	12.5
DNA	1
Total	25

Temp (°C)	Time (min:sec)	
94	03:00	
94	00:30	
53	01:00	
72	01:00	35x
72	03:00	
10	hold	

11.5.2. miR-17~92 transgene genotyping

Reagent	V/rxn
H2O	9.5
Primer 110 (10 µM)	1
Primer 111 (10 µM)	1
Go green Taq	12.5
DNA	1
Total	25

Temp (°C)	Time (min:sec)	
94	03:00	
94	00:30	
53	01:00	
72	01:00	35x
72	03:00	
10	hold	

11.5.3. SMARTA genotyping

Reagent	V/rxn
H2O	9.5
Primer 207 (10 µM)	1
Primer 208 (10 µM)	1
Go Green Taq	12.5
DNA	1
Total	25

Temp (°C)	Time (min:sec)	
94	02:00	
94	00:20	
52	00:15	
72	00:10	35x
72	02:00	
10	hold	

11.5.4. CD4cre genotyping

Reagent	V/rxn
H2O	9.5
Primer 112 (10 µM)	1
Primer 113 (10 µM)	1
Primer 174 (10 µM)	1
Primer 175 (10 µM)	1
Go green Taq	12.5
DNA	1
Total	25

Temp (°C)	Time (min:sec)	
94	03:00	
94	00:30	
58	01:00	
72	01:00	35x
72	03:00	
10	hold	

11.5.5. CD28 knockout genotyping

wt

Reagent	V/rxn
H2O	8.5
Primer 688 (10 µM)	1
Primer 689 (10 µM)	1
Go green Taq	12.5
DNA	2
Total	25

mut

Reagent	V/rxn
H2O	7.5
Primer 689 (10 µM)	1
Primer 690 (10 µM)	2
Go green Taq	12.5
DNA	2
Total	25

Temp (°C)	Time (min:sec)		
94	02:00		
94	00:20		-1.5°C per
65	00:15	10x	cycle
68	00:10		
94	00:15		
50	00:15		32x
72	00:10		
72	02:00		
4	hold		

12. Abbreviations

abbreviation	*meaning*
°C	degree Celsius
2-NBDG	2-deoxy-2-((7-nitro-2,1,3-benzoxadiazol-4-yl)amino)-D Glucose
80k	80'000
abs(log2FC)	absolute log2 fold change
ACK	Ammonium-Chloride-Potassium
Ago2	argonaute 2
AHC	Ago2 HITS CLIP
Akt	Protein Kinase B
AP-1	activator protein 1
APC	antigen presenting cell
ATP	adenosine tri phosphate
B6	Black 6 (mouse)
$Bcl\text{-}_{XL}$	B cell lymphoma-extra large
BFA	Brefeldin A
bp	base pairs
C13ORF25	chromosome 13 open reading frame 25
Ca^{2+}	Calcium
CAR	chimeric antigen receptor
CD	cluster of differentiation/ designation or classification determinant
CDF	cumulative distribution function
CPM	counts per million reads mapped
CRAC	calcium release activated calcium channels
CREB1	cAMP response element binding
CRISPR	clustered regularly interspaced short palindromic repeats
CsA	Cyclosporin A
Csk	C-terminal Src kinase
CTLA-4	cytotoxic T lymphocyte antigen 4
CTV	cell trace violet
d	day
DAG	diacylglycerol
DNA	Deoxyribonucleic acid
DAPI	4',6-diamidino-2-phenylindole
DE	differential expression
dH_2O	distilled water
DMSO	Dimethyl sulfoxide
e.g.	exempli gratia
EAE	experimental autoimmune encephalitis
ECAR	extracellular acidification rate
EISA	exon intron split analysis
ELISA	enzyme-linked immunosorbent assay
ENCODE	encyclopedia of DNA elements
ER	endoplasmic reticulum
FACS	fluorescence associated cell sorting

FCCP	Carbonyl cyanide-4-(trifluoromethoxy)phenylhydrazone
FDR	false discovery rate
FoxP3	forkhead box p3
FSC-A	forward scatter-area
G	Gauge
GC	germinal center
GC-MS	Gas chromatography- mass spectrometry
GLUT1	glucose transporter 1
GMPR	guanosine monophosphate reductase
GP	glycoprotein
GSEA	gene set enrichment analysis
h	hours
HITS CLIP	High-throughput sequencing of RNA isolated by crosslinking immunoprecipitation
i.e.	id est
i.p.	intra peritoneal
i.v.	intra veneous
IFNγ	interferon gamma
Ig	Immunoglobulin
IL	interleukin
Iono	Ionomycin
IP_3	inositol 1,4,5-triphosphate
ITAM	immunoreceptor tyrosine-based activation motifs
iT_{reg}	induced T regulatory cell
JNK	jun kinase
LAT	linker of activated T cells
LCMV	Lymphocytic choriomeningitis virus
LN	lymph node
logFC	log fold change
lox, miR1792lox	B6.CD4cre.miR-17~92lox
MFI	median fluorescence intensity
MHC	major histocompatibility complex
min	minutes
miR, miRNA	microRNA
MIR17HG	miR-17~92 host gene
ml	milliliter
mm	millimeters
mRNA	messenger RNA
ms	millisecond
mTORc	mammalian target of rapamycin complex
n.s.	not significant
NFAT	nuclear factor of activated T cells
NFκB	nuclear factor kappa-light-chain-enhancer of activated B cells
ng	nanogram
NIH	National Institute of Health

norm.	normalized
nt	nucleotide
OCR	oxygen consumption rate
p value	probability value
PAM	protospacer adjacent motif
PBMC	peripheral blood mononuclear cells
PBS	phosphate buffered saline
PC	principal component
PCA	principal component analysis
PCR	polymerase chain reaction
PD-1	Programmed death 1
PFU	plaque forming units
PHLPP2	PH domain and Leucine Rich Repeat Protein Phosphatase 2
PI3K	phosphatidyl inositol 3 kinase
PIP_2	phosphatidyl inositol 4,5-bisphosphate
PIP_3	phosphatidyl inositol 3,4,5-trisphosphate
PLC-γ	phospholipase C-γ
PMA	phorbol 12-myristate 13-acetate
PTEN	phosphatase and tensin homolog
qPCR	quantitative PCR
RCAN	Regulator of calcineurin, also known as members of Down's syndrome critical region
RISC	RNA induced silencing complex
RNA	Ribonucleic acid
Rorγt	RAR related orphan receptor gamma
rpm	rounds per minute
RT	room temperature or reverse transcription
SD	standard deviation
SH2	Src Homology 2
siRNA	small interfering RNA
SOCE	store operated calcium entry
STAT	Signal transducer and activator of transcription
STIM 1/2	stromal interaction molecules
Tbet	T-box expressed in T cells
TCR	T cell receptor
TF	Transcription factor
T_{FH}	T follicular Helper cell
tg, miR1792tg	B6.CD4cre.miR-17~92tg
TGFβRII	transforming growth factor beta receptor II
T_H	T Helper
TMB	3,3',5,5'-Tetramethylbenzidine
TNF	tumor necrosis factor
TS	TargetScan
U	Units
UTR	untranslated region

V	Volt
vs.	versus
wt	wild type
αCD3	anti CD3
µl	micro liter
µM	micro molar

13. Appendix

13.1. Gating strategy LCMV experiments

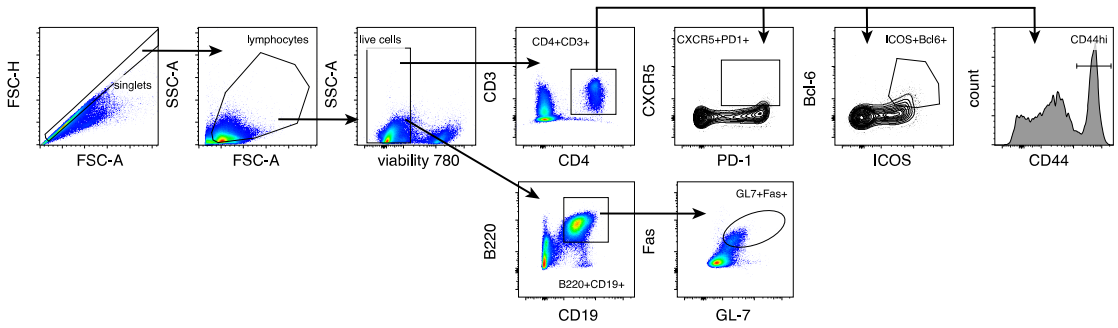

Figure 40. Gating strategy for LCMV infection experiments

Cell suspensions were pre-gated for singlets, lymphocytes and viability. CD4⁺ T cells were gated with CD3/CD4 (including the cells down-regulating CD3 as a consequence of antigen encountering, "smear"). CD4⁺ T cells were further displayed with CXCR57PD-1, ICOS/Bcl6 and CD44. B cells were gated from the viable cells as B220/CD19, and subsequently for Fas/GL-7

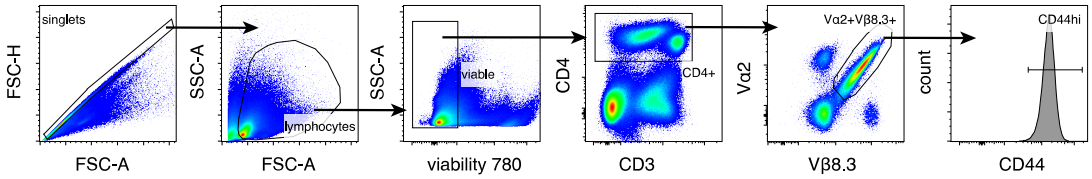

Figure 41. Gating strategy for adoptive transfer experiments

Cell suspensions were pre-gated for singlets, lymphocytes and viability. CD4⁺ T cells were gated with CD3/CD4 (including the cells down-regulating CD3 as a consequence of antigen encountering, "smear"). CD4⁺ T cells were further displayed Vα2/Vβ8.3 and these further with CD44.

13.2. GC-MS experimental procedure

The following protocol was obtained from the NIH West coast Metabolomics Center.

Data Dictionary Fiehn laboratory _NIH West Coast Metabolomics Center_09-27-2013

Primary metabolism by ALEX-CIS GCTOF MS

Glossary

ALEX automated liner exchange, produced by Gerstel corporation.
CIS cold injection system, produced by Gerstel corporation
GC gas chromatography
TOF time of flight mass spectrometer
MS mass spectrometry. After hard ionization by electron ionization, one electron gets abstracted from the intact molecules which hence become positively charged. The standardized ~70 eV ionization voltage is so high that molecules fragment into multiple product ions, which may also form rearrangements among each other. Fragments are then analyzed by time of flight mass spectrometry which is made here by the vendor Leco corporation not to obtain accurate mass information at high resolution but instead to obtain mass spectra at very high sensitivity and speed.
QC quality control
IS also istd, internal standards
FAME fatty acid methyl esters
v/v volumetric ratio
InChI International Chemical Identifier key. Denotes the exact stereochemical and atomic description of chemicals and used as universal identifier in chemical databases.
KEGG Kyoto Encyclopedia of Genes and Genomes
PubChem a public database of chemicals and chemical information.
rt retention time (seconds)
RI also ret.index, retention index, a conversion of absolute retention times to relative retention times based on a set of pre-defined internal standards. Classically, Kovats retention indices are used based on hydrocarbons. We use Fiehn retention indices based on FAME istd because FAME mass spectra are much easier to correctly annotate in automatic assays.
mz also m/z, or mass-to-charge ratio. In metabolomics, ions are almost exclusively detected as singly charged species.
s/n signal to noise ratios
IUPAC International Union of Pure and Applied Chemistry
NIST National Institute of Standards and Technology
PCA Principal Component Analysis

Data acquisition

Data are acquired using the following chromatographic parameters, with more details to be found in Fiehn O. et al. Plant J. 53 (2008) 691–704.
Column: Restek corporation Rtx-5Sil MS (30 m length x 0.25 mm internal diameter with 0.25 µm film made of 95% dimethyl/5%diphenylpolysiloxane)
Mobile phase: Helium
Column temperature: 50-330°C Flow-rate: 1 mL min^{-1}
Injection volume: 0.5 µL
Injection: 25 splitless time into a multi-baffled glass liner
Injection temperature: 50°C ramped to 250°C by 12°C s^{-1}
Oven temperature program: 50°C for 1 min, then ramped at 20°C min^{-1} to 330°C, held constant for 5 min.

The analytical GC column is protected by a 10 m long empty guard column which is cut by 20 cm intervals whenever the reference mixture QC samples indicate problems caused by column contaminations. We have validated that at this sequence of column cuts, no detrimental effects are detected with respect to peak shapes, absolute or relative metabolite retention times or reproducibility of quantifications. This chromatography method yields excellent retention and separation of primary metabolite classes (amino acids, hydroxyl acids, carbohydrates, sugar acids, sterols, aromatics, nucleosides, amines and miscellaneous compounds) with narrow peak widths of 2–3 s and very good within-series retention time reproducibility of better than 0.2 s absolute deviation of retention times. We use automatic liner exchanges after each set of 10 injections which we could show to reduce sample carryover for highly lipophilic compounds such as free fatty acids.
Mass spectrometry parameters are used as follows: a Leco Pegasus IV mass spectrometer is used with unit mass resolution at 17 spectra s^{-1} from 80-500 Da at ~70 eV ionization energy and 1800 V detector voltage with a 230°C transfer line and a 250°C ion source.

Data processing

Raw data files are preprocessed directly after data acquisition and stored as ChromaTOF-specific *.peg files, as generic *.txt result files and additionally as generic ANDI MS *.cdf files. ChromaTOF vs. 2.32 is used for data preprocessing without smoothing, 3 s peak width, baseline subtraction just above the noise level, and automatic mass spectral deconvolution and peak detection at signal/noise levels of 5:1 throughout the chromatogram. Apex masses are reported for use in the BinBase algorithm. Result *.txt files are exported to a data server with absolute spectra intensities and further processed by a filtering algorithm implemented in the metabolomics BinBase database.

The BinBase algorithm (rtx5) used the settings: validity of chromatogram (<10 peaks with intensity >10^7 counts s^{-1}), unbiased retention index marker detection (MS similarity>800, validity of intensity range for high m/z marker ions), retention index calculation by 5th order polynomial regression. Spectra are cut to 5% base peak abundance and matched to database entries from most to least abundant spectra using the following matching filters: retention index window ±2,000 units (equivalent to about ±2 s retention time), validation of unique ions and apex masses (unique ion must be included in apexing masses and present at >3% of base peak abundance), mass spectrum similarity must fit criteria dependent on peak purity and signal/noise ratios and a final isomer filter. Failed spectra are automatically entered as new database entries if s/n >25, purity <1.0 and presence in the biological study design class was >80%. All thresholds reflect settings for ChromaTOF v. 2.32. Quantification is reported as peak height using the unique ion as default, unless a different quantification ion is manually set in the BinBase administration software BinView. A quantification report table is produced for all database entries that are positively detected in more than 10% of the samples of a study design class (as defined in the miniX database) for unidentified metabolites. A subsequent post-processing module is employed to automatically replace missing values from the *.cdf files. Replaced values are labeled as 'low confidence' by color coding, and for each metabolite, the number of high-confidence peak detections is recorded as well as the ratio of the average height of replaced values to high-confidence peak detections. These ratios and numbers are used for manual curation of automatic report data sets to data sets released for submission.

Data reporting

Data are reported including metadata, see example below.

								Subject ID	223913	157B19	124940
								Local code	A0050702A	A0125621A	142363
								Vial Barcode	1RAR7	1GZR9	1AN1N
								Date received	4-Dec-12	4-Dec-12	4-Dec-12
								Date of evalu	3/17/2013	3/17/2013	3/17/2013
								Sample Status			
								REVISION			
								Comments	GCTOF MS_s	GCTOF MS_sa	GCTOF MS_s
								Acq. Time	5:18:33 AM	5:43:50 AM	6:09:05 AM
								Data File Nam	130328cmss	130328cmss	130328cms
								miniX id	118072	118073	118074
BinBase i	BinBase name	ret.index	quant mz	mass spec	InChI key	KEGG id	PubChem id				
14441	z C30 FAME internal stand	1113100	87	82:386.0 83:	BIRUBGLRQLAEFF-UHFFF	n/a	12400	16026	15203	18096	
14378	z C28 FAME internal stand	1061700	87	82:1635.0 83	ZKHOYAKAFALNQD-UHFF	n/a	41518	39317	228	11145	
14367	z C26 FAME internal stand	1006900	87	82:1915.0 83	VHUJBYYFFWDLNM-UHFF	n/a	22048	32809	30571	35507	
14373	z C24 FAME internal stand	948820	87	82:1153.0 83	XUDJZDNUVZHSKZ-UHFFF	n/a	75546	43836	43163	48731	
14350	z C22 FAME internal stand	886620	87	82:3004.0 83	QSQLTHMFHEFIY-UHFF	n/a	13584	53566	51781	58740	
14338	z C20 FAME internal stand	819620	87	82:5074.0 83	QGBRLVONZKHAKJ-UHFF	n/a	14259	57770	58877	63250	
14344	z C18 FAME internal stand	747420	87	82:1871.0 83	HPEIJPJOZXNMSJ-UHFFFA	n/a	8201	53466	52542	57091	
14328	z C16 FAME internal stand	668720	87	82:7874.0 83	FLIACVVOZYBSBS-UHFFF	C16995	8181	170150	166843	186189	
14330	z C14 FAME internal stand	582620	87	82:6846.0 83	ZAZKJZBWRNNLDS-UHFF	n/a	31284	117029	113463	131850	
15538	z C12 FAME internal stand	487220	87	87:89125.0 1	UQDUPQYQJKYHQI-UHFFF	n/a	8139	147184	142864	169095	
14348	z C10 FAME internal stand	381020	87	82:2900.0 83	YRHYCMZFEVDGFQ-UHFF	n/a	8050	131518	127669	150456	
14356	z C09 FAME internal stand	323120	87	82:1461.0 83	IJKHLVMUNBOGRR-UHFF	n/a	15606	119374	119013	137532	
14391	z C08 FAME internal stand	262320	87	82:81.6.0 83:	IGHZJRVDZXSNKQ-UHFFF	n/a	8091	79355	87424	91461	
231968	xylose	544673	103	85:5068.0 86	PYMYPHUHKUWMLA-VPE	C02205	644160	19097	1462	1642	
368041	xylitol	566570	217	86:588.0 87:	HEBKCHPVOIAQTA-NGQZ	C00379	6912	239	168	121	
203224	xanthine	702391	353	85:1361.0 86	LRFVTYWOQMYALW-UHF	C00385	1188	64	26	60	
199605	valine	313224	144	85:48.0 86:1	KZSNJWFQEVHDMF-BYPY	C00183	6287	108089	120432	133290	
213127	uridine	856953	258	85:2472.0 86	DRTQHJPVMGBUCF-XVFC	C00299	6029	256	63	60	
304993	uric acid	730534	441	85:1183.0 86	LEHOTFFKMJEONL-UHFF	C00366	1175	16528	13715	7856	
224322	urea	337230	171	87:1643.0 89	XSQUKJJJFZCRTK-UHFFFA	C00086	1176	334000	281631	313888	

The **'BinBase identifier column'** denotes the unique identifier for the GCTOFMS platform. It is given for both identified and unidentified metabolites in the same manner.

The **'BinBase name'** denotes the name of the metabolite, if the peak has been identified. A chemical name is not a unique identifier. We use names recognized by biologists instead of IUPAC nomenclature. If a compound is identified, it has a name, and external database identifiers such as InChI key, PubChem ID and KEGG ID. If a compound is unknown, the name is the same as given in the 'identifier column'.

The **'retention index'** column details the target retention index in the BinBase database system.
The **'quant mz'** column details the m/z value that was used to quantify the peak height of a BinBase entry.
The **'mass spec'** column details the complete mass spectrum of the metabolite given as mz: intensity values, separated by spaces.
The **'InChI key'** identifier gives the unique chemical identifier defined by the IUPAC and NIST consortia.
The **'KEGG'** identifier gives the unique identifier associated with an identified metabolite in the community database KEGG LIGAND DB.
The **'PubChem'** column denotes the unique identifier of a metabolite in the PubChem database.
The **'internal standard'** addition within the BinBase name clarifies if a specific chemical has been added into the extraction solvent as internal standard. These internal standards serve as retention time alignment markers, for quality control purposes and for quantification corrections.

Row metadata that are requested by a specific consortium are labeled in blue.
Consortium **'subject ID', 'local ID', 'vial barcode'** detail information given by a specific consortium.
The row **'date received'** is the date when samples were received in the metabolomics laboratory.
The row **'date of evaluation'** is the data of data acquisition, as given by the machine logbook.
The row **'sample status'** uses the consortium's sample status code if samples have errors. The consortium sample status code does not give a code when data acquisition occurred without problems. If a consortium does not use an authorized error code dictionary, plain text is given for errors.
The row **'revision'** details if data processing yields a new data sheet. Data revisions may be needed when new algorithms have been tested, validated and deployed that might yield better raw data analyses than prior submissions. By default, therefore, data revisions replace the (less valid) prior data submissions. However, data revisions may also indicate a different form of data treatment, e.g. data normalizations (see below). In this case, the 'revision' would indicate the type of normalization. Any information in the row 'revision' will have a date stamp when the revision was conducted in the form of *MMDDYY*.
The **'comments'** row gives comments about the platform and type of sample. A sample is given as "sample" in comparison to e.g. a quality control or a blank injection.
The **'Acq.Date-Time'** row details the acquisition time when the data acquisition was completed.
The **'Data File Name'** row denotes the name of the raw data file. Raw data files are secured at the NIH Metabolomics database, www.metabolomicsworkbench.org
Data file names are dictated by the laboratory's information and management system when the sequence starts running. GCTOF raw file names from the Leco instrumentation end with .peg (this ending is not given in the file name, but is found in the database repositories).
In case a sample will need to be reinjected, the file name will change from e.g. 130328cmssa40_1.peg to 130328cmssa40 _2.d for the second injection, 130328cmssa40_3.d for the third injection and subsequent injections. The file name itself denotes YYMMDD then the 'machine used for data acquisition' (here: c; we have four GCTOF MS machines a-d), 'person who operated the machine' (here: ms for Mimi Swe), 'sa' for sample (instead of e.g. 'qc' for a quality control or 'bl' for a blank sample), followed by the sequence number (here: the 40th sample within the sample sequence).
The **'miniX'** row shows the unique sample identifier in the Fiehnlab miniX laboratory information management system.

The **actual data** are given as peak heights for the quantification ion (mz value) at the specific retention index. We give peak heights instead of peak areas because peak heights are more precise for low abundant metabolites than peak areas, due to the larger influence of baseline determinations on areas

compared to peak heights. Also, overlapping (co-eluting) ions or peaks are harder to deconvolute in terms of precise determinations of peak areas than peak heights. Such data files are then called 'raw results data' in comparison to the raw data file produced during data acquisition (see 'data file name'). The worksheets are called 'Height'.

Raw results data need to be normalized to reduce the impact of between-series drifts of instrument sensitivity, caused by machine maintenance, aging and tuning parameters. Such normalization data sets are called 'norm data' worksheets.

There are many different types of normalizations in the scientific literature. We usually provide first a variant of a 'vector normalization' in which we calculate the sum of all peak heights for all identified metabolites (but not the unknowns!) for each sample. We call such peak-sums "mTIC" in analogy to the term TIC used in mass spectrometry (for 'total ion chromatogram'), but with the notification "mTIC" to indicate that we only use genuine metabolites (identified compounds) in order to avoid using potential non-biological artifacts for the biological normalizations, such as column bleed, plasticizers or other contaminants.
Subsequently, we determine if the mTIC averages are significantly different between treatment groups or cohorts. If these averages indeed are different by $p<0.05$, data will be normalized to the average mTIC of each group. If averages between treatment groups or cohorts are not different, or if treatment relations to groups are kept blinded, data will be normalized to the total average mTIC.

Following equation is then used for normalizations for metabolite *i* of sample *j*:

$$\text{metabolite}_{ij,\ \text{normalized}} = \frac{\text{metabolite}_{ij,\ \text{raw}}}{\text{mTIC}_j} \cdot \text{mTIC}_{\text{average}}$$

The worksheet is then called **'norm mTIC'**. Data are 'relative semi-quantifications', meaning they are normalized peak heights. Because the average mTIC will be different between series of analyses that are weeks or months apart (due to differences in machine sensitivity, tuning, maintenance status and other parameters), **additional normalizations** need to be performed. For this purpose, identical samples ('QC samples') must be analyzed multiple times in all series of data acquisitions. In fact, one must not exclude the possibility that even within a series of data acquisitions, a sensitivity shift or drift might occur.
Hence, the following statistical analyses are suggested: (a) compute univariate statistics for mTIC values in batches within-series and between-series of data injections, using time/date stamps to find potential breaks during which machine downtime may have occurred. If there are no mTIC differences between such time/date stamp batches, calculate an overall mTIC covering all samples. (b) compute multivariate PCA plots for the , marking the potentially different samples of individual time/date stamp batches using different colors. If there is no apparent separation between PCA clusters of different colors, there is no large between-series effect and these PCA clusters can be treated as indistinguishable. If there is suspicion of hidden features that might be masked by overall variance analysis in PCA, supervised statistics by Partial Least Square regression models can unravel such between-series differences.
Once different clusters (i.e. series of undistinguishable QC samples) have been identified, correction factor models need to be developed that correct differences between those QC samples. Subsequently, these correction factors can be applied to the actual analytical samples to remove overt quantification differences that are not related to biological causes but solely due to analytical errors.
Such correction factor models can be computed in different ways, e.g. by unit-variance mean centering or by calculating simple offset vectors for each individual metabolite. The best way of such types of normalizations is being explored in the Fiehn laboratory. However, in any case, such correction models can only be developed if a sufficient number of QC samples have been included in the analytical sequences. For that reason, the Fiehn laboratory uses a suitable QC sample for every 11th injection. Such QC samples need to be as similar to the actual biological specimen as possible, e.g. generated by pool samples during extractions or by obtaining typical community standard samples (e.g. the NIST standard blood plasma, or commercial serum or plasma samples as needed).

If appropriate internal standards are used for absolute quantifications, the following equation could be used for peak height normalizations for metabolite *i* of sample *j* and internal standard *k*

$$\text{metabolite}_{ij,\ \text{normalized}} = \frac{\text{metabolite}_{ij,\ \text{raw}}}{\text{istd}_k} \cdot \text{concentration istd}_k$$

However, there are few universal or class-specific internal standards in GC-MS based analysis, because within each chemical class, metabolites may have drastically different calibration curves (sensitivity or 'response') based on a combination of injection, volatilization and stability and ionization response properties. As surrogate, external calibration standards could be used for specific (important) metabolites which, however, cannot be applied for unidentified compounds and which of course would not account for recovery during extraction procedures.